Appendix F

Supplemental Performance Demonstration Information

F.1 Modeling the Test Results

General linear models (GLMs) were used to analyze the test data for each of the 23 electrical circuits in Table 4.1 at each test time. The GLM analysis determines which experimental factors or, when possible, combinations of factors (interactions) explain a statistically significant portion of the observed variation in the test results.

A GLM used to analyze the test results with respect to sites, flux type, and their interactions (where possible) is expressed as the following 22-term equation:

$$Y = \beta_0 + \beta_1 D_1 + \beta_2 D_2 + \beta_3 D_3 + \beta_4 D_4 + \beta_5 D_5 + \beta_6 D_6 + \beta_7 D_7 + \beta_8 D_8 + \beta_9 D_9 + \beta_{10} D_{10} + \beta_{11} D_{11} + \beta_{12} D_{12} + \beta_{13} D_{13} + \beta_{14} D_{14} + \beta_{15} D_{15} + \beta_{16} D_{16} \quad \text{(Main effects)} \quad \text{(F.1)}$$

$$+ \beta_{17} D_3 D_{16} + \beta_{18} D_4 D_{16} + \beta_{19} D_6 D_{16} + \beta_{20} D_{10} D_{16} + \beta_{21} D_{12} D_{16} + \beta_{22} D_{15} D_{16} \quad \text{(Two-factor interactions)}$$

The coefficients in the GLM (β_0, β_1, β_2, …) are estimated using ordinary least squares regression techniques. The dummy variables, D_1 to D_{16}, are set equal to 1 to identify type of surface finish/manufacturing site and type of flux that are associated with individual test results. Otherwise, the dummy variables are set to 0. The following dummy variables can be used to represent the experimental variables for each test environment for each electrical response variable.

D_1 = 0 if surface finish is not HASL – Site 2
= 1 if surface finish is HASL – Site 2
D_2 = 0 if surface finish is not HASL – Site 3
= 1 if surface finish is HASL – Site 3
D_3 = 0 if surface finish is not OSP – Site 4
= 1 if surface finish is OSP – Site 4
D_4 = 0 if surface finish is not OSP – Site 5
= 1 if surface finish is OSP – Site 5
D_5 = 0 if surface finish is not OSP – Site 6
= 1 if surface finish is OSP – Site 6
D_6 = 0 if surface finish is not immersion Sn – Site 7
= 1 if surface finish is immersion Sn – Site 7
D_7 = 0 if surface finish is not immersion Sn – Site 8
= 1 if surface finish is immersion Sn – Site 8
D_8 = 0 if surface finish is not immersion Sn – Site 9
= 1 if surface finish is immersion Sn – Site 9
D_9 = 0 if surface finish is not immersion Sn – Site 10
= 1 if surface finish is immersion Sn – Site 10
D_{10} = 0 if surface finish is not immersion Ag – Site 11
= 1 if surface finish is immersion Ag – Site 11
D_{11} = 0 if surface finish is not immersion Ag – Site 12
= 1 if surface finish is immersion Ag – Site 12
D_{12} = 0 if surface finish is not Ni / Au – Site 13
= 1 if surface finish is Ni / Au – Site 13
D_{13} = 0 if surface finish is not Ni / Au – Site 14
= 1 if surface finish is Ni / Au – Site 14
D_{14} = 0 if surface finish is not Ni / Au – Site 15
= 1 if surface finish is Ni / Au – Site 15
D_{15} = 0 if surface finish is not Ni / Pd / Au – Site 16
= 1 if surface finish is Ni / Pd / Au – Site 16
D_{16} = 0 if flux is not water soluble
= 1 if flux is water soluble

The "base case" is obtained by setting all $D_i = 0$. Note that the surface finish/manufacturing site is HASL / Site 1 if $D_1 = D_2 = D_3 = D_4 = D_5 = D_6 = D_7 = D_8 = D_9 = D_{10} = D_{11} = D_{12} = D_{13} = D_{14} = D_{15} = 0$. Likewise, if $D_{16} = 0$, the flux is low-residue. Thus, the base case is HASL / Site 1 with LR flux.

Note the GLM in Equation F.1 contains six interactions terms that represent the last six sites in Table 4.2 (5, 6, 7, 11, 13, and 16) for which both LR and WS fluxes were used.

The GLM approach provides a tool for identifying the statistically significant experimental variables and their interactions. That is, all terms in the model that are *significantly different from the base case* are identified through tests of statistical hypotheses of the form:

$$H_0: \beta_i = 0 \text{ versus } H_1: \beta_i \neq 0 \text{ for all i}$$

If the null hypothesis is rejected, then the coefficient of the corresponding term in the GLM is significantly different from 0, which means that the particular experimental conditions represented by that term (surface finish or flux type) differ significantly from the base case. If the null hypothesis is not rejected, then the coefficient of the corresponding term in the GLM is not significantly different from 0 and, therefore, the experimental conditions represented by that term *do not* differ significantly from the base case. Such terms are sequentially eliminated from the GLM (see Iman, 1994, for complete details).

The GLM approach is quite flexible and easily adaptable to a variety of requirements. For example, if the focus is on surface finishes and not sites; the GLM in Equation F.1 would be replaced by one of the following form:

$$Y = \beta_0 + \beta_1 D_1 + \beta_2 D_2 + \beta_3 D_3 + \beta_4 D_4 + \beta_5 D_5 + \beta_6 D_6 \qquad \text{F.2}$$

This model contains only main effects where the dummy variables are defined as follows.

D_1 = 0 if surface finish is not OSP
= 1 if surface finish is OSP
D_2 = 0 if surface finish is not immersion Sn
= 1 if surface finish is immersion Sn
D_3 = 0 if surface finish is not immersion Ag
= 1 if surface finish is immersion Ag
D_4 = 0 if surface finish is not Ni / Au
= 1 if surface finish is Ni / Au
D_5 = 0 if surface finish is not Ni / Pd / Au
= 1 if surface finish is Ni / Pd / Au
D_6 = 0 if flux is not water soluble
= 1 if flux is water soluble

As before, the "base case" is obtained by setting all $D_i = 0$, which is HASL with LR flux. Note that the base case associated with the GLM in Equation F.1 was also HASL with LR flux, but also required Site 1. That requirement is not part of the latter model since sites are not included in the model in Equation F.2.

As a final illustration of the flexibility of the GLM approach consider a subset of the data base that only includes the results for Sites 1, 4, 5, 7, 11, 13, and 16 in Table 4.2. These sites were selected because their surface finish was processed with both LR and WS fluxes, which allows an interaction term to be added to the model in Equation F.2 for each surface finish and flux combination. However, by excluding the other sites, the number of data points is reduced from 164 to 92.

Example of GLM Analysis

The data base for the electrical responses incorporates the dummy variables used to define the experimental parameters for each measurement. The data base contains 164 rows (one for each PWA). Sample data base entries for the GLM in Equation F.2 for leakage measurement on the 10-mil pads (response number 18 in Table 4.1) in $\log_{10}$ ohms could appear as follows:

Row	OSP	Imm Sn	Imm Ag	Ni/Au	Ni/Pd/Au	Flux	Leakage
1	0	0	0	0	0	0	12.8
2	1	0	0	0	0	1	11.9
3	0	1	0	0	0	0	12.1
4	0	0	0	0	1	1	11.8
•	•	•	•	•	•	•	•
•	•	•	•	•	•	•	•
•	•	•	•	•	•	•	•

The interpretation of these data base entries is as follows. The first row has zeros for OSP, immersion Sn, immersion Ag, Ni/Au, and Ni/Pd/Au. This implies that the surface finish is HASL. The surface finishes for rows 2, 3, and 4 are OSP, immersion Sn, and Ni/Pd/Au, respectively. Water soluble flux is used on rows 2 and 4. The leakage measurements are given in the last column. The above table would be expanded to include other experimental parameters or products (interactions) of the experimental parameters depending on the requirements of the GLM such as given in Equation F.1. The above table would also include columns containing the other 22 electrical measurements.

Computer software is used with the entries in the data base to find the least squares estimates of coefficients in the GLM. For example, such an analysis for the GLM in Equation F.2 could produce an estimated equation such as the following for leakage for the 10-mil pads.

$$Y = 12.5 - 0.200\ \text{OSP} + 0.192\ \text{Immersion Sn} - 0.164\ \text{Immersion Ag} + 0.006\ \text{Ni/Au} - 0.292\ \text{Ni/Pd/Au} - 1.04\ \text{Flux}$$

Note that the least squares process has simply solved a set of equations to determine an estimated coefficient for each term appearing in the GLM in Equation F.2. However, it does not necessarily follow that each of the terms in this estimated model makes a statistically significant contribution toward explaining the variation in the leakage measurements. Rather, this determination is accomplished by subjecting the coefficients in the *full* model to the following hypothesis test in a sequential (stepwise) manner to determine if they are significantly different from 0:

$$H_0: \beta_i = 0 \text{ versus } H_1: \beta_i \neq 0$$

If the coefficient is not significantly different from 0, it is eliminated from the model. Thus, the only terms remaining in the model at the conclusion of this sequence of tests are those that are declared to be significantly different from 0. This stepwise process eliminates some of the terms from the model and the least squares calculations are repeated without those terms, which produces a *reduced* model such as:

$$Y = 12.35 - 0.34\ \text{OSP} - 0.38\ \text{Immersion Ag} - 0.24\ \text{Ni/Pd/Au} - 1.06\ \text{Flux}$$

The intercept in this model, 12.35, is the estimated resistance for the base case—HASL processed with LR flux. Mean predictions for other combinations of the experimental parameters can be made by substituting the appropriate dummy variables into the model. For example, the mean prediction for a OSP (D_1=1, D_2=0, D_3=0, D_4=0, D_5=0) PWA processed with WS flux (D_6=1) is found as:

Y = 12.35 - 0.34 (1) - 1.06 (1) = 10.95

F.2 Overview of Test Results

Table F.1 Anomaly Summary by Surface Finish after Exposure to 85/85

MSN	Site	Flux		Circuit	Test Technician Comments
HASL					
083-2	1	WS	7	HF PTH 50MHz	Open PTH
			8	HF PTH f(-3dB)	Open PTH
			9	HF PTH f(-40dB)	Open PTH
OSP					
056-4	5	LR	7	HF PTH 50MHz	Open PTH
			8	HF PTH f(-3dB)	Open PTH
			9	HF PTH f(-40dB)	Open PTH
Immersion Sn					
030-4	9	WS	4	HVLC SMT	
032-4	8	LR	7	HF PTH 50MHz	Open PTH
			8	HF PTH f(-3dB)	Open PTH
086-2	7	WS	12	HF SMT f(-40dB)	Waveform did not go to -40dB
102-4	10	WS	17	HF TLC RNR	
Immersion Ag					
082-2	11	LR	21	Gull Wing	Burnt etch in multiple places
094-4	12	WS	7	HF PTH 50MHz	Open PTH
			8	HF PTH f(-3dB)	Open PTH
			9	HF PTH f(-40dB)	Open PTH
Ni/Au					
013-1	13	LR	6	HSD SMT	Device failed, U3
015-4	14	LR	9	HF PTH f(-40dB)	Wrong value capacitor

Table F.2 Anomaly Summary After Exposure to Thermal Shock

MSN	Site	Flux		Circuit	Test Technician Comments
HASL					
079-4	1	WS	12	HF SMT f(-40dB)	
083-2	1	WS	7	HF PTH 50MHz	Open PTH
			8	HF PTH f(-3dB)	Open PTH
			9	HF PTH f(-40dB)	Open PTH
			10	HF SMT 50MHz	Open PTH
			11	HF SMT f(-3dB)	Open PTH
			12	HF SMT f(-40dB)	Open PTH
096-4	3	WS	10	HF SMT 50MHz	Open PTH
			11	HF SMT f(-3dB)	Open PTH
			12	HF SMT f(-40dB)	Open PTH
098-3	3	WS	10	HF SMT 50MHz	Open PTH
			11	HF SMT f(-3dB)	Open PTH
			12	HF SMT f(-40dB)	Open PTH
098-4	3	WS	11	HF SMT f(-3dB)	Waveform shifted
099-1	3	WS	12	HF SMT f(-40dB)	Distorted Waveform (does not quite go to -40dB, reads at-3dB)
111-3	3	WS	23	Stranded Wire 2	Minor
OSP					
006-4	5	LR	12	HF SMT f(-40dB)	Distorted waveform (goes to 40db but flattens and crosses beyond 900mhz
009-2	6	LR	10	HF SMT 50MHz	Open PTH on coil
			11	HF SMT f(-3dB)	Open PTH on coil
			12	HF SMT f(-40dB)	Open PTH on coil

014-3	5	LR	10	HF SMT 50MHz	Open PTH
			11	HF SMT f(-3dB)	Open PTH
			12	HF SMT f(-40dB)	Open PTH
056-2	5	LR	7	HF PTH 50MHz	Open PTH
			8	HF PTH f(-3dB)	Open PTH
056-4	5	LR	7	HF PTH 50MHz	2 open PTHs
			8	HF PTH f(-3dB)	2 open PTHs
			9	HF PTH f(-40dB)	2 open PTHs
			10	HF SMT 50MHz	2 open PTHs
			11	HF SMT f(-3dB)	2 open PTHs
			12	HF SMT f(-40dB)	2 open PTHs
058-1	5	WS	10	HF SMT 50MHz	Open PTH
			12	HF SMT f(-40dB)	Open PTH
060-1	5	WS	12	HF SMT f(-40dB)	
060-2	5	WS	10	HF SMT 50MHz	Open PTH
			12	HF SMT f(-40dB)	Open PTH
Immersion Sn					
028-2	9	LR	10	HF SMT 50MHz	Open PTH
			12	HF SMT f(-40dB)	Open PTH
030-4	9	LR	4	HVLC SMT	Burnt etch (visual)
032-4	8	LR	7	HF PTH 50MHz	Open PTH
			8	HF PTH f(-3dB)	Open PTH
033-2	8	LR	17	HF TLC RNR	
037-2	9	LR	5	HSD PTH	Likely component failure
			10	HF SMT 50MHz	Open PTH
			11	HF SMT f(-3dB)	Open PTH
			12	HF SMT f(-40dB)	Open PTH
084-1	7	LR	10	HF SMT 50MHz	Open PTH
			11	HF SMT f(-3dB)	Open PTH
			12	HF SMT f(-40dB)	Open PTH
086-2	7	WS	5	HSD PTH	Likely component failure
		WS	12	HF SMT f(-40dB)	Distorted Waveform
087-3	7	WS	7	HF PTH 50MHz	High resistance on coil (acts like open PTH)
			8	HF PTH f(-3dB)	High resistance on coil (acts like open PTH)
			9	HF PTH f(-40dB)	High resistance on coil (acts like open PTH)
			12	HF SMT f(-40dB)	High resistance on coil (acts like open PTH)
088-3	7	LR	10	HF SMT 50MHz	Open PTH
			11	HF SMT f(-3dB)	Open PTH
			12	HF SMT f(-40dB)	Open PTH
089-1	7	WS	7	HF PTH 50MHz	Open PTH
			8	HF PTH f(-3dB)	Open PTH
			9	HF PTH f(-40dB)	Open PTH
			12	HF SMT f(-40dB)	Open PTH
089-2	7	WS	10	HF SMT 50MHz	High resistance on coil (acts like open PTH)
			11	HF SMT f(-3dB)	High resistance on coil (acts like open PTH)
			12	HF SMT f(-40dB)	High resistance on coil (acts like open PTH)
089-4	7	WS	10	HF SMT 50MHz	Open PTH
			11	HF SMT f(-3dB)	Open PTH
			12	HF SMT f(-40dB)	Open PTH
090-2	7	WS	7	HF PTH 50MHz	Open PTH on coil
			8	HF PTH f(-3dB)	Open PTH on coil
			9	HF PTH f(-40dB)	Open PTH on coil
102-4	10	WS	17	HF TLC RNR	
Immersion Ag					
071-1	11	LR	10	HF SMT 50MHz	Open PTH on coil
			11	HF SMT f(-3dB)	Open PTH on coil
			12	HF SMT f(-40dB)	Open PTH on coil
072-1	11	LR	7	HF PTH 50MHz	Open PTH

			8	HF PTH f(-3dB)	Open PTH
			9	HF PTH f(-40dB)	Open PTH
073-3	11	LR	7	HF PTH 50MHz	Open PTH
			8	HF PTH f(-3dB)	Open PTH
			9	HF PTH f(-40dB)	Open PTH
			15	HR TLC 1GHz	
082-2	11	WS	12	HF SMT f(-40dB)	Burnt etch
085-1	12	WS	7	HF PTH 50MHz	Open PTH
			8	HF PTH f(-3dB)	Open PTH
			9	HF PTH f(-40dB)	Open PTH
			10	HF SMT 50MHz	Open PTH
			11	HF SMT f(-3dB)	Open PTH
			12	HF SMT f(-40dB)	Open PTH
085-2	12	WS	7	HF PTH 50MHz	Open PTH (2 places)
			8	HF PTH f(-3dB)	Open PTH (2 places)
			9	HF PTH f(-40dB)	Open PTH (2 places)
			10	HF SMT 50MHz	Open PTH (2 places)
			11	HF SMT f(-3dB)	Open PTH (2 places)
			12	HF SMT f(-40dB)	Open PTH (2 places)
091-4	12	WS	12	HF SMT f(-40dB)	
094-1	12	WS	7	HF PTH 50MHz	Burnt Etch, High Resistance PTH, and Open PTH
			8	HF PTH f(-3dB)	Burnt Etch, High Resistance PTH, and Open PTH
			9	HF PTH f(-40dB)	Burnt Etch, High Resistance PTH, and Open PTH
			10	HF SMT 50MHz	Burnt Etch, High Resistance PTH, and Open PTH
			11	HF SMT f(-3dB)	Burnt Etch, High Resistance PTH, and Open PTH
			12	HF SMT f(-40dB)	Burnt Etch, High Resistance PTH, and Open PTH
094-4	12	WS	7	HF PTH 50MHz	Open PTH
			8	HF PTH f(-3dB)	Open PTH
			9	HF PTH f(-40dB)	Open PTH
Ni/Au					
013-1	13	LR	6	HSD SMT	Device failed, U3
015-2	14	LR	7	HF PTH 50MHz	Open PTH on coil
			8	HF PTH f(-3dB)	Open PTH on coil
			9	HF PTH f(-40dB)	Open PTH on coil
055-1	13	WS	7	HF PTH 50MHz	Open PTH
			8	HF PTH f(-3dB)	Open PTH
			9	HF PTH f(-40dB)	Open PTH
Ni/Pd/Au					
036-1	16	WS	6	HSD SMT	Likely component failure

Table F.3 Anomaly Summary After Mechanical Shock
(shaded entries signify carry over TS anomalies)

HASL					
MSN	**Site**	**Flux**		**Circuit**	**Test Technician Comments**
039-2	2	LR	12	HF SMT f(-40dB)	Waveform distorted
046-1	2	LR	10	HF SMT 50MHz	Open PTH
			11	HF SMT f(-3dB)	
			12	HF SMT f(-40dB)	
046-2	2	LR	10	HF SMT 50MHz	Open PTH
			11	HF SMT f(-3dB)	
			12	HF SMT f(-40dB)	
046-4	2	LR	12	HF SMT f(-40dB)	Distorted waveform
076-1	1	LR	10	HF SMT 50MHz	High resistance
			11	HF SMT f(-3dB)	
			12	HF SMT f(-40dB)	
076-2	1	LR	1	HCLV PTH	
079-4	1	WS	12	HF SMT f(-40dB)	Waveform does not go to -40dB

080-4	1	WS	12	HF SMT f(-40dB)	
083-2	1	WS	7	HF PTH 50MHz	Open PTH
			8	HF PTH f(-3dB)	
			9	HF PTH f(-40dB)	
			11	HF SMT f(-3dB)	
			12	HF SMT f(-40dB)	
096-4	3	WS	7	HF PTH f(-3dB)	Open PTH, distorted waveform
			10	HF SMT 50MHz	
			11	HF SMT f(-3dB)	
			12	HF SMT f(-40dB)	
			13	HF TLC 50MHz	
098-2	3	WS	12	HF SMT f(-40dB)	
098-3	3	WS	10	HF SMT 50MHz	Open PTH
			11	HF SMT f(-3dB)	
			12	HF SMT f(-40dB)	
098-4	3	WS	10	HF SMT 50MHz	Open PTH
			11	HF SMT f(-3dB)	Waveform shifted
			12	HF SMT f(-40dB)	
099-1	3	WS	12	HF SMT f(-40dB)	Distorted waveform
099-4	3	WS	12	HF SMT f(-40dB)	Distorted waveform
100-3	3	WS	12	HF SMT f(-40dB)	Distorted waveform
OSP					
006-4	6	LR	12	HF SMT f(-40dB)	Distorted waveform
007-3	6	LR	12	HF SMT f(-40dB)	
009-2	6	LR	10	HF SMT 50MHz	Open PTH
			11	HF SMT f(-3dB)	
			12	HF SMT f(-40dB)	
010-1	4	LR	1	HCLV PTH	Distorted waveform
			12	HF SMT f(-40dB)	
010-2	4	LR	12	HF SMT f(-40dB)	
010-4	4	LR	14	HF TLC 500MHz	
014-1	5	LR	10	HF SMT 50MHz	Open etch
			11	HF SMT f(-3dB)	
			12	HF SMT f(-40dB)	
014-3	5	LR	1	HCLV PTH	Open PTH
056-1	5	LR	12	HF SMT f(-40dB)	Waveform does not go to -40 at the correct frequency
056-2	5	LR	1	HCLV PTH	Open PTH
			7	HF PTH 50MHz	
			8	HF PTH f(-3dB)	
			9	HF SMT 50MHz	
			10	HF SMT f(-3dB)	
			12	HF SMT f(-40dB)	
056-3	5	LR	12	HF SMT f(-40dB)	Waveform shifted
056-4	5	LR	7	HF PTH 50MHz	Open PTH - 2 places
			8	HF PTH f(-3dB)	
			9	HF PTH f(-40dB)	
			10	HF SMT 50MHz	
			11	HF SMT f(-3dB)	
			12	HF SMT f(-40dB)	
057-1	5	WS	12	HF SMT f(-40dB)	Waveform does not go to -40dB
058-1	5	WS	10	HF SMT 50MHz	Open PTH
			11	HF SMT f(-3dB)	
			12	HF SMT f(-40dB)	
060-1	5	WS	12	HF SMT f(-40dB)	Distorted waveform
060-2	5	WS	7	HF SMT 50MHz	Open PTH
			9	HF SMT f(-40dB)	
060-4	5	WS	12	HF SMT f(-40dB)	Distorted waveform
061-4	4	WS	12	HF SMT f(-40dB)	

062-1	4	WS	12	HF SMT f(-40dB)	Distorted waveform
062-4	4	WS	12	HF SMT f(-40dB)	Waveform shifted
065-1	4	WS	12	HF SMT f(-40dB)	High resistance
065-4	4	WS	12	HF SMT f(-40dB)	
Immersion Sn					
026-4	9	LR	5	HSD PTH	Bad HSD PTH device
028-2	9	LR	10	HF SMT 50MHz	Open etch
			11	HF SMT f(-3dB)	
			12	HF SMT f(-40dB)	
029-1	9	LR	1	HCLV PTH	
029-2	9	LR	17	HF TLC RNR	
030-4	9	LR	9	HF PTH f(-40dB)	Burnt etch (visual)
032-4	8	LR	7	HF PTH 50MHz	Open PTH
			9	HF PTH f(-40dB)	
033-2	8	LR	17	HF TLC RNR	
037-2	9	LR	5	HSD PTH	Open etch
			10	HF SMT 50MHz	
			11	HF SMT f(-3dB)	
			12	HF SMT f(-40dB)	
040-3	8	LR	9	HF PTH f(-40dB)	Distorted waveform
084-1	7	LR	10	HF SMT 50MHz	Open PTH
			11	HF SMT f(-3dB)	
			12	HF SMT f(-40dB)	
084-2	7	LR	9	HF PTH f(-40dB)	Open PTH
			10	HF SMT 50MHz	
			11	HF SMT f(-3dB)	
			12	HF SMT f(-40dB)	
084-4	7	LR	10	HF SMT 50MHz	Open PTH
			11	HF SMT f(-3dB)	
			12	HF SMT f(-40dB)	
			15	HF TLC 1GHz	
086-2	7	WS	1	HCLV PTH	Distorted waveform
			12	HF SMT f(-40dB)	
087-1	7	WS	12	HF SMT f(-40dB)	
087-3	7	WS	8	HF PTH f(-3dB)	Open PTH 2 places SMT & PTH
			10	HF SMT 50MHz	
			11	HF SMT f(-3dB)	
			12	HF SMT f(-40dB)	
087-4	7	WS	12	HF SMT f(-40dB)	Distorted waveform
088-3	7	LR	10	HF SMT 50MHz	Open PTH
			11	HF SMT f(-3dB)	
			12	HF SMT f(-40dB)	
089-1	7	WS	7	HF PTH 50MHz	Open PTH
			8	HF PTH f(-3dB)	Waveform does not go to -40dB
			9	HF PTH f(-40dB)	
			12	HF SMT f(-40dB)	
089-2	7	WS	10	HF SMT 50MHz	Open PTH
			11	HF SMT f(-3dB)	
			12	HF SMT f(-40dB)	
089-4	7	WS	7	HF PTH 50MHz	Open PTH - 2 places
			8	HF PTH f(-3dB)	
			10	HF SMT 50MHz	
			11	HF SMT f(-3dB)	
			12	HF SMT f(-40dB)	
090-2	7	WS	7	HF PTH 50MHz	Open PTH 2 places SMT & PTH
			8	HF PTH f(-3dB)	
			10	HF SMT 50MHz	
			11	HF SMT f(-3dB)	

			12	HF SMT f(-40dB)	
102-4	10	WS	17	HF TLC RNR	
104-4	10	WS	12	HF SMT f(-40dB)	
113-1	10	WS	10	HF SMT 50MHz	Open PTH
			11	HF SMT f(-3dB)	
			12	HF SMT f(-40dB)	
Immersion Ag					
072-1	11	LR	7	HF PTH 50MHz	Open PTH
			8	HF PTH f(-3dB)	
			9	HF PTH f(-40dB)	
072-2	11	LR	12	HF SMT f(-40dB)	Waveform shifted
072-4	11	LR	12	HF SMT f(-40dB)	Waveform does not go to -40dB
073-3	11	LR	7	HF PTH 50MHz	Open PTH
			8	HF PTH f(-3dB)	
			9	HF PTH f(-40dB)	
075-2	11	LR	12	HF SMT f(-40dB)	
075-3	11	LR	13	HF TLC 50MHz	Distorted waveform
082-2	11	WS	10	HF SMT 50MHz	Open PTH
			12	HF SMT f(-40dB)	
			13	HF TLC 50MHz	
082-3	11	WS	12	HF SMT f(-40dB)	Open PTH, distorted waveform
085-1	12	WS	7	HF PTH 50MHz	Open PTH - 2 places
			8	HF PTH f(-3dB)	
			9	HF PTH f(-40dB)	
			10	HF SMT 50MHz	
			11	HF SMT f(-3dB)	
085-2	12	WS	1	HCLV PTH	Open PTH
			7	HF PTH 50MHz	
			8	HF PTH f(-3dB)	
			9	HF PTH f(-40dB)	
			10	HF SMT 50MHz	
			11	HF SMT f(-3dB)	
			12	HF SMT f(-40dB)	
091-4	12	WS	1	HCLV PTH	Open etch
			10	HF SMT 50MHz	
			11	HF SMT f(-3dB)	
			12	HF SMT f(-40dB)	
094-1	12	WS	7	HF PTH 50MHz	Open PTH - 2 places
			8	HF PTH f(-3dB)	
			9	HF PTH f(-40dB)	
			10	HF SMT 50MHz	
			11	HF SMT f(-3dB)	
			12	HF SMT f(-40dB)	
			13	HF TLC 50MHz	
094-3	12	WS	9	HF PTH f(-40dB)	Waveform distorted
			12	HF SMT f(-40dB)	
			13	HF TLC 50MHz	
			17	HF TLC RNR	
094-4	12	WS	1	HCLV PTH	Open PTH - 2 places
			7	HF PTH 50MHz	
			8	HF PTH f(-3dB)	
			9	HF PTH f(-40dB)	
			10	HF SMT 50MHz	
			11	HF SMT f(-3dB)	
			12	HF SMT f(-40dB)	
			13	HF TLC 50MHz	
095-4	12	WS	1	HCLV PTH	Open etch

Ni/Au					
013-1	13	LR	6	HSD SMT	HSD device fail
015-2	14	LR	7	HF PTH 50MHz	Open etch
			9	HF PTH f(-40dB)	
051-2	13	WS	8	HF PTH f(-3dB)	
054-4	13	WS	8	HF PTH f(-3dB)	
055-1	13	WS	7	HF PTH 50MHz	Open etch
			8	HF PTH f(-3dB)	
			9	HF PTH f(-40dB)	
055-4	13	WS	12	HF SMT f(-40dB)	Waveform distorted
Ni/Pd/Au					
036-2	16	WS	12	HF SMT f(-40dB)	

F.3 HCLV Circuitry

Pre-test measurements and deltas were analyzed with the GLM in Equation F.1 for the main effects site and flux and their interactions. These data were also subjected to a second GLM analysis based on Equation F.2 for the main effects surface finish and flux. The base case for the GLM in Equation F.1 is defined as HASL at Site 1 and processed with LR flux. The base case for the GLM in Equation F.2 is defined as HASL processed with LR flux.

Tables F.4 and F.5 summarize the results of these GLM analyses for HCLV PTH and HCLV SMT. The upper portion of these tables contain the GLM results for Equation F.1 while the lower portion of these tables contain the GLM results for Equation F.2. The rows labeled "Constant" in these tables contain the least squares estimates of β_0 in Equations F.1 and F.2 for each test time. The numbers in the columns beneath the "Constants" are the estimated coefficients of the terms in Equations F.1 and F.2 that are *significantly different* from the base case. Shaded cells signify that the corresponding term in the GLM is not significantly different from the base case.

The rows labeled Model R^2 in Tables F.4 and F.5 show the percent of variation in the voltage measurements explained by the respective estimated model. This value can range from 0% to 100%. The model R^2s for Equations F.1 and F.2 for the HCLV circuitry are summarized as follows for each test time.

GLM	Circuit	Pre-test	85/85	TS	MS
Site and Flux	HCLV PTH	2.0%	2.3%	3.7%	19.1%
	HCLV SMT	4.2%	7.7%	10.9%	2.1%
Surface Finish and Flux	HCLV PTH	0.7%	1.3%	1.7%	7.7%
	HCLV SMT	1.5%	0.3%	9.8%	0.7%

High R^2 values would indicate a strong cause and effect relationship between the parameters of surface finish, site, flux, and the voltage measurements at pretest. However, these R^2s are all quite small, which indicates that the experimental parameters: surface finish, site, and flux do not significantly affect the HCLV voltage measurements at Pre-test nor do they affect the changes in the voltage after exposure to each of the three test environments. That is, the HCLV measurements are robust with respect to surface finish, site, and flux. The results for the two GLMs used in the analysis are now examined in more detail.

GLM Results for Site and Flux

The uppermost portion of Table F.4 for HCLV PTH shows that only two experimental factors (Site 2 and Site 8) are significantly different from the base case for the GLM in Equation F.1. The

estimated GLM at Pre-test for Equation F.1 is obtained from the estimated coefficients in the second column of Table F.4 as:

$$Y = 7.14 + 0.06\ \text{Site2} + 0.07\ \text{Site 8}$$

where Y represents the voltage response. The predicted voltage from this estimated model is 7.14V for all site and flux combinations except Sites 2 and 8. The predictions for these two sites are 7.14V + 0.06V = 7.20V and 7.14V + 0.07V = 7.21V, respectively. Note that even though these two terms are *statistically significant*, they represent very small changes from the base case voltage and, as such, are not of practical interest. Moreover, the model R^2 is only 2.0%, which has no practical value. Similar comments hold for the GLM analyses at Pre-test for HCLV SMT.

Columns 3 to 5 in Tables F.4 and F.5 give the HCLV PTH and HCLV SMT GLM results for Delta 1, 2, and 3, respectively. Note that these latter three analyses are based on changes in the voltage measurements from Pre-test. The model R^2 values after 85/85 and TS are also quite small, which implies that the experimental parameters did not influence the HCLV measurements after exposure to the 85/85, TS, and MS test environments.

In spite of the lack of significant experimental parameters in the HCLV GLMs, there is one very interesting aspect of the model for HCLV SMT at Post MS. Note that the estimate of the constant term in the last column of Table F.5 is 2.48, whereas, the estimated constants at Post 85/85 and Post TS were 0.04 and 0.05, respectively. This is an increase of approximately 2.43V. The explanation of this increase requires a review of the HCLV circuit, which is given in Section F.10. In particular, Section F.10 explains that the HCLV circuit has seven 10Ω resistors, R_1, R_2, ..., R_7 in parallel. The overall circuit resistance, R_{total}, is the parallel combination of these seven resistors, which is given as:

$$\frac{1}{R_{total}} = \frac{1}{R_1} + \frac{1}{R_2} + \frac{1}{R_2} + \cdots + \frac{1}{R_7} = \frac{7}{10\Omega} \tag{F.3}$$

$$R_{total} = \frac{10\Omega}{7} \tag{F.4}$$

Since a current (I) of 5A was applied to the circuit, Ohm's Law gives the resulting voltage (V) as

$$V = IR = 5A \times \frac{10\Omega}{7} = 7.14V \tag{F.5}$$

During the MS test, it was noted that one to three of the resistors frequently fell off the board. In fact, 158 of the 164 PWAs were missing at least one of these resistors. If a single resistor is missing, Equation F.5 would be revised as follows:

$$V = IR = 5A \times \frac{10\Omega}{6} = 8.33V \tag{F.6}$$

Likewise, two missing resistors increase the voltage to 10V. Next consider the following dotplot of voltage measurements at Post MS.

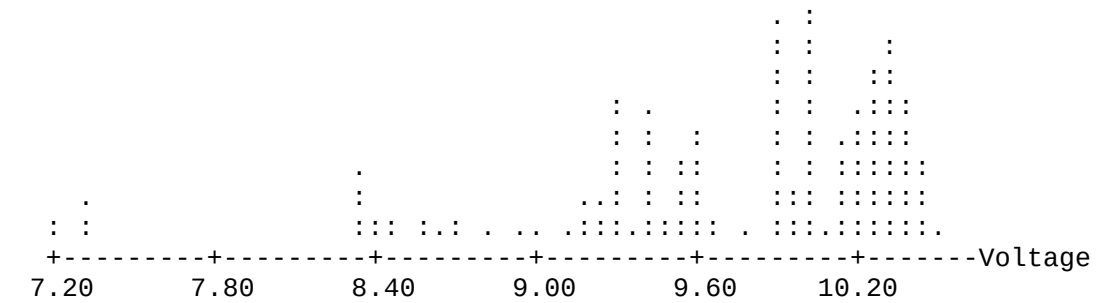

Note how the voltages are lumped around the points at 7.14V, 8.33V, and 10V, which corresponds to the loss of no, one, or two resistors. Thus, the constant term in the GLM represents an average increase in voltage of 2.48V over the nominal expected value of 7.14V, which is between one and two missing resistors.

GLM Results for Surface Finish and Flux

The lower portion of Table F.4 for HCLV PTH shows that only one experimental factor (Ni/Pd/Au) is significantly from the base case at Pre-test for the GLM in Equation F.2. The estimated model is:

$$Y = 7.15 - 0.04 \text{ Ni/Pd/Au}$$

where Y represents the voltage response. The predicted voltage from this estimated model is 7.15V for all surface finish and flux combinations except for Ni/Pd/Au processed with either flux, in which case the prediction is decreased by 0.04V or 7.15V - 0.04V = 7.11V. As was just discussed with the previous GLM, even though the coefficient for Ni/Pd/Au is statistically significant, it actually represents a very small change from the base case and, as such, is not of practical interest. Moreover, the model R^2 is only 0.7%, which has no practical value. Similar comments hold for the GLM analyses at Pre-test for HCLV SMT.

These low R^2 values imply that the experimental parameters do not differ significantly from the base case in terms of their impact on the voltage of the HCLV PTH and HCLV SMT circuits. That is, there is no practical difference from the base case voltage measurements due to surface finish or flux type. This result is to be expected since there were no difference among sites for these circuits in the GLM analysis based on Equation F.1.

Columns 3 to 5 in Tables F.4 and F.5 give the HCLV PTH and HCLV SMT GLM results for Delta 1, 2, and 3, respectively. The model R^2 values at Post 85/85, Post TS, and Post MS are also quite small, which implies that the experimental parameters did not influence the HCLV measurements after exposure to the 85/85 and TS test environments. However, as just explained for the Site and Flux model, the constant term in the last column of Table F.5 is affected by the missing resistors.

Table F.4 Significant Coefficients for the Two GLM Analyses by Test Time for HCLV PTH

GLM from Eq. F.1: Sites and Interactions with Flux

Experimental Factor	Pre-Test	85/85 (Delta 1)	Thermal Shock (Delta 2)	Mech Shock (Delta 3)
Constant	7.14	0.04	0.05	0.14
Flux				
Site 2	0.06		-0.17	
Site 3				
Site 4				
Site 5				
Site 6				
Site 7				
Site 8	0.07			
Site 9				
Site 10				
Site 11		0.13		
Site 12				0.80
Site 13				
Site 14				
Site 15				
Site 16				
Site 4 * Flux				
Site 5 * Flux				
Site 7 * Flux				
Site 11 * Flux		-0.16		
Site 13 * Flux				
Site 16 * Flux				
Model R^2	2.0%	2.3%	3.7%	19.1%
Standard Deviation	0.13	0.18	0.17	0.36

GLM from Eq. F.2: Surface Finishes and Flux

Experimental Factor	Pre-Test	85/85 (Delta 1)	Thermal Shock (Delta 2)	Mech Shock (Delta 3)
Constant	7.15	0.03	0.04	0.13
OSP				
Immersion Sn				
Immersion Ag		0.07	0.07	0.34
Ni/Au				
Ni/Pd/Au	-0.04			
Flux				
Model R^2	0.7%	1.3%	1.7%	7.7%
Standard Deviation	0.10	0.10	0.17	0.38

Table F.5 Significant Coefficients for the Two GLM Analyses by Test Time for HCLV SMT

GLM from Eq. F.1: Sites and Interactions with Flux

Experimental Factor	**Pre-Test**	**85/85 (Delta 1)**	**Thermal Shock (Delta 2)**	**Mech Shock (Delta 3)**
Constant	7.26	0.04	0.05	2.48
Flux				
Site 2				-0.48
Site 3				
Site 4				
Site 5			-0.10	
Site 6				
Site 7				
Site 8	0.06	-0.09		
Site 9				
Site 10	-0.07		0.11	
Site 11				
Site 12				
Site 13				
Site 14				
Site 15				
Site 16				
Site 4 * Flux				
Site 5 * Flux		-0.14		
Site 7 * Flux				
Site 11 * Flux				
Site 13 * Flux			-0.11	
Site 16 * Flux				
Model R^2	4.2%	7.7%	10.9%	2.1%
Standard Deviation	0.09	0.12	0.13	0.70

GLM from Eq. F.2: Surface Finishes and Flux

Experimental **Factor**	**Pre-Test**	**85/85 (Delta 1)**	**Thermal Shock (Delta 2)**	**Mech Shock (Delta 3)**
Constant	7.26	0.03	0.07	2.49
OSP			-0.08	
Immersion Sn				-0.15
Immersion Ag		-0.02		
Ni/Au			-0.10	
Ni/Pd/Au				
Flux	-0.02			
Model R^2	1.5%	0.3%	9.8%	0.7%
Standard Deviation	0.09	0.1	0.13	0.70

F.4 HVLC Circuitry

Results of the GLM analyses for HVLC PTH and HVLC SMT circuits are given in Tables F.6 and F.7, respectively. Columns 3 to 5 in these tables give the GLM results for 85/85, TS, and MS, respectively. The model R^2s for Equations F.1 and F.2 for the HVLC circuitry are summarized as follows for each test time.

GLM	Circuit	Pre-test	85/85	TS	MS
Site and Flux	HVLC PTH	13.3%	5.2%	0.0%	3.2%
	HVLC SMT	20.9%	14.0%	18.7%	NA
Surface Finish and Flux	HVLC PTH	7.6%	2.5%	2.6%	3.2%
	HVLC SMT	14.0%	15.3%	12.9%	NA

These model R^2 values are generally higher that those observed for the HCLV measurements. However, the magnitudes of the coefficients were too small to be of practical significance relative to the JTP acceptance criteria, which indicates that these parameters do not influence the HVLC measurements. To further explain this point, consider the coefficients for site and flux in Table F.6 at Pre-test where the constant term is 5.018μA. The largest coefficient at Pre-test is -0.008μA for the interaction of Site 4 and Flux. Thus, this interaction can decrease the constant term to 5.018μA - 0.008μA = 5.010μA, which is so far from the lower and upper limits of 4μA and 6μA that it is not of practical interest. Note that there are no R^2 values listed for HVLC SMT at Post MS. This is due to resistors coming off the PWA during the MS test, which caused the HVLC SMT circuit to give a constant response for reasons that will now be explained.

Boxplot Displays of Multiple Comparison Results

Figures F.1 to F.8 give boxplots for the HVLC PTH and SMT circuits. It is important to keep the vertical scale in mind relative to the acceptance criteria when viewing these boxplots. That is, the acceptance criteria indicates that the current should be between 4μA and 6μA. These boxplots are centered close to 5μA and the total spread is on the order of 0.02μA for the PTH circuits and approximately 0.5μA for SMT circuits. Hence, even though there are some statistically significantly differences, they are not likely to be of practical concern. Note the boxplots in Figure F.8 for HCLV SMT at Post MS. These values are all either 0μA for very close to it, reflecting the fact that the resistors came off the PWA during the MS test.

Table F.6 Significant Coefficients for the Two GLM Analyses by Test Time for HVLC PTH

GLM from Eq. F.1: Sites and Interactions with Flux

Experimental Factor	Pre-Test	85/85	Thermal Shock	Mech Shock
Constant	**5.018**	**5.004**	**4.999**	**4.998**
Flux				
Site 2				
Site 3				
Site 4	0.007			
Site 5				
Site 6				
Site 7				
Site 8	0.005			
Site 9	0.004			
Site 10				
Site 11				
Site 12	0.004	0.006		
Site 13				
Site 14				-0.005
Site 15				
Site 16				
Site 4 * Flux	-0.008			
Site 5 * Flux				
Site 7 * Flux				
Site 11 * Flux		0.006		
Site 13 * Flux				
Site 16 * Flux				
Model R^2	13.3%	5.2%	0.0%	3.2%
Standard Deviation	0.005	0.006	0.006	0.006

GLM from Eq. F.2: Surface Finishes and Flux

Experimental Factor	Pre-Test	85/85	Thermal Shock	Mech Shock
Constant	5.018	5.004	4.998	4.998
OSP				
Immersion Sn	0.003		0.002	
Immersion Ag	0.003	0.003		
Ni/Au				-0.003
Ni/Pd/Au				
Flux				
Model R^2	7.6%	2.5%	2.6%	3.2%
Standard Deviation	0.005	0.006	0.006	0.006

Table F.7 Significant Coefficients for the Two GLM Analyses by Test Time for HVLC SMT

GLM from Eq. F.1: Sites and Interactions with Flux

Experimental Factor	Pre-Test	85/85	Thermal Shock	Mech Shock
Constant	5.038	5.034	5.039	
Flux				
Site 2				
Site 3				
Site 4				
Site 5				
Site 6				
Site 7				
Site 8	0.172	0.173	0.170	
Site 9				
Site 10	0.111	0.111	0.109	
Site 11				
Site 12	0.122	0.125	0.120	
Site 13				
Site 14				
Site 15	0.125	0.126	0.125	
Site 16				
Site 4 * Flux				
Site 5 * Flux				
Site 7 * Flux				
Site 11 * Flux				
Site 13 * Flux				
Site 16 * Flux				
Model R^2	20.9%	21.5%	18.7%	
Standard Deviation	0.100	0.100	0.112	

GLM from Eq. F.2: Surface Finishes and Flux

Experimental Factor	Pre-Test	85/85	Thermal Shock	Mech Shock
Constant	5.032	5.027	5.033	
OSP				
Immersion Sn	0.095	0.100	0.097	
Immersion Ag	0.087	0.090	0.085	
Ni/Au				
Ni/Pd/Au				
Flux				
Model R^2	14.0%	15.3%	12.9%	
Standard Deviation	0.100	0.100	0.110	

F.5 HSD Circuitry

The complete results of the GLM analyses are given in Tables F.8 and F.9, respectively. Columns 3 to 5 in these tables give the GLM results for 85/85, TS, and MS, respectively. Note that these latter three analyses are based on changes in total propagation delay from Pre-test. The model R^2s for Equations F.1 and F.2 for the HSD circuitry are summarized as follows for each test time.

GLM	Circuit	Pre-test	85/85	TS	MS
Site and Flux	HSD PTH	5.1%	9.8%	4.3%	9.5%
	HSD SMT	6.1%	6.4%	0.0%	2.3%
Surface Finish and Flux	HSD PTH	0.9%	1.6%	1.8%	6.7%
	HSD SMT	1.0%	0.3%	0.8%	0.2%

All these model R^2 values are quite small at each test time, which indicates that the experimental parameters under evaluation do not influence the HSD total propagation delay measurements.

Boxplot Displays of Multiple Comparison Results

Figures F.9 and F.10 give boxplots of Pre-test measurements of total propagation delay for the HSD PTH and HSD SMT circuits, respectively. Note that most total propagation delays in Figure F.9 for HSD PTH are a little over 17 ns with a range of about 1ns. Figure F.10 shows that the total propagation delays for HSD SMT have a range of about 0.4ns and are centered about 9.2ns. The percentage changes in the total propagation delay measurements were small and well within the acceptance criteria so boxplot displays of these measurements are not presented.

Table F.8 Significant Coefficients for the Two GLM Analyses by Test Time for HSD PTH

GLM from Eq. F.1: Sites and Interactions with Flux

Experimental Factor	Pre-Test	85/85 (Delta 1)	Thermal Shock (Delta 2)	Mech Shock (Delta 3)
Constant	17.13	0.55	0.98	0.37
Flux			-0.46	
Site 2				
Site 3				2.60
Site 4	0.14			
Site 5		0.61		
Site 6			-1.00	
Site 7				
Site 8				
Site 9		1.89		
Site 10				
Site 11				-2.30
Site 12				-3.50
Site 13				
Site 14				
Site 15				
Site 16				
Site 4 * Flux				
Site 5 * Flux				
Site 7 * Flux				
Site 11 * Flux				
Site 13 * Flux				
Site 16 * Flux	0.19			
Model R^2	5.1%	9.8%	4.3%	9.5%
Standard Deviation	0.19	1.30	1.33	3.52

GLM from Eq. F.2: Surface Finishes and Flux

Experimental Factor	Pre-Test	85/85 (Delta 1)	Thermal Shock (Delta 2)	Mech Shock (Delta 3)
Constant	17.13	0.88	0.88	0.52
OSP	0.05			
Immersion Sn				
Immersion Ag				-2.89
Ni/Au				
Ni/Pd/Au				
Flux		-0.35	-0.36	
Model R^2	0.9%	1.6%	1.8%	6.7%
Standard Deviation	0.20	1.00	1.30	3.5

Table F.9 Significant Coefficients for the Two GLM Analyses by Test Time for HSD SMT

GLM from Eq. F.1: Sites and Interactions with Flux

Experimental Factor	Pre-Test	85/85 (Delta 1)	Thermal Shock (Delta 2)	Mech Shock (Delta 3)
Constant	9.23	0.94	1.16	-0.002
Flux				
Site 2		-1.59		
Site 3				
Site 4				
Site 5				
Site 6				
Site 7				
Site 8				-1.60
Site 9				
Site 10				
Site 11				
Site 12		-1.27		
Site 13				
Site 14				
Site 15	0.12			
Site 16				
Site 4 * Flux				
Site 5 * Flux	-0.10			
Site 7 * Flux				
Site 11 * Flux				
Site 13 * Flux				
Site 16 * Flux				
Model R^2	6.1%	6.4%	0.0%	2.3%
Standard Deviation	0.13	1.65	1.99	2.25

GLM from Eq. F.2: Surface Finishes and Flux

Experimental Factor	Pre-Test	85/85 (Delta 1)	Thermal Shock (Delta 2)	Mech Shock (Delta 3)
Constant	9.21	0.77	1.23	-0.04
OSP				
Immersion Sn				
Immersion Ag			-0.56	
Ni/Au				-0.25
Ni/Pd/Au		0.35		
Flux	0.03			
Model R^2	1.0%	0.3%	0.8%	0.2%
Standard Deviation	0.10	1.00	1.90	2.2

F.6 HF LPF Circuitry

Pre-test measurements for all HF LPF circuits were subjected to GLM analyses, as were the deltas after 85/85, TS, and MS. The results of the GLM analyses are given in Tables F.10 to F.15. Columns 3 to 5 in these tables give the GLM results for 85/85, TS, and MS, respectively.

Note that these latter three analyses are based on changes from Pre-test measurements. The model R^2s for Equations F.1 and F.2 for the HF LPF circuitry are summarized as follows for each test time.

GLM	Circuit	Pre-test	85/85	TS	MS
Site and Flux	PTH 50MHz	20.6%	29.5%	24.1%	20.5%
	PTH f(-3dB)	7.1%	10.8%	10.2%	23.4%
	PTH f(-40dB)	14.3%	9.6%	7.6%	13.5%
	SMT 50MHz	3.9%	10.3%	21.1%	32.2%
	SMT f(-3dB)	8.8%	10.5%	19.1%	14.3%
	SMT f(-40dB)	5.3%	2.3%	16.1%	29.4%
Surface Finish and Flux	PTH 50MHz	4.3%	2.3%	0.3%	8.1%
	PTH f(-3dB)	7.8%	0.2%	1.6%	10.9%
	PTH f(-40dB)	4.5%	1.8%	1.6%	10.9%
	SMT 50MHz	2.7%	0.6%	0.8%	6.1%
	SMT f(-3dB)	0.7%	1.5%	5.0%	3.0%
	SMT f(-40dB)	5.2%	0.3%	4.9%	14.4%

The model R^2 values are quite small at Pre-test, which indicates that the parameters under evaluation do not influence the HF LPF measurements. The same is true at Post 85/85. The model R^2 values are also quite small at Post TS and Post MS. However, the test measurements contained many extreme outlying observations at both of these later two test times, which greatly increases the sample variance and in turn hinders the interpretation of the GLM results. As indicated in Tables F.1, F.2, and F.3 there were many anomalous HF LPF test measurements (171 at Post MS).

Boxplot Displays of Multiple Comparison Results

Boxplot displays of all test results for HF LPF circuits have been created to aid in the interpretation of the results. Figures 4.9 to 4.15 in Chapter 4 show the boxplots for the analyses with significant differences or values not meeting acceptance criteria. Figures F.11 to F.27 show all remaining boxplots associated with the HF LPF results.

Table F.10 Significant Coefficients for the Two GLM Analyses by Test Time for HF PTH 50 MHz

GLM from Eq. F.1: Sites and Interactions with Flux

Experimental Factor	Pre-Test	85/85 (Delta 1)	Thermal Shock (Delta 2)	Mech Shock (Delta 3)
Constant	-0.721	-0.034	-0.002	-2.666
Flux				
Site 2				
Site 3				
Site 4				
Site 5				
Site 6				
Site 7				
Site 8				
Site 9				
Site 10				
Site 11				
Site 12				-28.1
Site 13	-0.180	0.197	0.192	
Site 14			-0.073	
Site 15				
Site 16				
Site 4 * Flux				
Site 5 * Flux				
Site 7 * Flux				-18.5
Site 11 * Flux				
Site 13 * Flux	0.160	-0.206	-0.180	
Site 16 * Flux				
Model R^2	20.6%	29.5%	24.1%	20.5%
Standard Deviation	0.055	0.048	0.063	14.1

GLM from Eq. F.2: Surface Finishes and Flux

Experimental Factor	Pre-Test	85/85 (Delta 1)	Thermal Shock (Delta 2)	Mech Shock (Delta 3)
Constant	-0.720	-0.034	0.003	-3.28
OSP			-0.010	
Immersion Sn				
Immersion Ag				-13.6
Ni/Au	-0.034	0.023		
Ni/Pd/Au				
Flux				
Model R^2	4.3%	2.3%	0.3%	8.1%
Standard Deviation	0.060	0.050	0.072	15.00

Table F.11 Significant Coefficients for the Two GLM Analyses by Test Time for HF PTH f(-3dB)

GLM from Eq. F.1: Sites and Interactions with Flux

Experimental Factor	Pre-Test	85/85 (Delta 1)	Thermal Shock (Delta 2)	Mech Shock (Delta 3)
Constant	283.0	-0.9	0.5	-1.05
Flux				
Site 2				
Site 3				
Site 4				
Site 5				
Site 6			-2.2	
Site 7				
Site 8				
Site 9				
Site 10				
Site 11				
Site 12				-116
Site 13	-1.8			
Site 14				
Site 15	-1.5			
Site 16				
Site 4 * Flux				
Site 5 * Flux		0.7		
Site 7 * Flux		-1.2		-68
Site 11 * Flux				
Site 13 * Flux				-79
Site 16 * Flux				
Model R^2	7.1%	10.8%	10.2%	23.4%
Standard Deviation	2.0	0.9	1.5	58.5

GLM from Eq. F.2: Surface Finishes and Flux

Experimental Factor	Pre-Test	85/85 (Delta 1)	Thermal Shock (Delta 2)	Mech Shock (Delta 3)
Constant	283.0	-1.0	0.5	4.19
OSP		0.1	-0.5	
Immersion Sn				
Immersion Ag				-53.0
Ni/Au	-1.6			
Ni/Pd/Au				
Flux				-23.8
Model R^2	7.8%	0.2%	1.6%	10.9%
Standard Deviation	2.0	0.9	1.5	62.0

Table F.12 Significant Coefficients for the Two GLM Analyses by Test Time for HF PTH f(-40dB)

GLM from Eq. F.1: Sites and Interactions with Flux

Experimental Factor	Pre-Test	85/85 (Delta 1)	Thermal Shock (Delta 2)	Mech Shock (Delta 3)
Constant	472.9	-0.2	-0.2	-11.7
Flux				
Site 2				
Site 3				
Site 4				
Site 5	-3.8		-1.8	
Site 6		0.9		
Site 7				
Site 8		-1.5		
Site 9	-5.7			
Site 10				
Site 11				
Site 12				-140
Site 13	-5.1			
Site 14				
Site 15	-4.5			
Site 16				
Site 4 * Flux				
Site 5 * Flux			2.6	
Site 7 * Flux				
Site 11 * Flux				
Site 13 * Flux				
Site 16 * Flux				
Model R^2	14.3%	9.6%	7.6%	13.5%
Standard Deviation	5.1	1.2	1.5	77.1

GLM from Eq. F.2: Surface Finishes and Flux

Experimental Factor	Pre-Test	85/85 (Delta 1)	Thermal Shock (Delta 2)	Mech Shock (Delta 3)
Constant	472.2	-0.1	-0.3	-8.41
OSP				
Immersion Sn		-0.4		
Immersion Ag				-83.0
Ni/Au	-3.2			
Ni/Pd/Au			0.71	
Flux				
Model R^2	4.5%	1.8%	1.6%	10.9%
Standard Deviation	5.0	1.0	1.5	78.0

Table F.13 Significant Coefficients for the Two GLM Analyses by Test Time for HF SMT 50 MHz

GLM from Eq. F.1: Sites and Interactions with Flux

Experimental Factor	Pre-Test	85/85 (Delta 1)	Thermal Shock (Delta 2)	Mech Shock (Delta 3)
Constant	-0.733	-0.018	0.005	-3.1
Flux				
Site 2				
Site 3			-0.112	-19.2
Site 4				
Site 5				-13.5
Site 6				
Site 7			-0.126	-49.7
Site 8				
Site 9		-0.049		
Site 10				
Site 11				
Site 12	0.031			-31.4
Site 13				
Site 14				
Site 15				
Site 16				
Site 4 * Flux	0.021			
Site 5 * Flux				
Site 7 * Flux				25.0
Site 11 * Flux		-0.047		
Site 13 * Flux				
Site 16 * Flux				
Model R^2	3.9%	10.3%	21.1%	32.2%
Standard Deviation	0.039	0.037	0.069	17.2

GLM from Eq. F.2: Surface Finishes and Flux

Experimental Factor	Pre-Test	85/85 (Delta 1)	Thermal Shock (Delta 2)	Mech Shock (Delta 3)
Constant	-0.733	-0.023	-0.010	-5.62
OSP			0.017	
Immersion Sn				-10.6
Immersion Ag	0.020			-10.7
Ni/Au		0.008		
Ni/Pd/Au				
Flux				
Model R^2	2.7%	0.6%	0.8%	6.1%
Standard Deviation	0.030	0.030	0.077	20.0

Table F.14 Significant Coefficients for the Two GLM Analyses by Test Time for HF SMT f(-3dB)

GLM from Eq. F.1: Sites and Interactions with Flux

Experimental Factor	Pre-Test	85/85 (Delta 1)	Thermal Shock (Delta 2)	Mech Shock (Delta 3)
Constant	319.8	-1.3	0.7	-15.5
Flux				
Site 2		1.0		108
Site 3				
Site 4				
Site 5				
Site 6				
Site 7			-15.3	
Site 8				
Site 9			-4.0	
Site 10				
Site 11		1.5		
Site 12				-143
Site 13	3.7			
Site 14			-3.9	
Site 15				
Site 16				
Site 4 * Flux				
Site 5 * Flux			-3.7	
Site 7 * Flux			11.9	-102
Site 11 * Flux		-2.2		
Site 13 * Flux	-4.4			
Site 16 * Flux				
Model R^2	8.8%	10.5%	19.1%	14.3%
Standard Deviation	1.9	1.1	4.7	112

GLM from Eq. F.2: Surface Finishes and Flux

Experimental Factor	Pre-Test	85/85 (Delta 1)	Thermal Shock (Delta 2)	Mech Shock (Delta 3)
Constant	319.7	-1.3	0.4	-1.98
OSP	0.4			
Immersion Sn			-2.8	
Immersion Ag		0.5		
Ni/Au				
Ni/Pd/Au				
Flux				-41.0
Model R^2	0.7%	1.5%	5.0%	3.0%
Standard Deviation	2.0	1.0	5.0	11.0

Table F.15 Significant Coefficients for the Two GLM Analyses by Test Time for HF SMT f(-40dB)

GLM from Eq. F.1: Sites and Interactions with Flux

Experimental Factor	Pre-Test	85/85 (Delta 1)	Thermal Shock (Delta 2)	Mech Shock (Delta 3)
Constant	865.5	1.7	-8.1	-80.3
Flux				
Site 2				
Site 3				-244
Site 4				
Site 5	-10.7			-171
Site 6				
Site 7				-430
Site 8		4.9		
Site 9				
Site 10				
Site 11		2.2		
Site 12	-19.7			-365
Site 13				
Site 14				
Site 15				
Site 16				
Site 4 * Flux				
Site 5 * Flux				
Site 7 * Flux				
Site 11 * Flux			-23.7	
Site 13 * Flux				
Site 16 * Flux				
Model R^2	5.3%	2.3%	16.1%	29.4%
Standard Deviation	21.0	7.6	9.1	221

GLM from Eq. F.2: Surface Finishes and Flux

Experimental Factor	Pre-Test	85/85 (Delta 1)	Thermal Shock (Delta 2)	Mech Shock (Delta 3)
Constant	861.2	2.0	-6.8	-146.2
OSP				
Immersion Sn				
Immersion Ag				
Ni/Au	13.4	1.0		192.0
Ni/Pd/Au				171.0
Flux			-4.4	-117.0
Model R^2	5.2%	0.3%	4.9%	14.4%
Standard Deviation	21.0	7.0	9.7	24.0

F.7 HF TLC Circuitry

Pre-test measurements for all HF TLC circuits except RNF were subjected to GLM analyses, as were the deltas after 85/85, TS, and MS. The results of the GLM analyses are given in Tables F.16 to F.20. Columns 3 to 5 in those tables give the HF TLC PTH and HF TLC SMT GLM results for 85/85, TS, and MS, respectively. Note that these latter three analyses are based on changes from Pre-test measurements. The model R^2s for Equations F.1 and F.2 for the HF TLC circuitry are summarized as follows for each test time, except for HF TLC RNF, which gave a constant response.

GLM	Circuit	Pre-test	85/85	TS	MS
Site and Flux	50MHz	62.3%	6.7%	0.0%	14.7%
	500MHz	10.7%	8.1%	0.0%	8.1%
	1GHz	13.2%	10.9%	6.1%	7.9%
	RNF				
	RNR	2.7%	8.2%	2.4%	6.2%
Surface Finish and Flux	50MHz	48.1%	6.6%	5.0%	9.1%
	500MHz	2.5%	0.9%	1.8%	1.4%
	1GHz	0.9%	2,8%	4.1%	0.7%
	RNF				
	RNR	3.6%	0.6%	3.5%	2.0%

The model R^2 values for HF TLC are all quite small at Pre-test except for those at 50MHz, which are of moderate size. The small R^2 values indicate that the experimental parameters do not influence the Pre-test HF TLC measurements. The moderate sized R^2 values for the 50MHz case are examined in further detail below (repeated from Chapter 4).

The predicted response at Pre-test for HF TLC 50MHz for the base case (HASL at Site 1 processed with LR flux) based on the Site & Flux GLM was -47.43dB. The predicted differences from the base case are given in Appendix F in Table F.21. The results show that the sites that produced Ni/Au and Ni/Au/Pd (#13-16) have predicted increases of less than 3dB. While statistically significant, this change is rather small compared to the base case value and is probably not of practical utility. Overall, some of the sites differ from the base case by approximately –1.5dB to 2.9dB. These changes again may not have any practical significance since the important concept is not so much the magnitude of the response, but rather its stability when subject to environmental stress conditions, which is the basis for the acceptance criteria.

The predicted response at Pre-test for HF TLC 50MHz for the base case (HASL processed with LR flux) based on the Surface Finish & Flux GLM was -46.73dB, which is almost identical to that for the Site & Flux GLM. The predicted differences from the base case are given in Appendix F in Table F.22. These predictions are consistent with those in Table F.21 and show that immersion Sn and immersion Ag are approximately 1.0dB lower than the base case and Ni/Au and Ni/Pd/Au are approximately 1 to 2 dB higher than the base case. Again, these differences are most likely not of practical utility.

Boxplot Displays of Multiple Comparison Results

HF TLC 50MHz. A boxplot display of the Post MS test results is given in Figure 4.16. Boxplots for the other three test times are displayed in Figures F.28 to F.30.

HF TLC 500MHz. A boxplot display of the Post MS test results is given in Figure 4.17. Boxplots for the other three test times are displayed in Figures F.31 to F.33.

HF TLC 1GHz. Boxplots displays for are not given for the HF TLC 1GHz test results to conserve space. The total variation at Pre-test for HF TLC 1GHz was only 2dB and there was only one slight anomaly of -5dB at Post MS, which is not of concern.

HF TLC RNR. A boxplot display of the Post MS test results is given in Figure 4.18. Boxplots for the other three test times are displayed in Figures F.34 to F.36.

Table F.16 Significant Coefficients for the Two GLM Analyses by Test Time for HF TLC 50 MHz Forward

GLM from Eq. F.1: Sites and Interactions with Flux

Experimental Factor	Pre-Test	85/85 (Delta 1)	Thermal Shock (Delta 2)	Mech Shock (Delta 3)
Constant	-47.43	0.22	-0.08	0.04
Flux				
Site 2				
Site 3	0.98			4.40
Site 4				
Site 5	1.19			
Site 6	1.48			
Site 7	-1.51			
Site 8				
Site 9				
Site 10	0.90			
Site 11				3.20
Site 12	-1.40			7.60
Site 13	2.90	-1.17		
Site 14	2.69			
Site 15	2.05			
Site 16	2.19			
Site 4 * Flux		0.96		
Site 5 * Flux	-1.37			
Site 7 * Flux				
Site 11 * Flux				
Site 13 * Flux		1.41		
Site 16 * Flux	-1.50			
Model R^2	62.3%	6.7%	0.0%	14.7%
Standard Deviation	1.00	1.0	1.01	4.80

GLM from Eq. F.2: Surface Finishes and Flux

Experimental Factor	Pre-Test	85/85 (Delta 1)	Thermal Shock (Delta 2)	Mech Shock (Delta 3)
Constant	-46.73	0.09	-0.30	0.29
OSP				
Immersion Sn	-0.71			
Immersion Ag	-0.97			4.7
Ni/Au	2.24	-0.45		
Ni/Pd/Au	1.19			
Flux	-0.59	0.48	0.45	
Model R^2	48.1%	6.6%	5.0%	9.1%
Standard Deviation	1.00	1.00	0.99	4.9

Table F.17 Significant Coefficients for the Two GLM Analyses by Test Time for HF TLC 500 MHz Forward

GLM from Eq. F.1: Sites and Interactions with Flux

Experimental Factor	Pre-Test	85/85 (Delta 1)	Thermal Shock (Delta 2)	Mech Shock (Delta 3)
Constant	-17.48	0.06	-0.23	-0.14
Flux				
Site 2				
Site 3	0.64			
Site 4				-1.32
Site 5	0.45			
Site 6	0.53			
Site 7				
Site 8				
Site 9				
Site 10	0.56			
Site 11				
Site 12				-0.85
Site 13		-1.13		
Site 14				
Site 15				
Site 16				
Site 4 * Flux				1.50
Site 5 * Flux				
Site 7 * Flux				
Site 11 * Flux				
Site 13 * Flux		1.35		
Site 16 * Flux				
Model R^2	10.7%	8.1%	0.0%	8.1%
Standard Deviation	0.66	0.62	0.60	0.93

GLM from Eq. F.2: Surface Finishes and Flux

Experimental Factor	Pre-Test	85/85 (Delta 1)	Thermal Shock (Delta 2)	Mech Shock (Delta 3)
Constant	-17.41	0.02	-0.28	-0.09
OSP	0.27			
Immersion Sn			0.20	
Immersion Ag				
Ni/Au				
Ni/Pd/Au		0.23		
Flux				-0.22
Model R^2	2.5%	0.9%	1.8%	1.4%
Standard Deviation	0.60	0.60	0.59	0.96

Table F.18 Significant Coefficients for the Two GLM Analyses by Test Time for HF TLC 1 GHz Forward

GLM from Eq. F.1: Sites and Interactions with Flux

Experimental Factor	Pre-Test	85/85 (Delta 1)	Thermal Shock (Delta 2)	Mech Shock (Delta 3)
Constant	-14.11	0.11	-0.39	-0.22
Flux	-0.16			
Site 2	-0.30			
Site 3	0.37			
Site 4				
Site 5	0.21			
Site 6				
Site 7				-1.26
Site 8				
Site 9				
Site 10	0.46			
Site 11			-0.51	
Site 12				
Site 13		-0.46		
Site 14				
Site 15		-0.35		
Site 16				
Site 4 * Flux				
Site 5 * Flux				
Site 7 * Flux				1.00
Site 11 * Flux				
Site 13 * Flux		0.59		
Site 16 * Flux				
Model R^2	13.2%	10.9%	6.1%	7.9%
Standard Deviation	0.37	0.31	0.52	0.69

GLM from Eq. F.2: Surface Finishes and Flux

Experimental Factor	Pre-Test	85/85 (Delta 1)	Thermal Shock (Delta 2)	Mech Shock (Delta 3)
Constant	-14.16	0.11	-0.38	-0.30
OSP	0.09			0.14
Immersion Sn				
Immersion Ag			-0.33	
Ni/Au		-0.15		
Ni/Pd/Au				
Flux				
Model R^2	0.9%	2.8%	4.1%	0.7%
Standard Deviation	0.30	0.30	0.52	0.71

Table F.19 Significant Coefficients for the Two GLM Analyses by Test Time for HF TLC Rev Null Freq

GLM from Eq. F.1: Sites and Interactions with Flux

Experimental Factor	Pre-Test	85/85 (Delta 1)	Thermal Shock (Delta 2)	Mech Shock (Delta 3)
Constant				
Flux Site 2 Site 3				
Site 4 Site 5 Site 6				
Site 7 Site 8 Site 9				
Site 10 Site 11 Site 12				
Site 13 Site 14 Site 15				
Site 16 Site 4 * Flux Site 5 * Flux				
Site 7 * Flux Site 11 * Flux Site 13 * Flux Site 16 * Flux				
Model R^2 Standard Deviation				

GLM from Eq. F.2: Surface Finishes and Flux

Experimental Factor	Pre-Test	85/85 (Delta 1)	Thermal Shock (Delta 2)	Mech Shock (Delta 3)
Constant				
OSP Immersion Sn Immersion Ag				
Ni/Au Ni/Pd/Au Flux				
Model R^2 Standard Deviation				

Table F.20 Significant Coefficients for the Two GLM Analyses by Test Time for HF TLC Rev Null Resp

GLM from Eq. F.1: Sites and Interactions with Flux

Experimental Factor	Pre-Test	85/85 (Delta 1)	Thermal Shock (Delta 2)	Mech Shock (Delta 3)
Constant	-33.90	0.20	-0.05	0.02
Flux				
Site 2				
Site 3				
Site 4				
Site 5	1.13			
Site 6				
Site 7				
Site 8				
Site 9				
Site 10				
Site 11				-3.50
Site 12			-1.60	
Site 13		-3.23		
Site 14				
Site 15				
Site 16				
Site 4 * Flux				
Site 5 * Flux	-1.25			
Site 7 * Flux				
Site 11 * Flux				
Site 13 * Flux		3.60		
Site 16 * Flux				
Model R^2	2.7%	8.2%	2.4%	6.2%
Standard Deviation	1.40	1.70	2.20	3.56

GLM from Eq. F.2: Surface Finishes and Flux

Experimental Factor	Pre-Test	85/85 (Delta 1)	Thermal Shock (Delta 2)	Mech Shock (Delta 3)
Constant	-33.70	0.07	0.03	-0.74
OSP				
Immersion Sn	-0.68	0.34		
Immersion Ag			-1.26	
Ni/Au				
Ni/Pd/Au				
Flux				1.03
Model R^2	3.6%	0.6%	3.5%	2.0%
Standard Deviation	1.00	1.00	2.1	3.6

Table F.21 Predicted Changes from the Base Case at Pre-test for HF TLC 50MHz for the GLM in Equation F.1

	LR Flux	WS Flux
Site 2		
Site 3	0.98	0.98
Site 4		
Site 5	1.19	-0.18
Site 6	1.48	1.48
Site 7	-1.51	-1.51
Site 8		
Site 9		
Site 10	0.90	0.90
Site 11		
Site 12	-1.40	-1.40
Site 13	2.90	2.90
Site 14	2.69	2.69
Site 15	2.05	2.05
Site 16	2.19	0.69

Table F.22 Predicted Changes from the Base Case at Pre-test for HF TLC 50MHz for the GLM in Equation F.2

	LR Flux	WS Flux
OSP		-0.59
Immersion Sn	-0.71	-1.30
Immersion Ag	-0.97	-1.56
Ni/Au	2.24	1.65
Ni/Pd/Au	1.19	0.60

F.8 Leakage Measurements

The results of the GLM analyses are given in Tables F.23 to F.26. Columns 3 to 5 in these tables give the GLM results for 85/85, TS, and MS, respectively. The model R^2s for Equations F.1 and F.2 for the GLM analyses of the leakage measurements are summarized as follows.

GLM	Circuit	Pre-test	85/85	TS	MS
Site and Flux	10-Mil Pads	85.6%	22.7%	10.8%	8.6%
	PGA-A	88.4%	3.9%	9.7%	9.0%
	PGA-B	89.4%	5.6%	15.5%	12.5%
	Gull Wing	55.4%	3.3%	2.8%	1.7%
Surface Finish and Flux	10-Mil Pads	74.8%	1.9%	3.4%	1.7%
	PGA-A	81.3%	2.0%	9.7%	6.3%
	PGA-B	88.7%	5.6%	16.0%	6.7%
	Gull Wing	48.2%	1.9%	2.8%	2.6%

It is of interest to note that the model R^2 values at Pre-test for all but the Gull Wing are all quite large. However, these values decrease to close to zero after exposure to the 85/85 environment. These results are now examined in detail for each of the four leakage circuits.

Tables F.27 and F.28 give the predicted changes from their respective base cases for all leakage measurements at Pre-test for the GLMs in Equations F.1 and F.2, respectively.

Table F.23 Significant Coefficients for the Two GLM Analyses by Test Time for 10-Mil Pads

GLM from Eq. F.1: Sites and Interactions with Flux

Experimental Factor	Pre-Test	85/85	Thermal Shock	Mech Shock
Constant	12.20	13.29	14.45	14.76
Flux	0.74			
Site 2	-0.97			
Site 3	1.02			
Site 4	0.93			
Site 5	0.85			
Site 6				
Site 7				
Site 8				
Site 9		-1.24	-0.95	-0.84
Site 10	1.00			
Site 11				
Site 12	0.91			
Site 13	-0.89	0.23		
Site 14	-0.75			
Site 15	0.98		0.55	
Site 16	-0.76			
Site 4 * Flux				
Site 5 * Flux				
Site 7 * Flux	0.85			
Site 11 * Flux	1.06			
Site 13 * Flux	1.95			
Site 16 * Flux	1.74			
Model R^2	85.6%	22.7%	10.8%	8.6%
Standard Deviation	0.42	0.51	0.70	0.59

GLM from Eq. F.2: Surface Finishes and Flux

Experimental Factor	Pre-Test	85/85	Thermal Shock	Mech Shock
Constant	11.75	13.21	14.30	14.69
OSP	0.73			
Immersion Sn	0.33			
Immersion Ag	0.48			
Ni/Au		0.21		
Ni/Pd/Au				0.31
Flux	1.77		0.27	
Model R^2	74.8%	1.9%	3.4%	1.7%
Standard Deviation	0.50	0.50	0.72	0.61

Table F.24 Significant Coefficients for the Two GLM Analyses by Test Time for PGA-A

GLM from Eq. F.1: Sites and Interactions with Flux

Experimental Factor	Pre-Test	85/85	Thermal Shock	Mech Shock
Constant	11.88	12.50	13.66	13.69
Flux	1.58		0.348	0.22
Site 2	-1.19			
Site 3				
Site 4				-0.54
Site 5				
Site 6				
Site 7				
Site 8				
Site 9	-0.81			
Site 10				
Site 11	-0.34			
Site 12				
Site 13	-0.64			
Site 14	-0.94			
Site 15				
Site 16	-1.14			
Site 4 * Flux		-0.50		0.63
Site 5 * Flux				
Site 7 * Flux				
Site 11 * Flux		-0.64		
Site 13 * Flux	0.91			
Site 16 * Flux	1.34			
Model R^2	88.4%	3.9%	9.7%	9.0%
Standard Deviation	0.40	0.71	0.52	0.49

GLM from Eq. F.2: Surface Finishes and Flux

Experimental Factor	Pre-Test	85/85	Thermal Shock	Mech Shock
Constant	11.38	12.41	13.66	13.66
OSP	0.35			
Immersion Sn		0.25		
Immersion Ag				
Ni/Au				
Ni/Pd/Au	-0.35			
Flux	2.05		0.34	0.256
Model R^2	81.3%	2.0%	9.7%	6.3%
Standard Deviation	0.5	0.70	0.51	0.49

Table F.25 Significant Coefficients for the Two GLM Analyses by Test Time for PGA-B

GLM from Eq. F.1: Sites and Interactions with Flux

Experimental Factor	Pre-Test	85/85	Thermal Shock	Mech Shock
Constant	10.71	12.52	13.69	13.83
Flux	2.77		0.40	
Site 2				-0.49
Site 3				
Site 4				
Site 5			-0.44	-0.63
Site 6		-0.41		-0.42
Site 7				
Site 8	0.57			
Site 9				
Site 10				
Site 11				
Site 12				
Site 13				
Site 14				
Site 15				
Site 16	-0.34	-0.61		
Site 4 * Flux				
Site 5 * Flux				0.69
Site 7 * Flux				
Site 11 * Flux				
Site 13 * Flux				
Site 16 * Flux		0.72		
Model R^2	89.4%	8.0%	15.5%	12.5%
Standard Deviation	0.47	0.53	0.56	0.50

GLM from Eq. F.2: Surface Finishes and Flux

Experimental Factor	Pre-Test	85/85	Thermal Shock	Mech Shock
Constant	10.77	12.55	13.72	13.70
OSP		-0.23	-0.33	-0.21
Immersion Sn				
Immersion Ag				
Ni/Au				
Ni/Pd/Au	-0.38	-0.40		
Flux	2.71		0.39	0.20
Model R^2	88.7%	5.6%	16.0%	6.7%
Standard Deviation	0.4	0.50	0.56	0.51

Table F.26 Significant Coefficients for the Two GLM Analyses by Test Time for the Gull Wing

GLM from Eq. F.1: Sites and Interactions with Flux

Experimental Factor	Pre-Test	85/85	Thermal Shock	Mech Shock
Constant	11.72	12.59	13.76	13.32
Flux	0.81		-0.37	
Site 2				
Site 3				
Site 4				
Site 5	0.37			
Site 6				
Site 7				
Site 8				-0.64
Site 9				
Site 10	0.47			
Site 11	-0.65			
Site 12	0.54			
Site 13				
Site 14				
Site 15		0.67		
Site 16		0.66		
Site 4 * Flux				
Site 5 * Flux				
Site 7 * Flux	0.47			
Site 11 * Flux	1.61			
Site 13 * Flux				
Site 16 * Flux				
Model R^2	55.4%	3.3%	2.8%	1.7%
Standard Deviation	0.54	1.1	1.10	1.06

GLM from Eq. F.2: Surface Finishes and Flux

Experimental Factor	Pre-Test	85/85	Thermal Shock	Mech Shock
Constant	11.55	12.62	13.76	13.22
OSP	0.30			
Immersion Sn	0.27			
Immersion Ag				
Ni/Au				0.46
Ni/Pd/Au		0.63		
Flux	1.09		-0.37	
Model R^2	48.2%	1.9%	2.8%	2.6%
Standard Deviation	0.50	1.00	1.10	1.0

Table F.27 Predicted Changes from the Base Case at Pre-test for the Leakage Measurements for the GLM in Equation F.1

	10-Mil Pads		PGA-A		PGA-B		Gull Wing	
	LR Flux	WS Flux	LR Flux	WS Flux	LR Flux	WS Flux	LR Flux	WS Flux
Site 2	-0.97	-0.23	-1.19	0.39		2.77		0.81
Site 3	1.02	1.76		1.58		2.77		0.81
Site 4	0.93	1.67		1.58		2.77		0.81
Site 5	0.85	1.59		1.58		2.77	0.37	1.18
Site 6		0.74		1.58		2.77		0.81
Site 7		1.59		1.58		2.77		1.28
Site 8		0.74		1.58	0.57	3.34		0.81
Site 9		0.74	-0.81	0.77		2.77		0.81
Site 10		1.74		1.58		2.77	0.47	1.28
Site 11		1.80	-0.34	1.24		2.77	-0.65	1.77
Site 12	0.91	1.65		1.58		2.77	0.54	1.35
Site 13	-0.89	1.80	-0.64	1.85		2.77		0.81
Site 14	-0.75	-0.01	-0.94	0.64		2.77		0.81
Site 15	0.98	1.72		1.58		2.77		0.81
Site 16	-0.76	1.72	-1.14	1.78	-0.34	2.43		0.81

Table F.28 Predicted Changes from the Base Case at Pre-test for the Leakage Measurements for the GLM in Equation F.2

	10-Mil Pads		PGA-A		PGA-B		Gull Wing	
	LR Flux	WS Flux	LR Flux	WS Flux	LR Flux	WS Flux	LR Flux	WS Flux
OSP	0.73	2.50	0.35	2.40		2.71	0.30	1.39
Imm Sn	0.33	2.10		2.05		2.71	0.27	1.36
Imm Ag	0.48	2.25		2.05		2.71		1.09
Ni/Au		1.77		2.05		2.71		1.09
Ni/Pd/Au		1.77	-0.35	1.70	-0.38	2.33		1.09

10-Mil Pads

Examination of the GLM results in Table F.27 for 10-mil pads shows an effect due to flux of approximately 0.74 orders of magnitude (see column 1 in uppermost portion of Table F.23). There is also evidence of site-to-site variation and some interaction between site and flux that affects resistance either positively or negatively by up to an order of magnitude. Sites applying the OSP surface finish (Sites 6, 7, 8, and 9) as will as Sites 10 and 11 with immersion Sn do not differ from the base case when LR flux is used.

Table F.28 shows a flux effect of approximately 1.77 orders of magnitude when sites are dropped from the GLM and replaced by surface finishes. These results show slight increases in resistance over the base case for OSP, immersion Sn, and immersion Ag.

The differences in the model R^2s for both GLMS essentially disappear after exposure to the 85/85 test environment. This result is not unusual and may be due to a *cleansing effect* from the 85/85 test environment that removes residues resulting from board fabrication, assembly, and handling. This same phenomenon was observed for the other three leakage circuits.

Boxplot Displays of Multiple Comparison Results. Boxplot displays of the Pre-test and Post 85/85 test results are given in Figure 4.19 and 4.20. Boxplots for the other test times are displayed in Figures F.37 and F.38. There are not great changes in the leakage measurements at Post TS and Post MS as shown in the boxplots.

PGA-A

Examination of the GLM results in Table F.27 for PGA-A shows an effect due to flux of approximately 1.58 orders of magnitude. There is also evidence of site-to-site variation and some interaction between site and flux that affects resistance either positively on negatively by up to an order of magnitude. Nine of the sites do not differ from the base case when LR flux is used.

Table F.28 shows a flux effect of approximately 2.05 orders of magnitude when sites are dropped from the GLM and replaced by surface finishes, but no meaningful differences due to surface finishes. As was the case with the 10-mil pads, the differences in the model R^2s for both GLMS essentially disappear after exposure to the 85/85 test environment.

Boxplot Displays of Multiple Comparison Results. A boxplot display of the Pre-test results is given in Figure 4.21. Boxplots for the other three test times are displayed in Figures F.39 to F.41.

PGA-B

Examination of the GLM results in Table F.27 for PGA-B shows a strong effect due to flux of approximately 2.77 orders of magnitude. Thirteen of the sites do not differ from the base case when LR flux is used and the other two only differ slightly. Table F.28 also shows a strong flux effect of approximately 2.71 orders of magnitude when sites are dropped from the GLM and replaced by surface finishes, but no meaningful differences due to surface finishes.

As was the case with the 10-mil pads and PGA-A, the differences in the model R^2s for both GLMS essentially disappear after exposure to the 85/85 test environment.

Boxplot Displays of Multiple Comparison Results. A boxplot display of the Pre-test results is given in Figure 4.22. Boxplots for the other three test times are displayed in Figures F.42 to F.44.

Gull Wing

Examination of the GLM results in Table F.27 for the Gull Wing shows a moderate effect due to flux of approximately 0.81 orders of magnitude. There is evidence of modest site-to-site variation and some interaction between site and flux. Eleven of the sites do not differ from the base case when LR flux is used and the other two only differ slightly. Table F.28 shows a flux effect of approximately 1.09 orders of magnitude when sites are dropped from the GLM and replaced by surface finishes, but no meaningful differences due to surface finishes.

As was the case with the 10-mil pads, PGA-A, and PGA-B the differences in the model R^2s for both GLMS essentially disappear after exposure to the 85/85 test environment.

Boxplot Displays of Multiple Comparison Results. A boxplot display of the Pre-test results is given in Figure 4.23. Boxplots for the other three test times are displayed in Figures F.45 to F.47.

F.9 Stranded Wires

Pre-test measurements for the stranded wire circuits were subjected to GLM analyses, as were the deltas after 85/85, thermal shock, and mechanical shock. The results of the GLM analyses are given in Tables F.29 and F.30. Columns 3 to 5 in these tables give the results for 85/85, TS, and MS, respectively. Note that these latter three analyses are based on changes from Pre-test measurements. The model R^2s for Equations F.1 and F.2 for the stranded wire circuitry are summarized as follows for each test time.

GLM	Circuit	Pre-test	85/85	TS	MS
Site and Flux	St. Wire 1	3.6%	6.5%	12.5%	11.7%
	St. Wire 2	8.6%	8.2%	8.2%	4.1%
Surface Finish and Flux	St. Wire 1	1.8%	1.6%	4.5%	2.1%
	St. Wire 2	0.8%	0.9%	7.4%	2.2%

The model R^2 values are all near zero at each test time, which indicates that the experimental parameters do not influence the stranded wire voltage measurements.

Boxplot Displays of Multiple Comparison Results. Boxplots displays of the Pre-test voltage measurements (mV) for both stranded wires are displayed in Figures F.48 and F.49.

Table F.29 Significant Coefficients for the Two GLM Analyses by Test Time for Stranded Wire

GLM from Eq. F.1: Sites and Interactions with Flux

Experimental Factor	Pre-Test	85/85 (Delta 1)	Thermal Shock (Delta 2)	Mech Shock (Delta 3)
Constant	12.90	0.000	0.001	0.005
Flux	0.55			
Site 2				
Site 3				
Site 4		-0.001		
Site 5		-0.001		
Site 6				
Site 7				
Site 8				
Site 9				
Site 10				
Site 11				
Site 12			0.024	0.042
Site 13				
Site 14				
Site 15				
Site 16				
Site 4 * Flux				
Site 5 * Flux		0.002		
Site 7 * Flux				
Site 11 * Flux				
Site 13 * Flux	-2.21			
Site 16 * Flux				0.079
Model R^2	3.6%	6.5%	12.5%	11.7%
Standard Deviation	2.57	0.002	0.014	0.041

GLM from Eq. F.2: Surface Finishes and Flux

Experimental Factor	Pre-Test	85/85 (Delta 1)	Thermal Shock (Delta 2)	Mech Shock (Delta 3)
Constant	12.94	0.000	0.001	0.006
OSP		-0.001		
Immersion Sn				
Immersion Ag	1.06		0.010	0.019
Ni/Au				
Ni/Pd/Au				
Flux				
Model R^2	1.8%	1.6%	4.5%	2.1%
Standard Deviation	2.00	0.001	0.014	0.043

Table F.30 Significant Coefficients for the Two GLM Analyses by Test Time for Stranded Wire 2

GLM from Eq. F.1: Sites and Interactions with Flux

Experimental Factor	Pre-Test	85/85 (Delta 1)	Thermal Shock (Delta 2)	Mech Shock (Delta 3)
Constant	23.44	-.000	0.011	0.033
Flux				
Site 2				
Site 3		0.003		
Site 4				
Site 5				
Site 6				
Site 7				
Site 8				
Site 9				
Site 10	-1.56			
Site 11				
Site 12			0.077	
Site 13				
Site 14				
Site 15				
Site 16				
Site 4 * Flux				
Site 5 * Flux	-2.31			
Site 7 * Flux				
Site 11 * Flux		-0.002	0.074	
Site 13 * Flux				
Site 16 * Flux				0.130
Model R^2	8.6%	8.2%	8.2%	4.1%
Standard Deviation	1.90	0.003	0.067	0.098

GLM from Eq. F.2: Surface Finishes and Flux

Experimental Factor	Pre-Test	85/85 (Delta 1)	Thermal Shock (Delta 2)	Mech Shock (Delta 3)
Constant	23.34	0.000	-0.001	0.021
OSP	-0.43			
Immersion Sn				
Immersion Ag		-0.001	0.038	
Ni/Au				
Ni/Pd/Au				
Flux			0.026	0.029
Model R^2	0.8%	0.9%	7.4%	2.2%
Standard Deviation	2.00	0.002	0.067	0.099

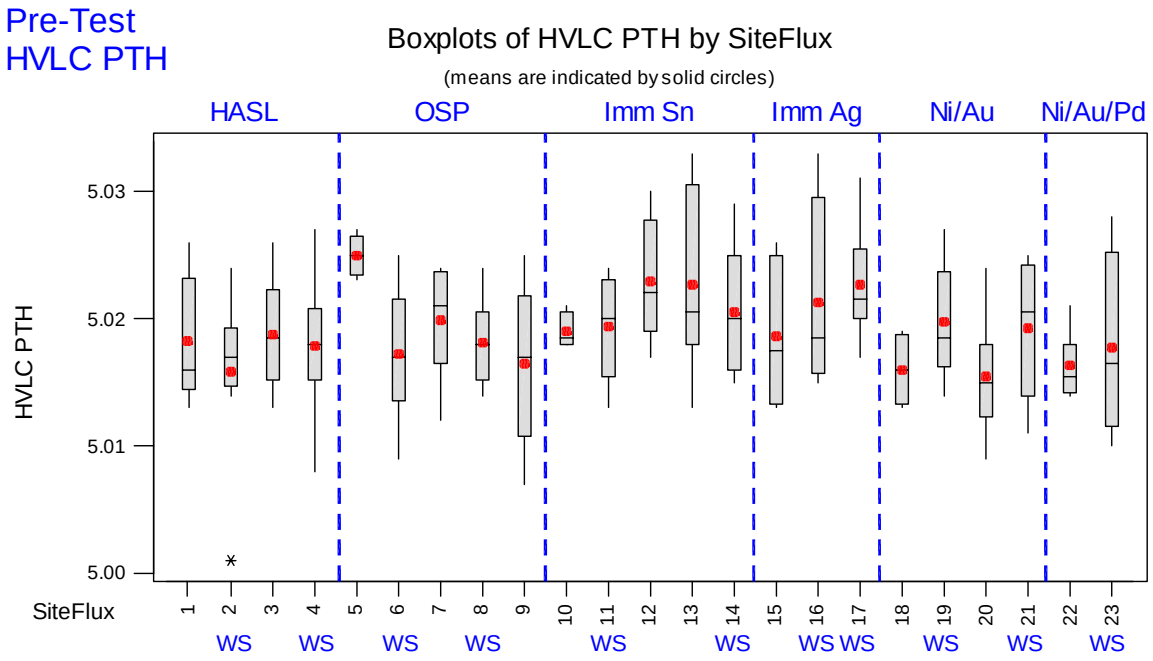

Figure F.1 Boxplot Displays for HVLC PTH Measurements (µA) at Pre-test by Surface Finish
(Acceptance Criterion = 4µA< X <6µA)

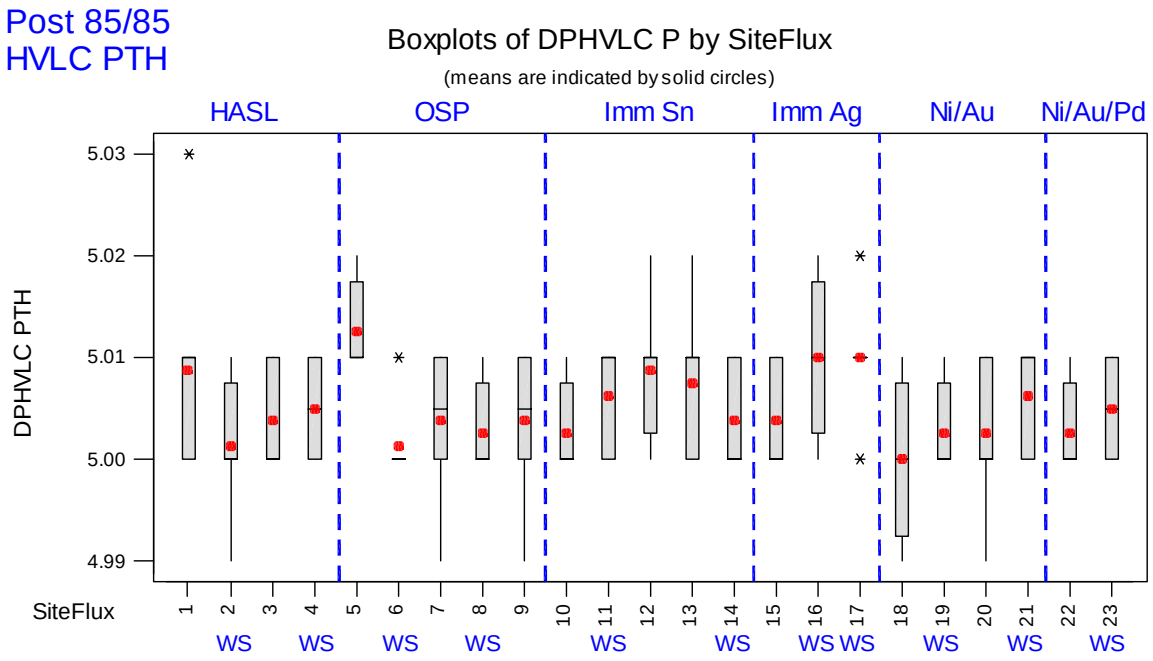

Figure F.2 Boxplot Displays for HVLC PTH Post 85/85 - Pre-test Measurements (µA) by Surface Finish
(Acceptance Criterion = 4µA< X <6µA)

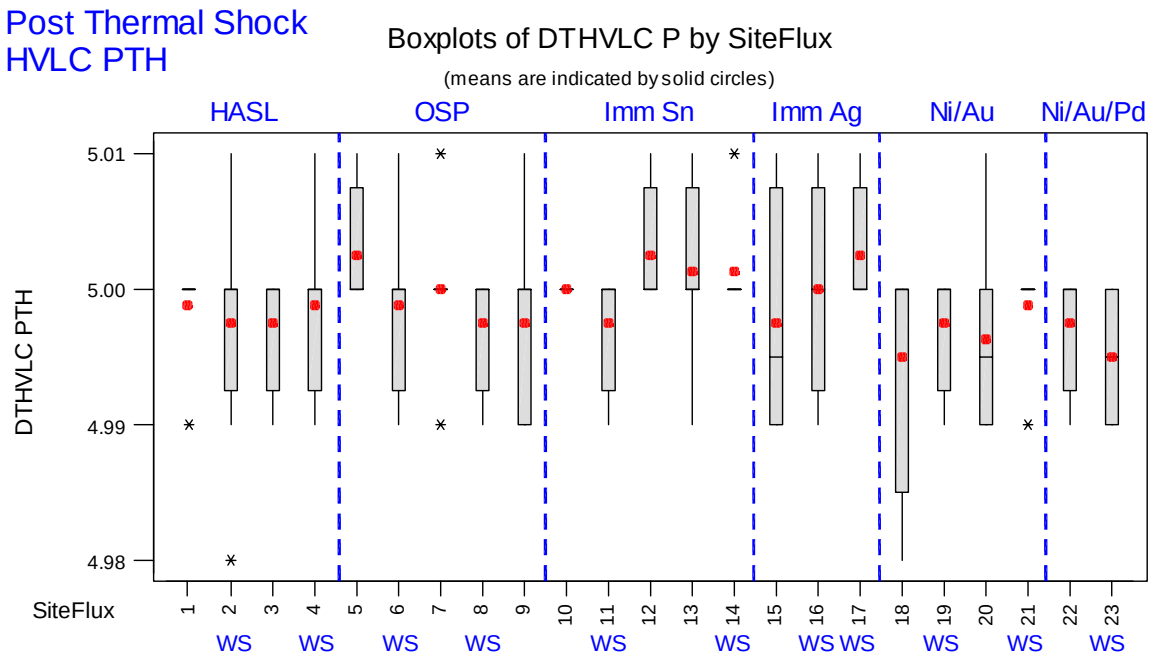

Figure F.3 Boxplot Displays for HVLC PTH Post TS - Pre-test Measurements (µA) by Surface Finish
(Acceptance Criterion = 4µA< X <6µA)

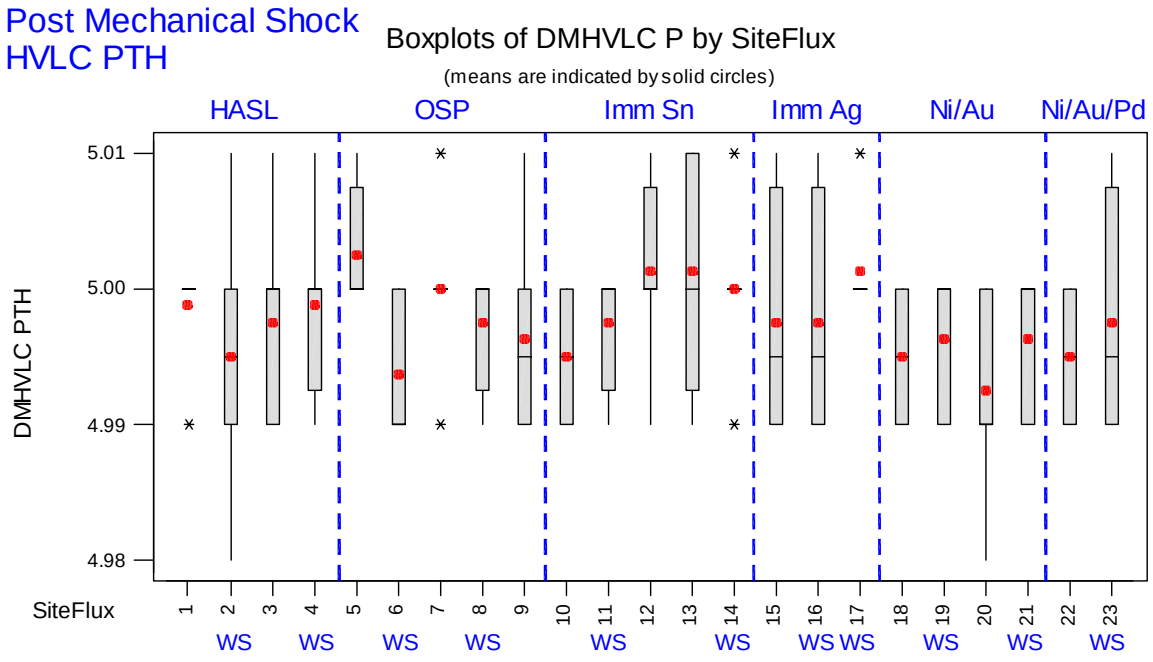

Figure F.4 Boxplot Displays for HVLC PTH Post MS - Pre-test Measurements (µA) by Surface Finish
(Acceptance Criterion = 4µA< X <6µA)

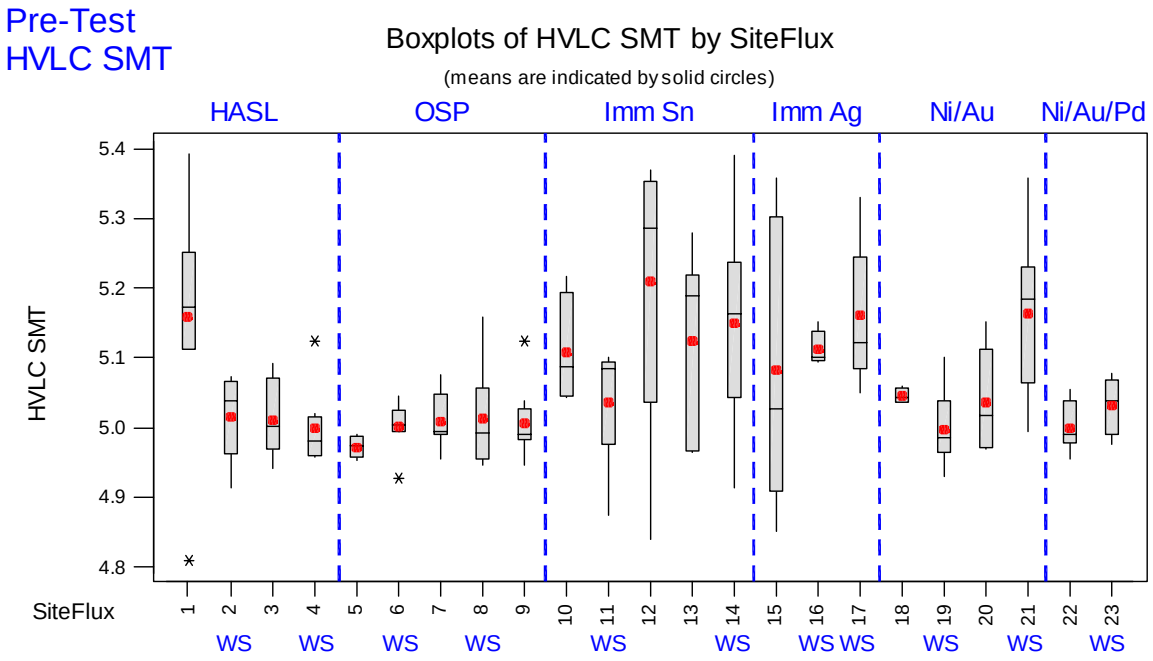

Figure F.5 Boxplot Displays for HVLC SMT Measurements (µA) at Pre-test by Surface Finish
(Acceptance Criterion = 4µA< X <6µA)

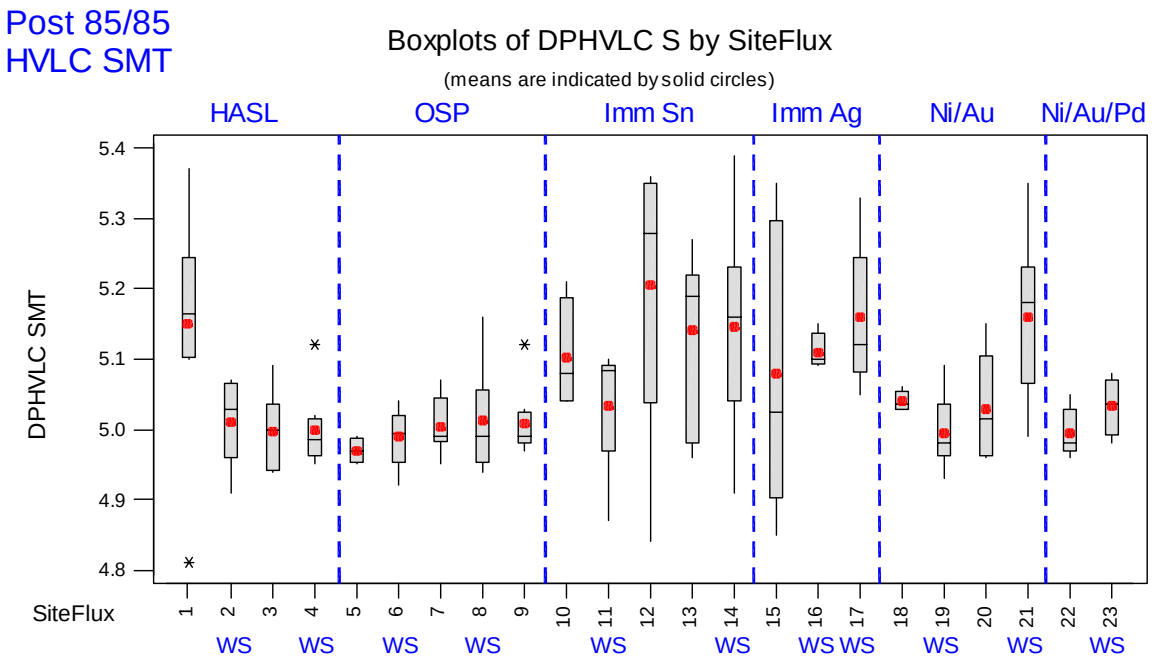

Figure F.6 Boxplot Displays for HVLC PTH Post 85/85 - Pre-test Measurements (µA) by Surface Finish
(Acceptance Criterion = 4µA< X <6µA)

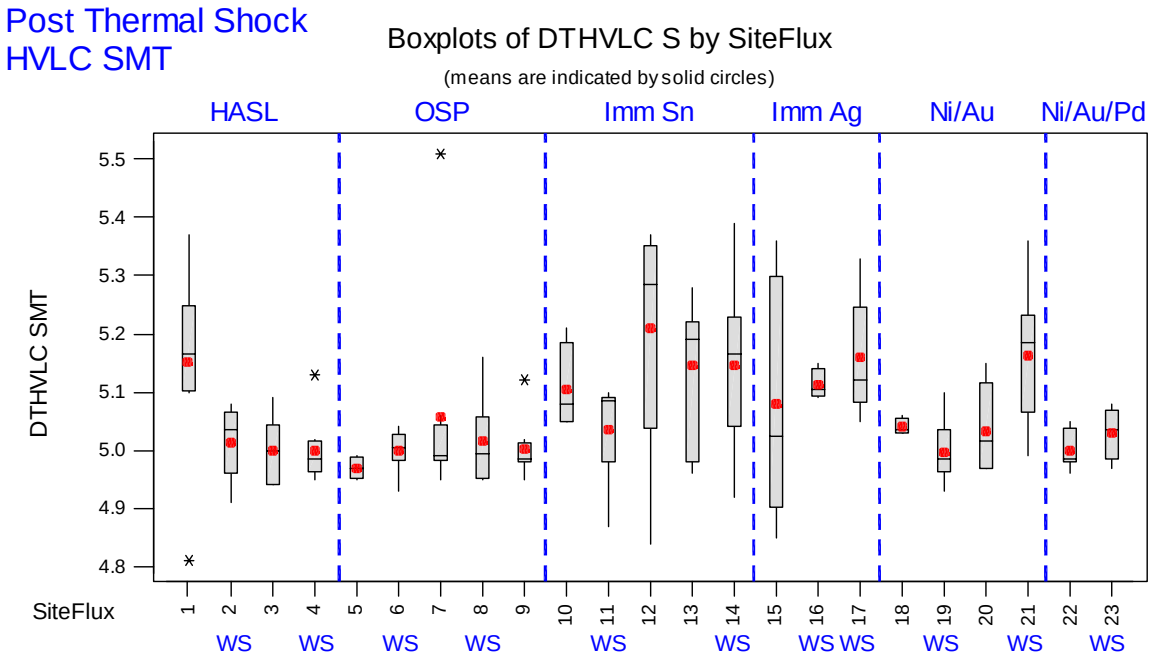

Figure F.7 Boxplot Displays for HVLC PTH Post TS - Pre-test Measurements (µA) by Surface Finish
(Acceptance Criterion = 4µA< X <6µA)

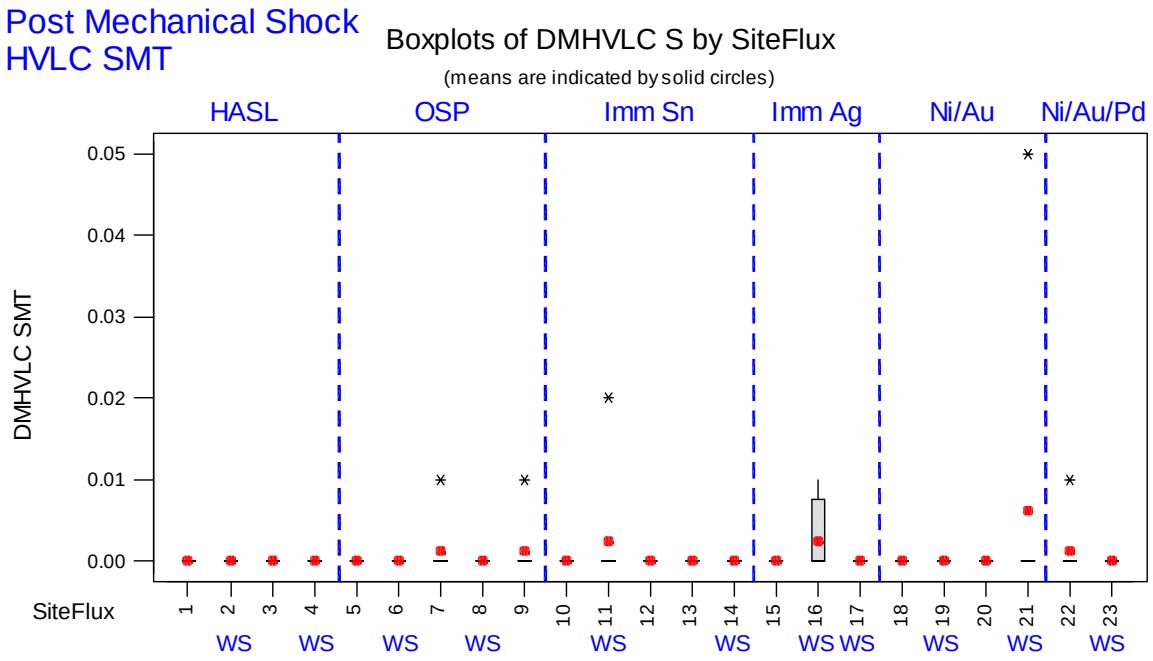

Figure F.8 Boxplot Displays for HVLC PTH Post MS - Pre-test Measurements by Surface Finish
(Acceptance Criterion = 4µA< X <6µA)

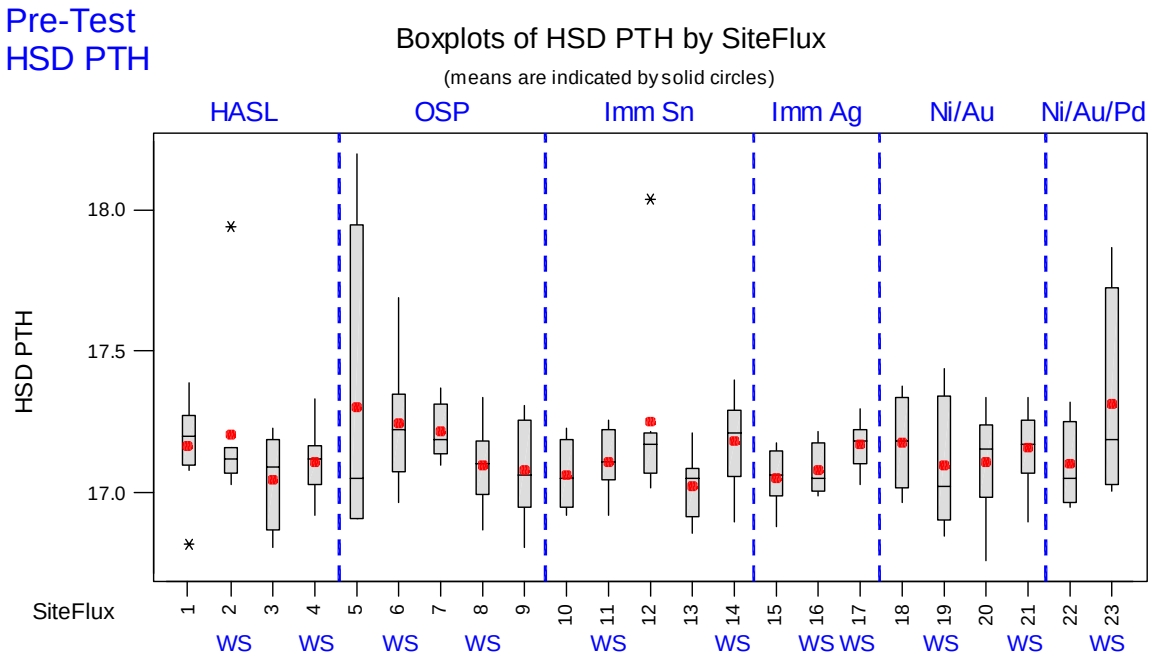

Figure F.9 Boxplot Displays for HSD PTH Measurements (nsec) at Pre-test by Surface Finish

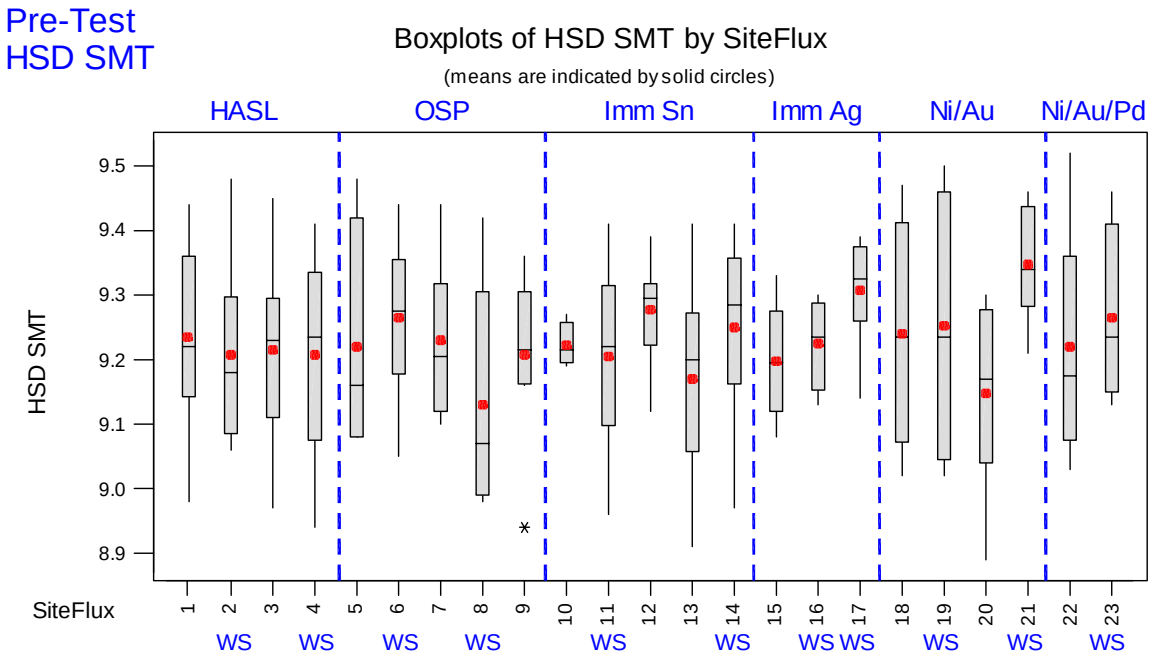

Figure F.10 Boxplot Displays for HSD SMT Measurements (nsec) at Pre-test by Surface Finish

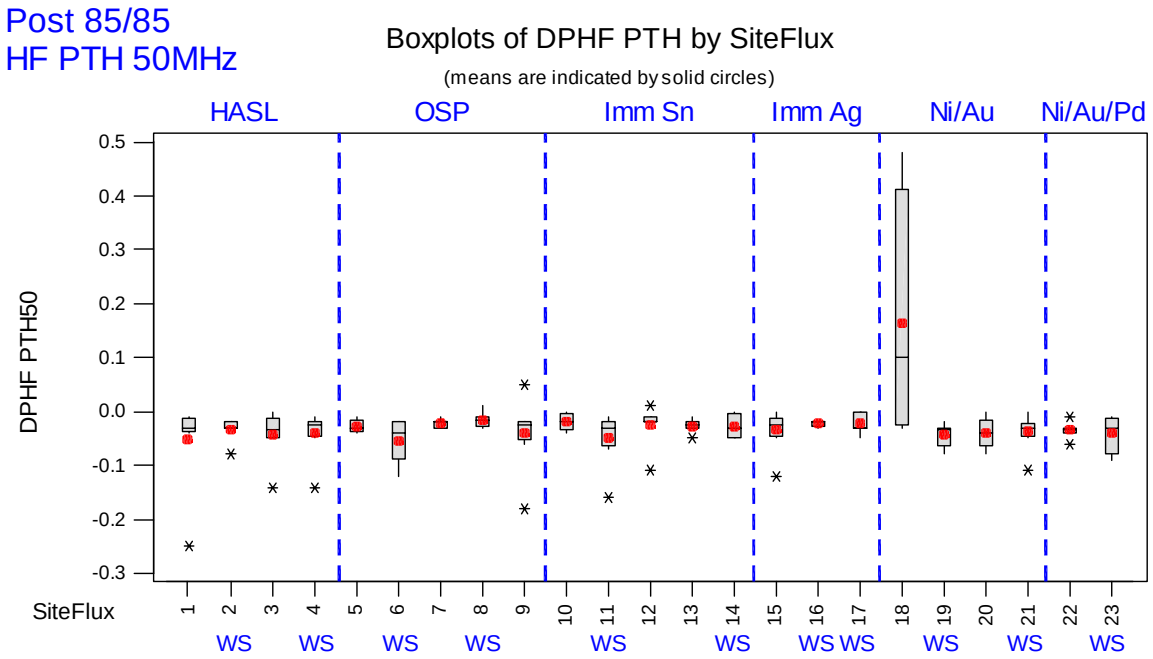

Figure F.11 Boxplot Displays for HF PTH 50MHz Post 85/85 - Pre-test Measurements (dB) by Surf. Finish
(Acceptance Criterion = ±5dB of Pre-test)

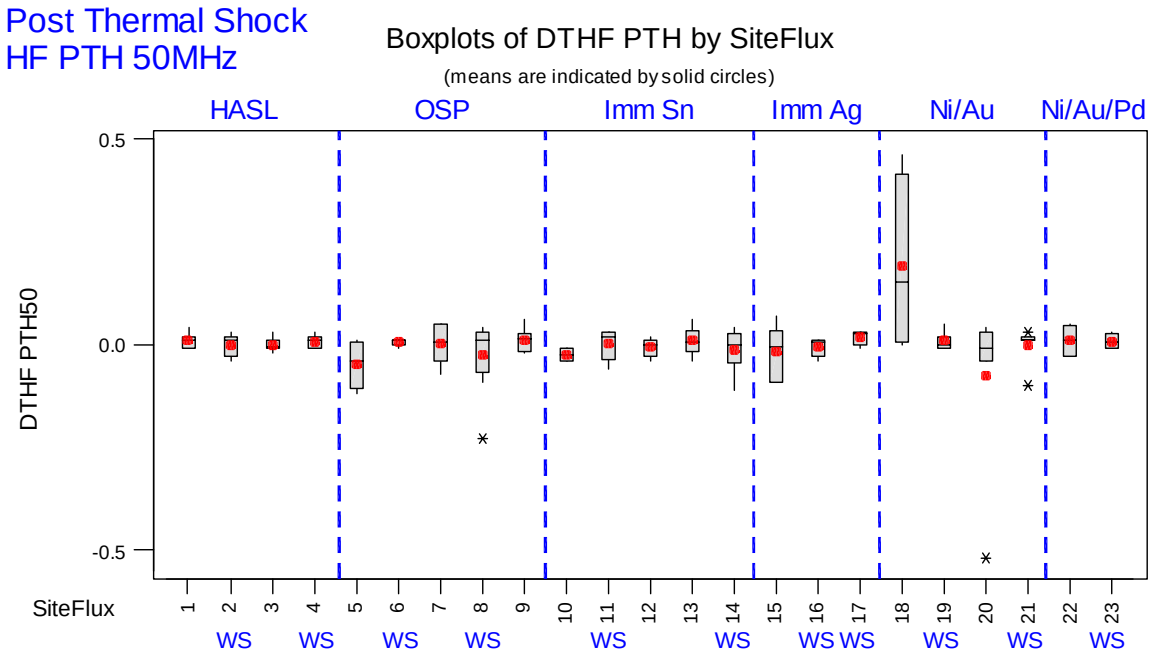

Figure F.12 Boxplot Displays for HF PTH 50MHz Post TS - Pre-test Measurements (dB) by Surface Finish
(Acceptance Criterion = ±5dB of Pre-test)

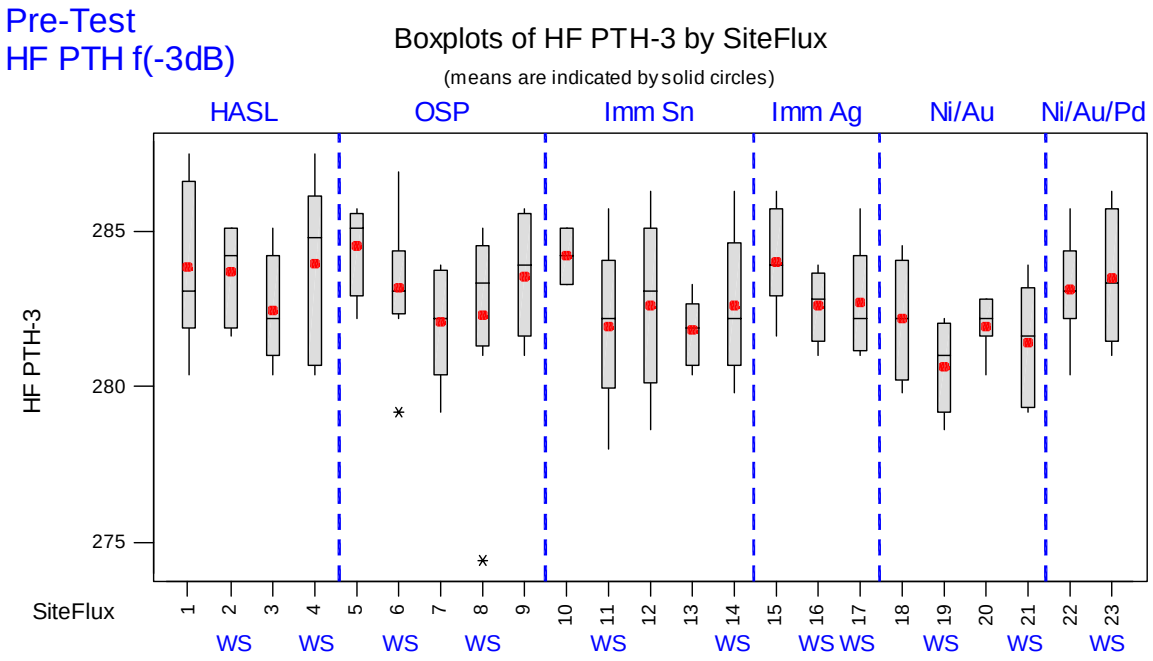

Figure F.13 Boxplot Displays for HF PTH f(-3dB) Measurements (MHz) at Pre-test by Surface Finish
(Acceptance Criterion = ±50Mhz of Pre-test)

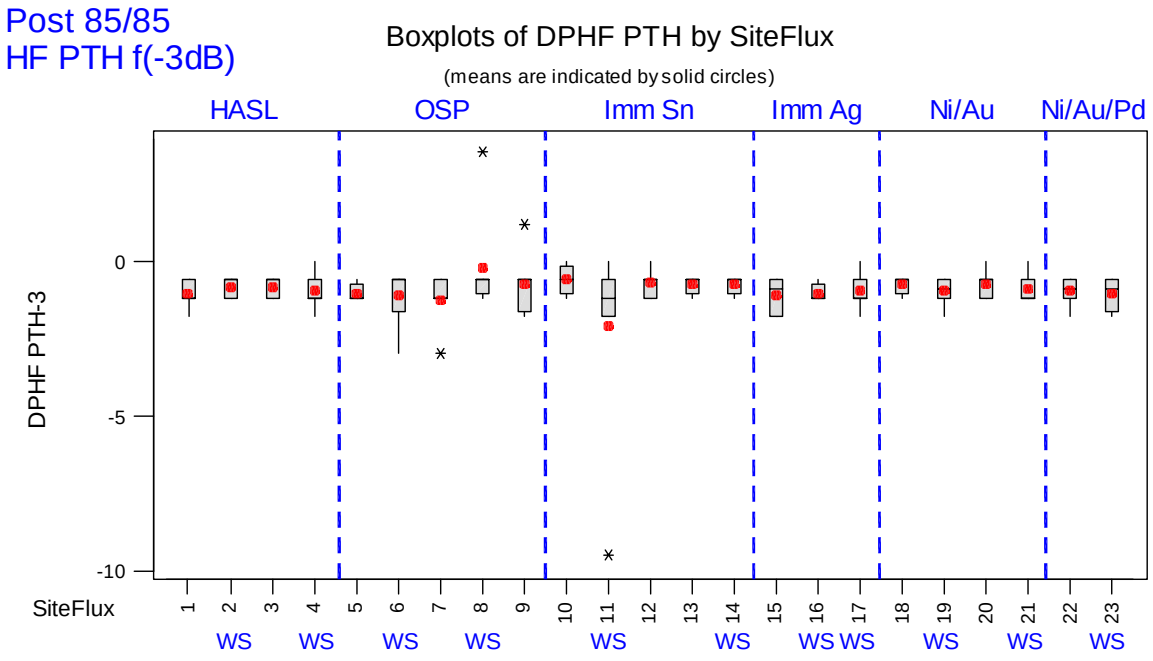

Figure F.14 Boxplot Displays for HF PTH f(-3dB) Post 85/85 - Pre-test Measurements (MHz) by Surf. Finish
(Acceptance Criterion = ±50Mhz of Pre-test)

Post Thermal Shock
HF PTH f(-3dB)

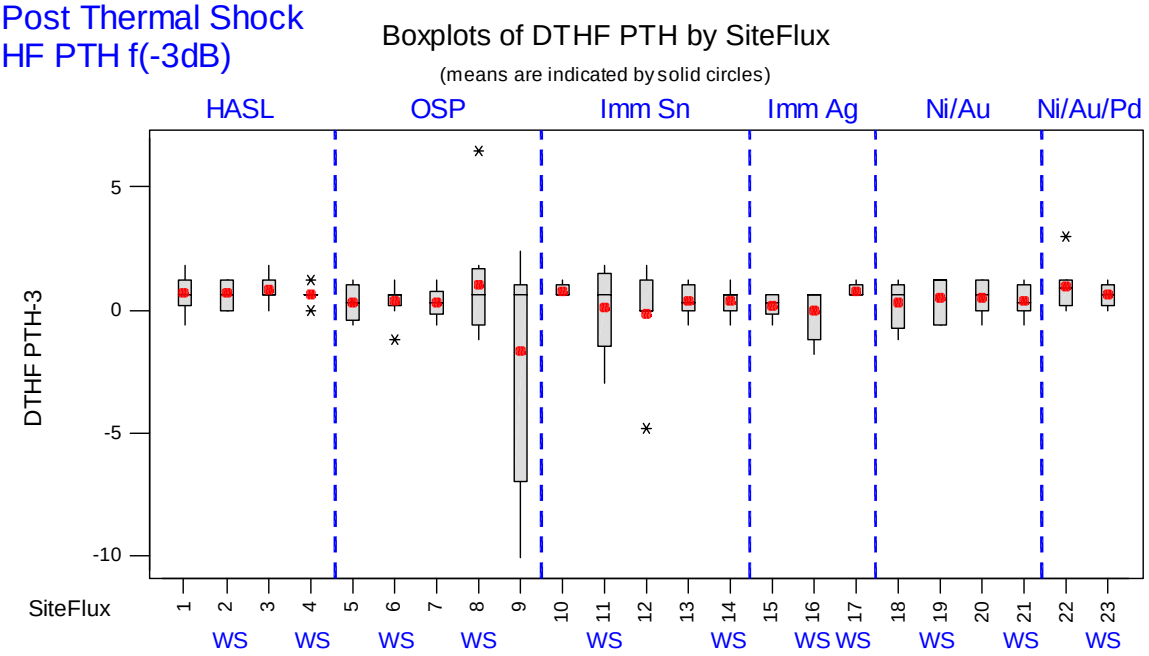

Figure F.15 Boxplot Displays for HF PTH f(-3dB) Post TS - Pre-test Measurements (Mhz) by Surface Finish
(Acceptance Criterion = ±50Mhz of Pre-test)

Pre-Test
HF PTH f(-40dB)

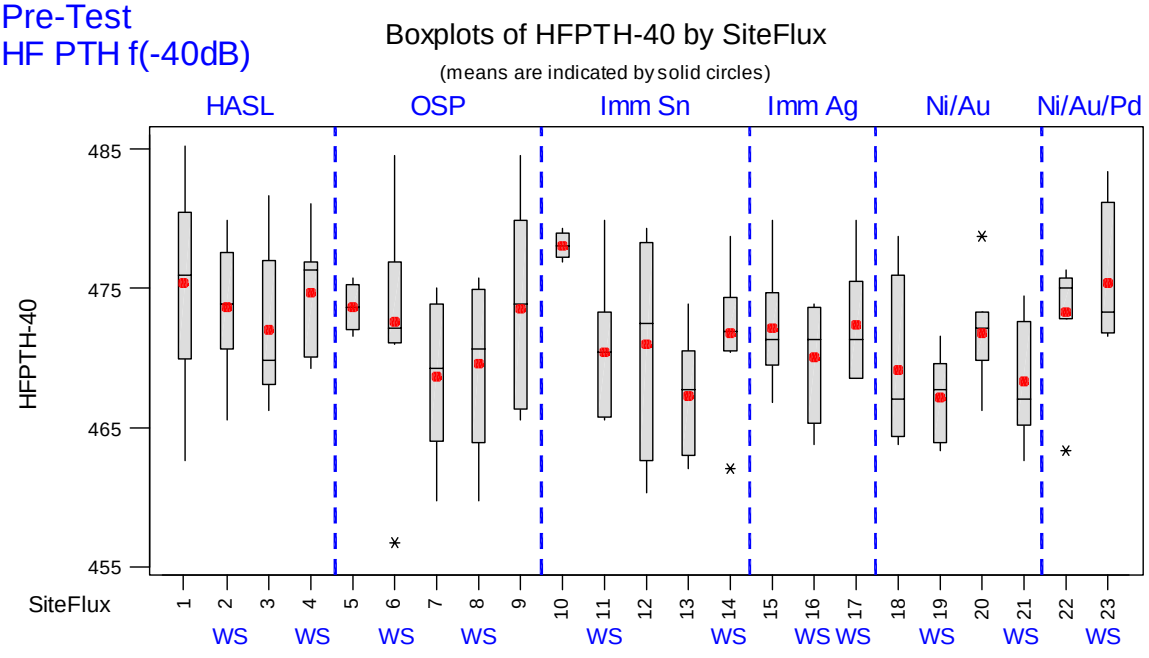

Figure F.16 Boxplot Displays for HF PTH f(-40dB) Measurements (MHz) at Pre-test by Surface Finish
(Acceptance Criterion = ±50Mhz of Pre-test)

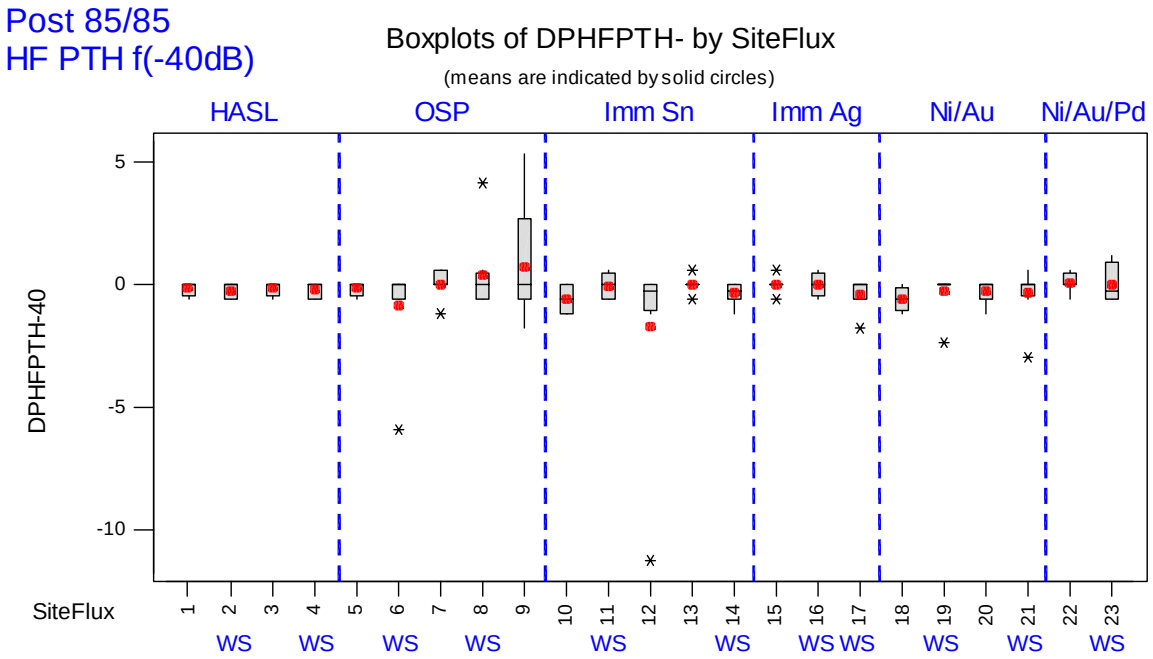

Figure F.17 Boxplot Displays for HF PTH f(-40dB) Post 85/85 - Pre-test Measurements (MHz) by Surf. Fin.
(Acceptance Criterion = ±50Mhz of Pre-test)

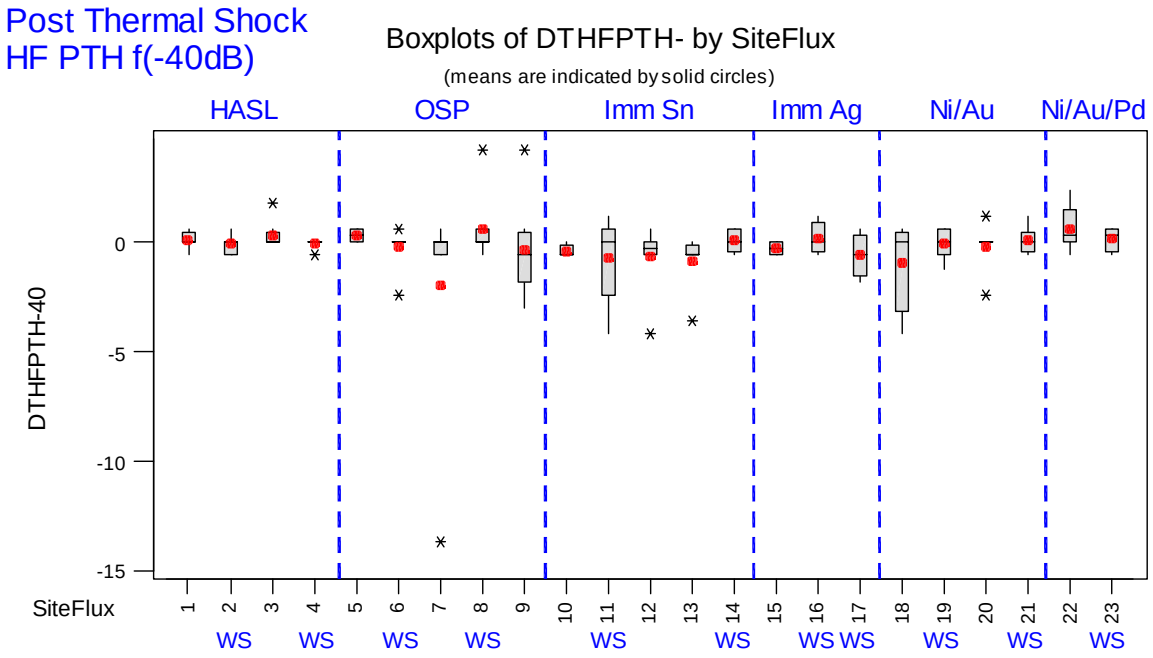

Figure F.18 Boxplot Displays for HF PTH f(-40dB) Post TS - Pre-test Measurements (MHz) by Surf. Finish
(Acceptance Criterion = ±50Mhz of Pre-test)

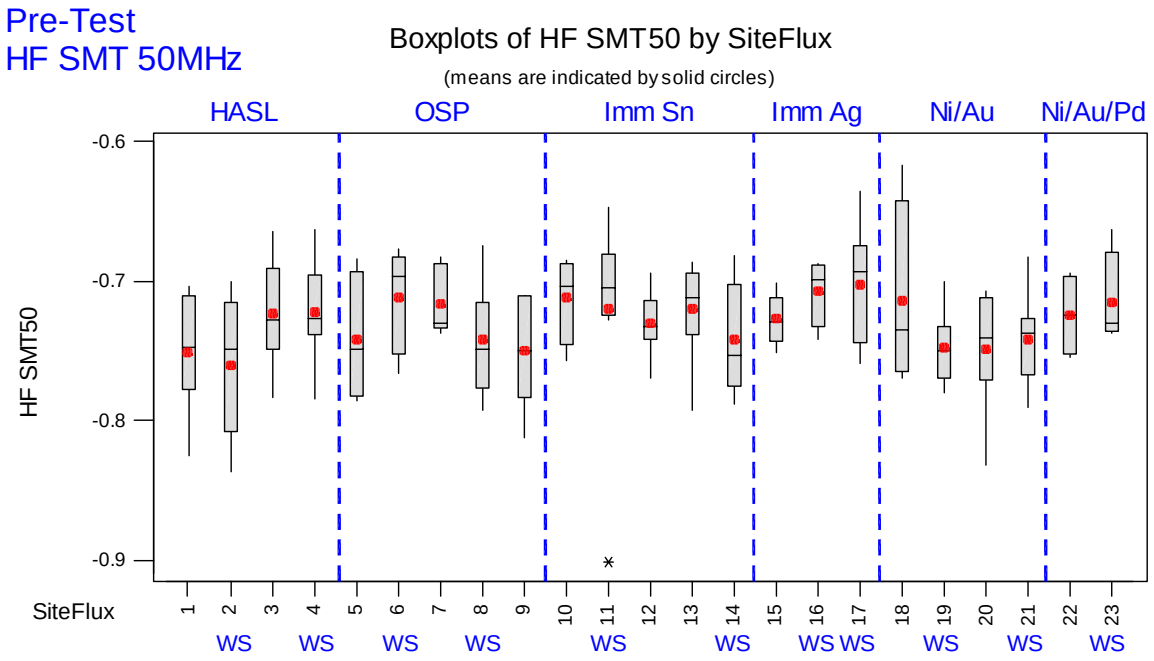

Figure F.19 Boxplot Displays for HF SMT 50MHz Measurements (dB) at Pre-test by Surface Finish

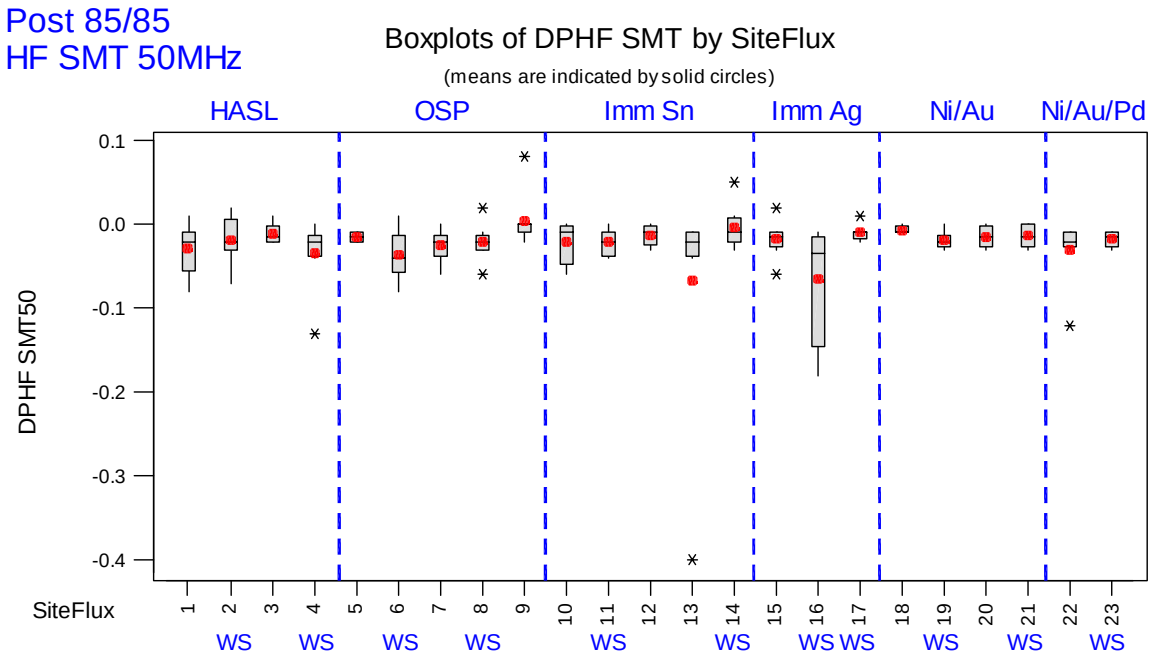

Figure F.20 Boxplot Displays for HF SMT 50MHz Post 85/85 - Pre-test Measurements (dB) by Surf. Finish
(Acceptance Criterion = ±5 dB of Pre-test)

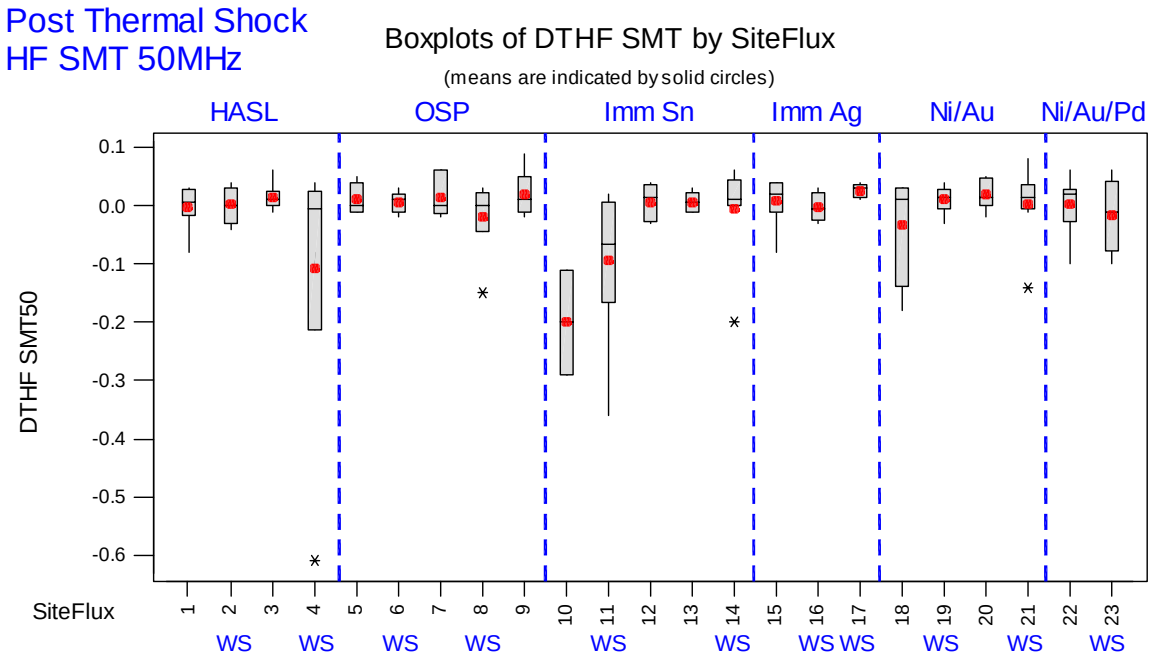

Figure F.21 Boxplot Displays for HF SMT 50MHz Post TS - Pre-test Measurements (dB) by Surface Finish
(Acceptance Criterion = ±5 dB of Pre-test)

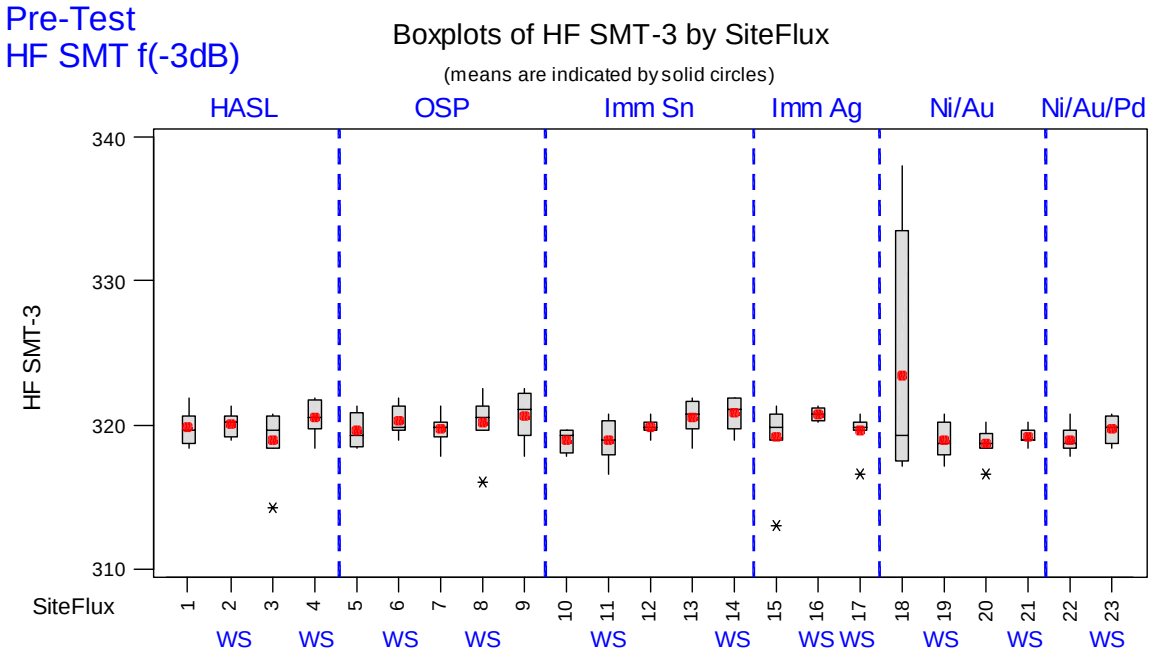

Figure F.22 Boxplot Displays for HF SMT f(-3dB) Measurements (MHz) at Pre-test by Surface Finish
(Acceptance Criterion = ±50Mhz of Pre-test)

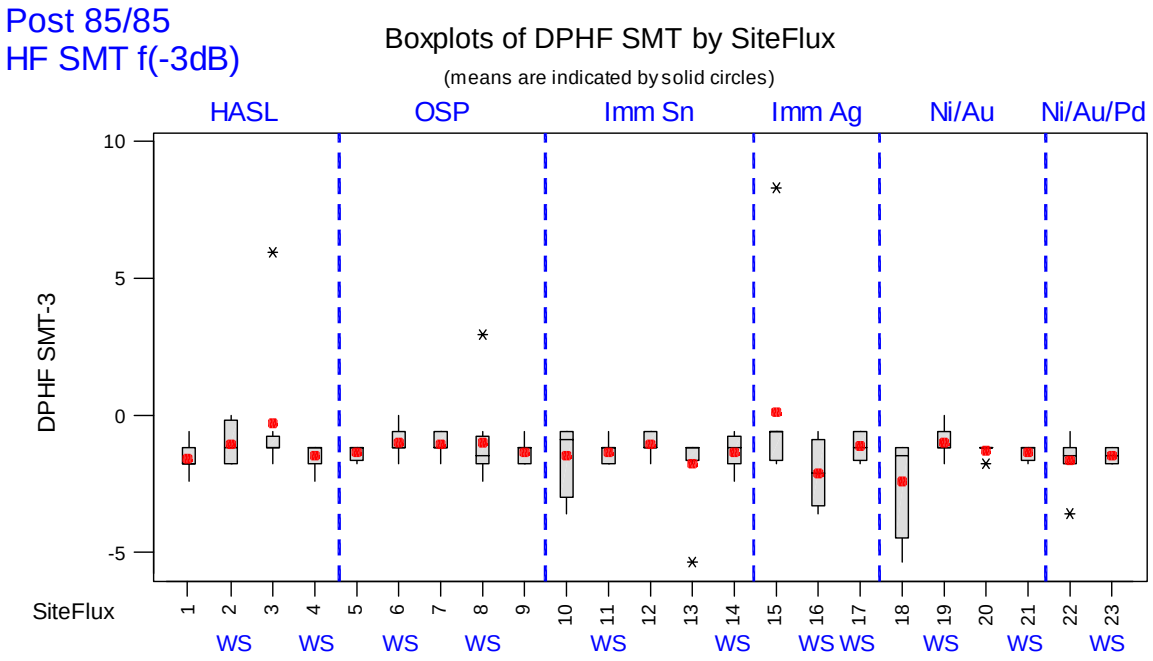

Figure F.23 Boxplot Displays for HF SMT f(-3dB) Post 85/85 - Pre-test Measurements (MHz) by Surf. Finish
(Acceptance Criterion = ±50Mhz of Pre-test)

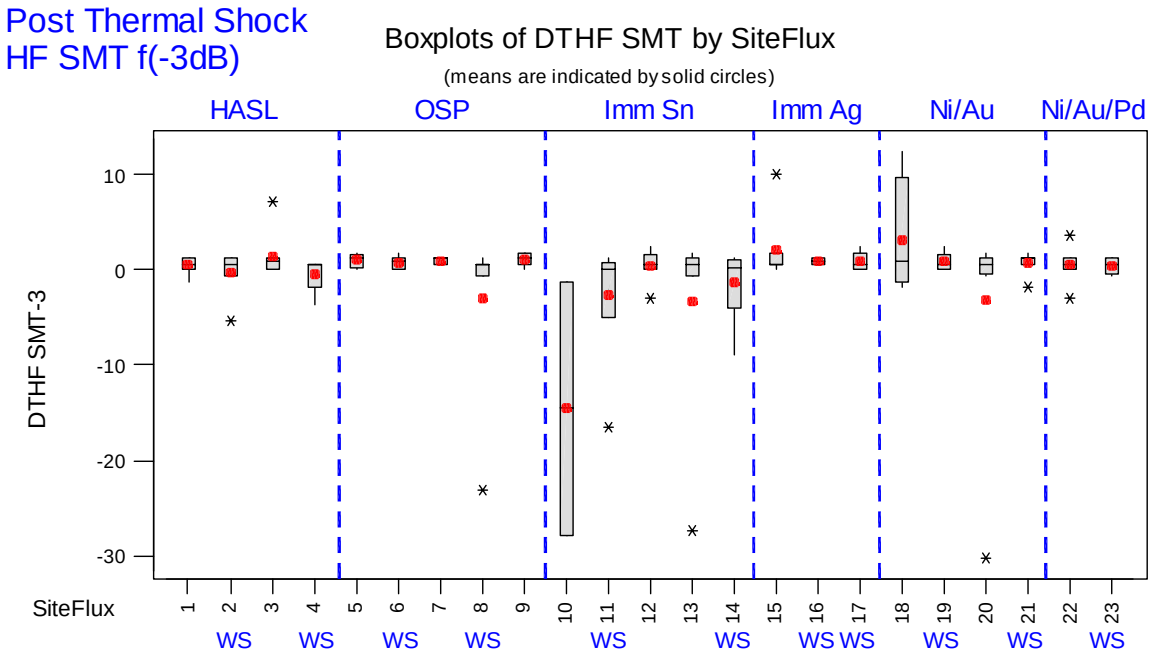

Figure F.24 Boxplot Displays for HF SMT f(-3dB) Post TS - Pre-test Measurements (MHz) by Surface Finish
(Acceptance Criterion = ±50Mhz of Pre-test)

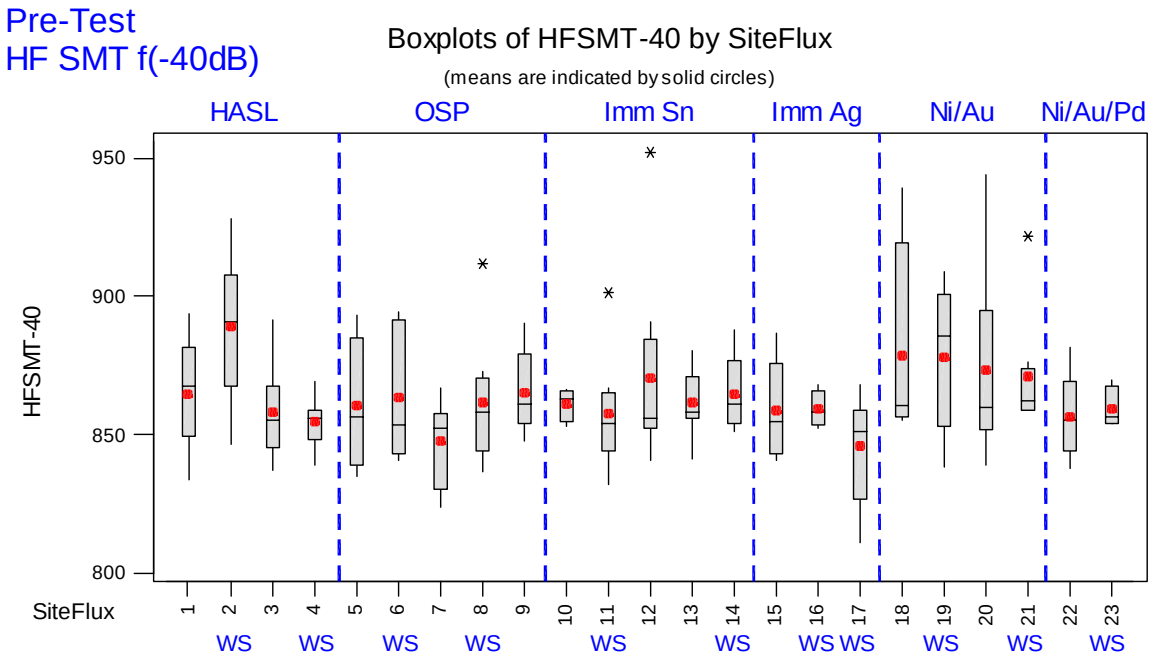

Figure F.25 Boxplot Displays for HF SMT f(-40dB) Measurements (MHz) at Pre-test by Surface Finish
(Acceptance Criterion = ±50Mhz of Pre-test)

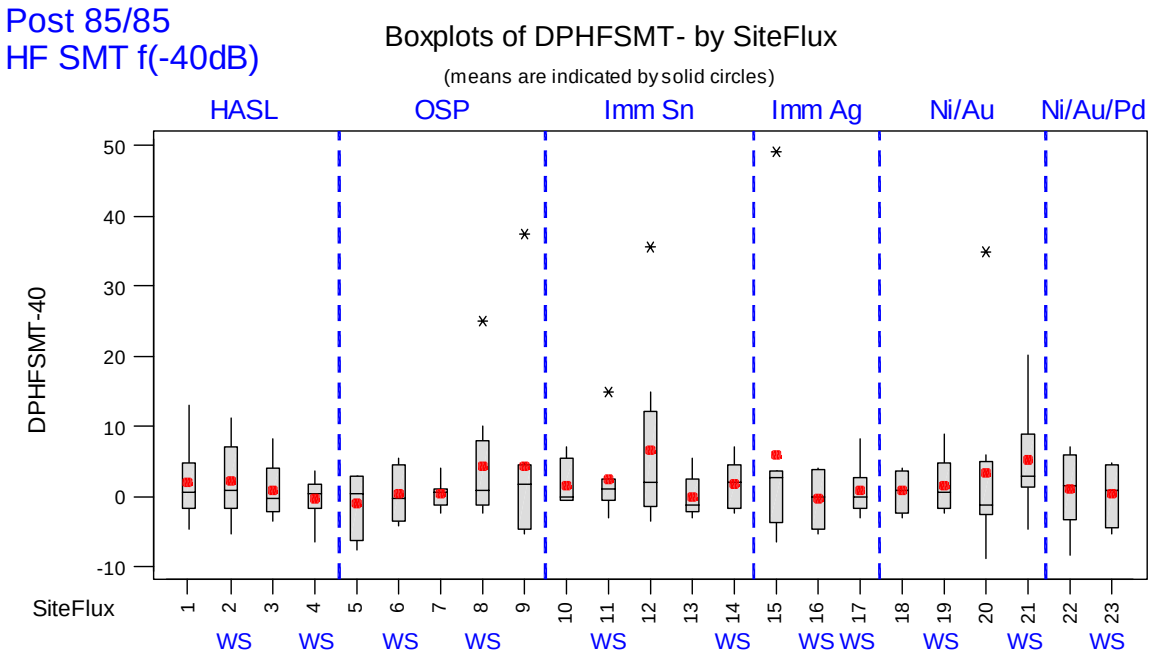

Figure F.26 Boxplot Displays for HF SMT f(-40dB) Post 85/85 - Pre-test Measurements (MHz) by Surf. Fin.
(Acceptance Criterion = ±50Mhz of Pre-test)

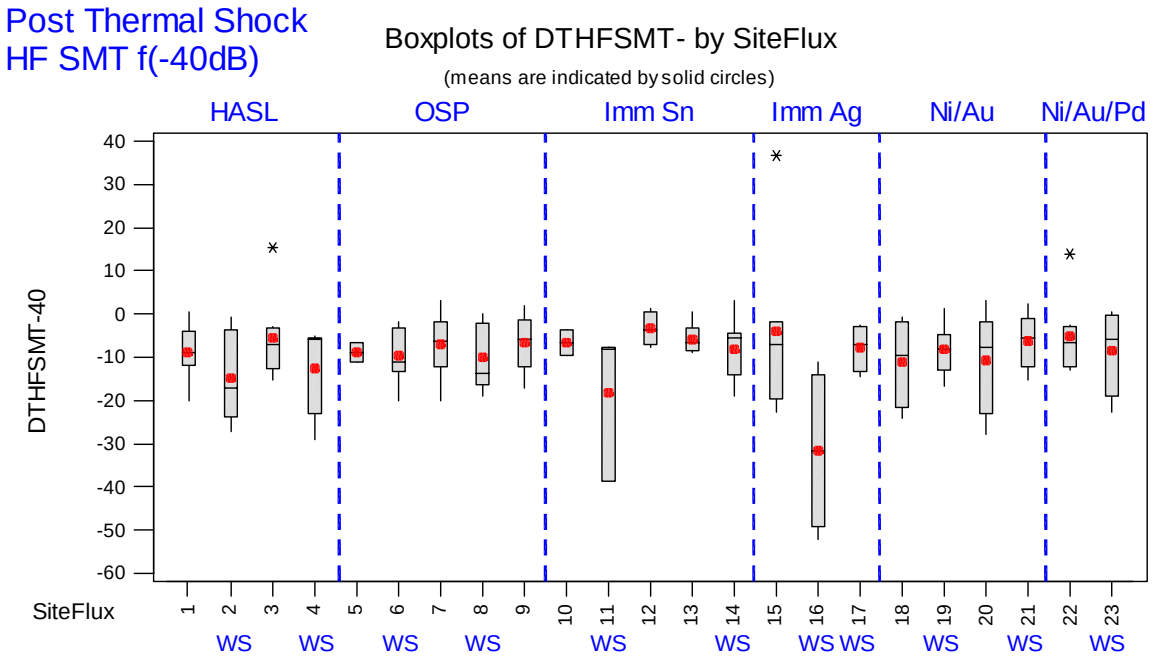

Figure F.27 Boxplot Displays for HF SMT f(-40dB) Post TS - Pre-test Measurements (MHz) by Surf. Finish
(Acceptance Criterion = ±50Mhz of Pre-test)

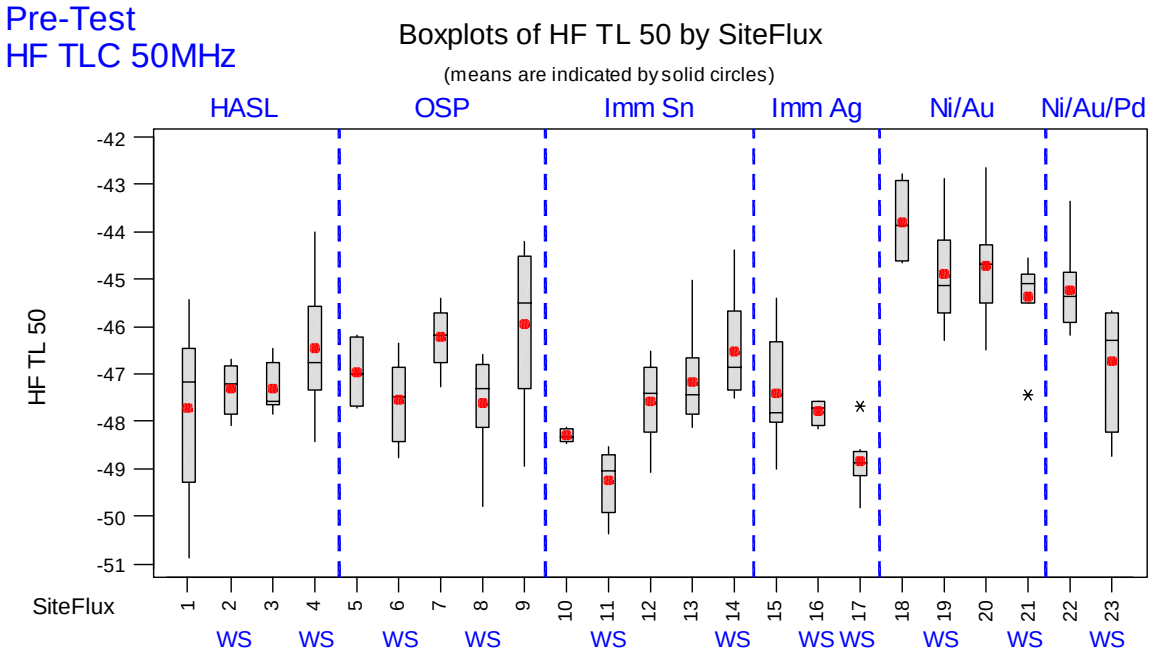

Figure F.28 Boxplot Displays for HF TLC 50MHz Measurements (dB) at Pre-test by Surface Finish

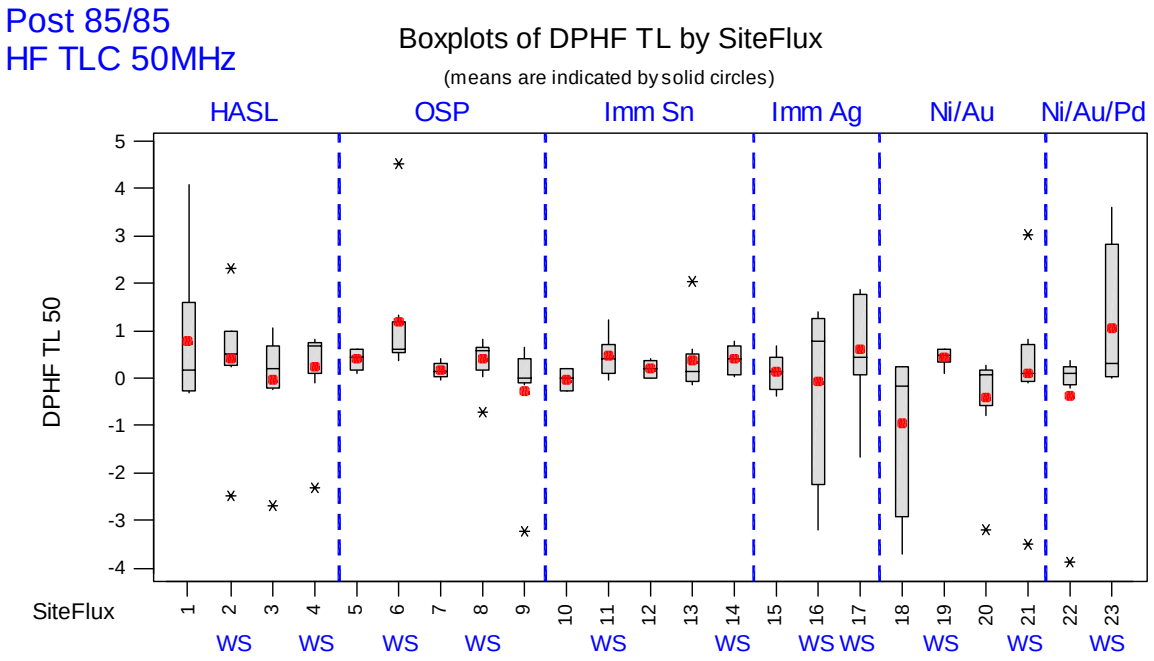

Figure F.29 Boxplot Displays for HF TLC 50MHz Post 85/85 - Pre-test Measurements (dB) by Surf. Finish
(Acceptance Criterion = ±5 dB of Pre-test)

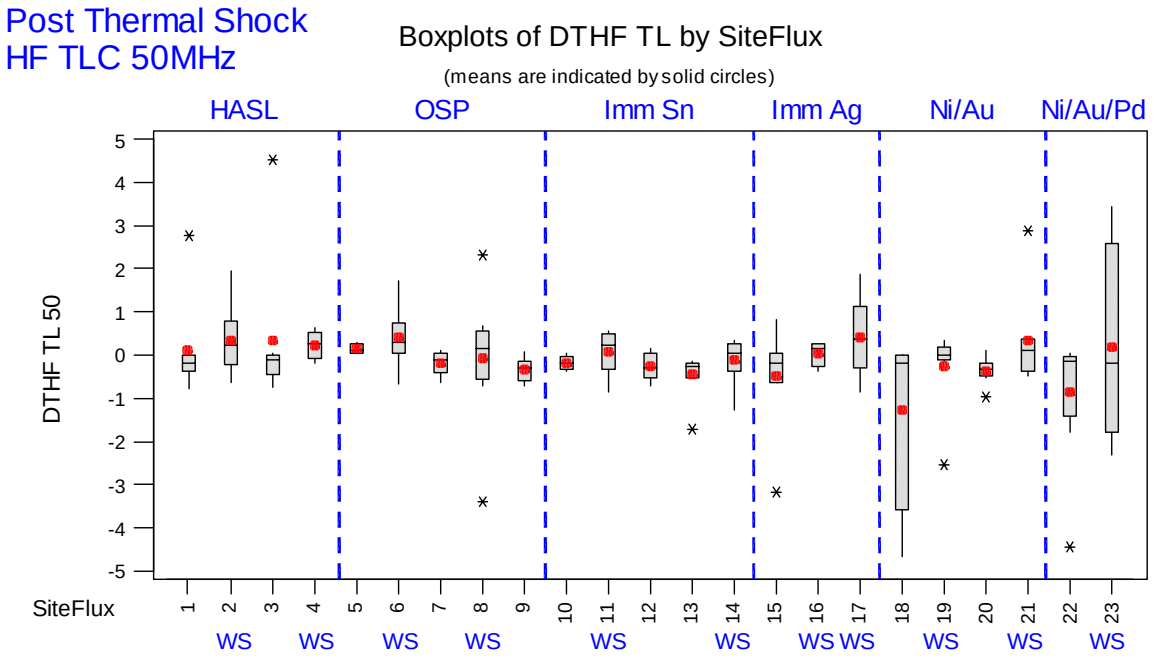

Figure F.30 Boxplot Displays for HF TLC 50MHz Post TS - Pre-test Measurements (dB) by Surface Finish
(Acceptance Criterion = ±5 dB of Pre-test)

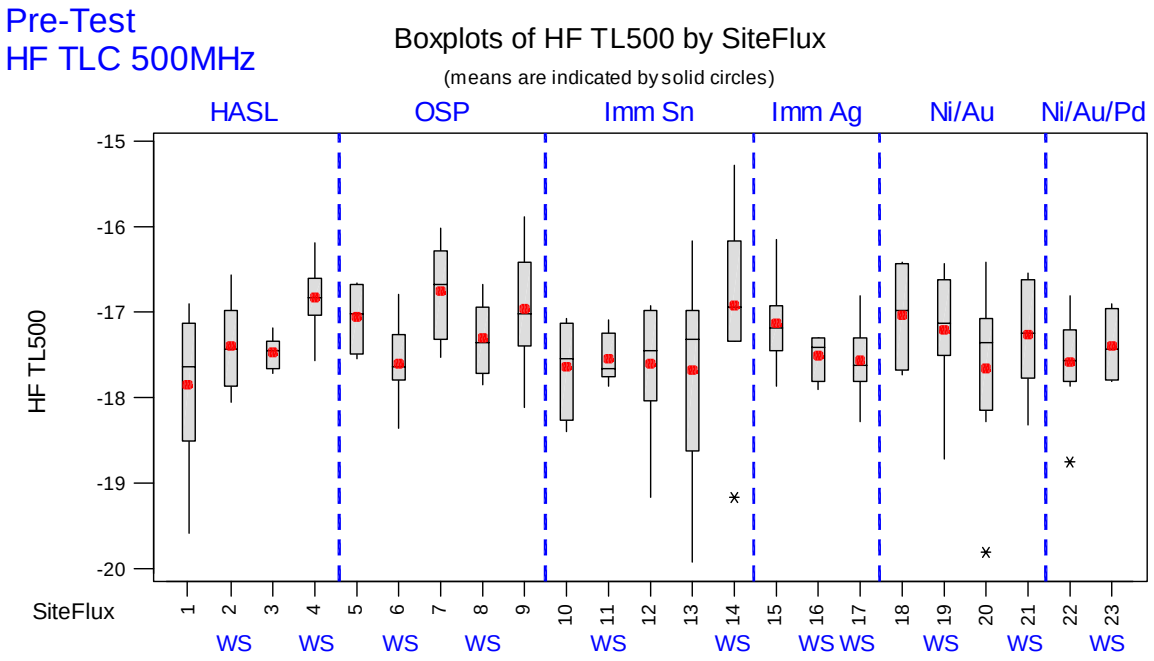

Figure F.31 Boxplot Displays for HF TLC 500MHz Measurements (dB) at Pre-test by Surface Finish

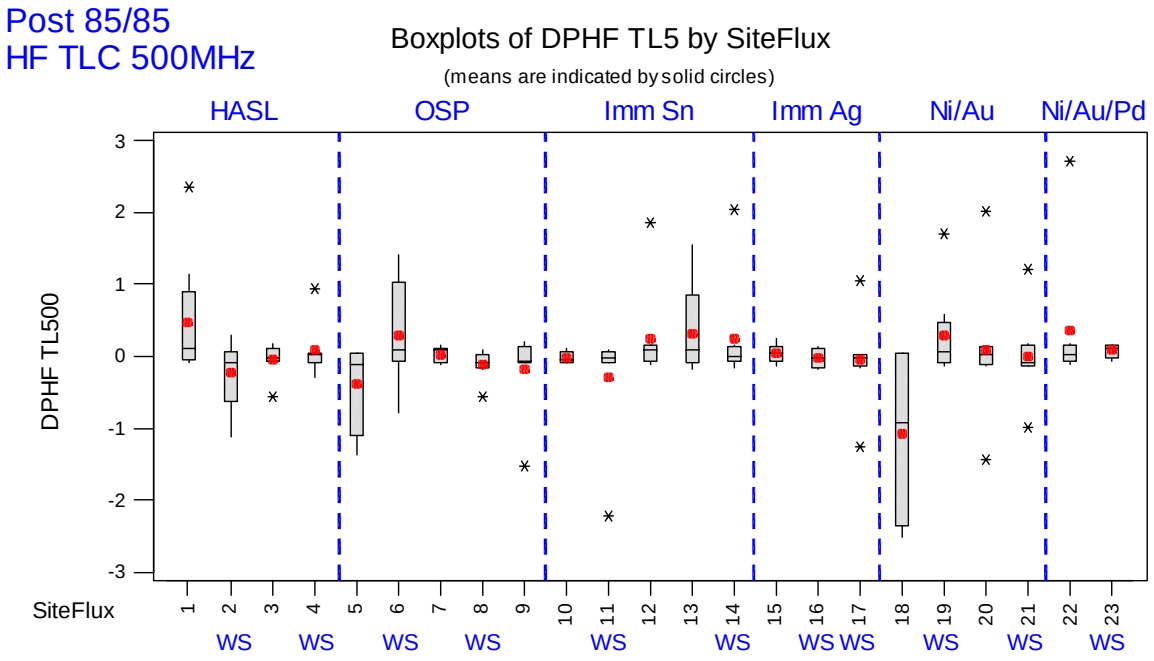

Figure F.32 Boxplot Displays for HF TLC 500MHz Post 85/85 - Pre-test Measurements (dB) by Surf. Finish
(Acceptance Criterion = ±5 dB of Pre-test)

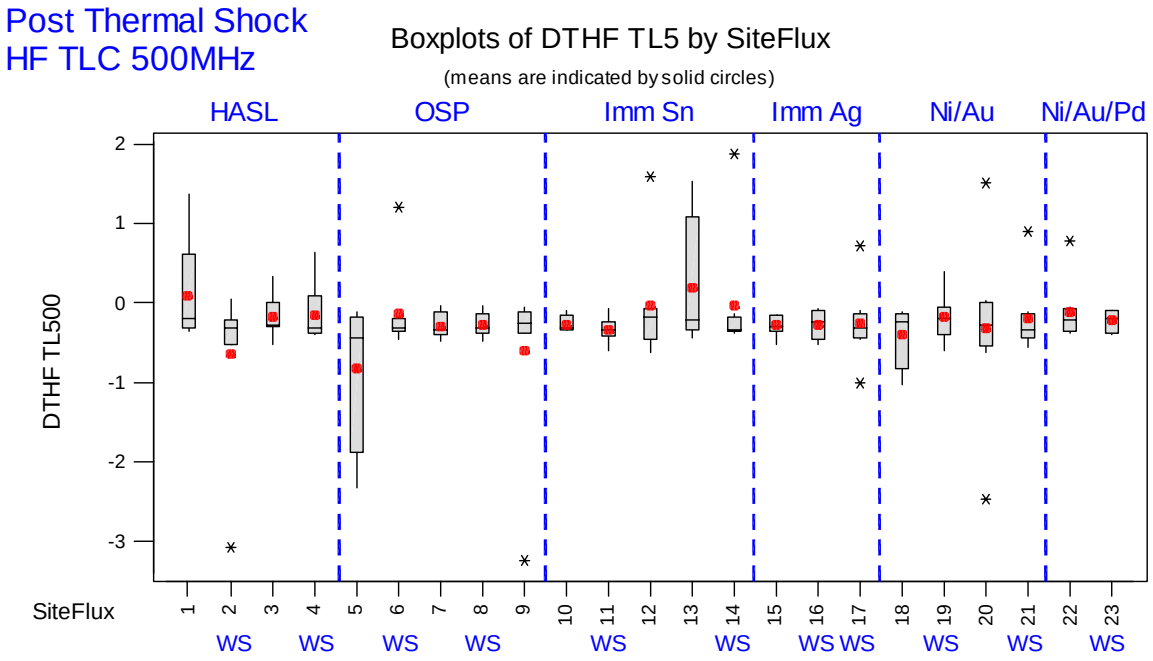

Figure F.33 Boxplot Displays for HF TLC 500MHz Post TS - Pre-test Measurements (dB) by Surface Finish
(Acceptance Criterion = ±5 dB of Pre-test)

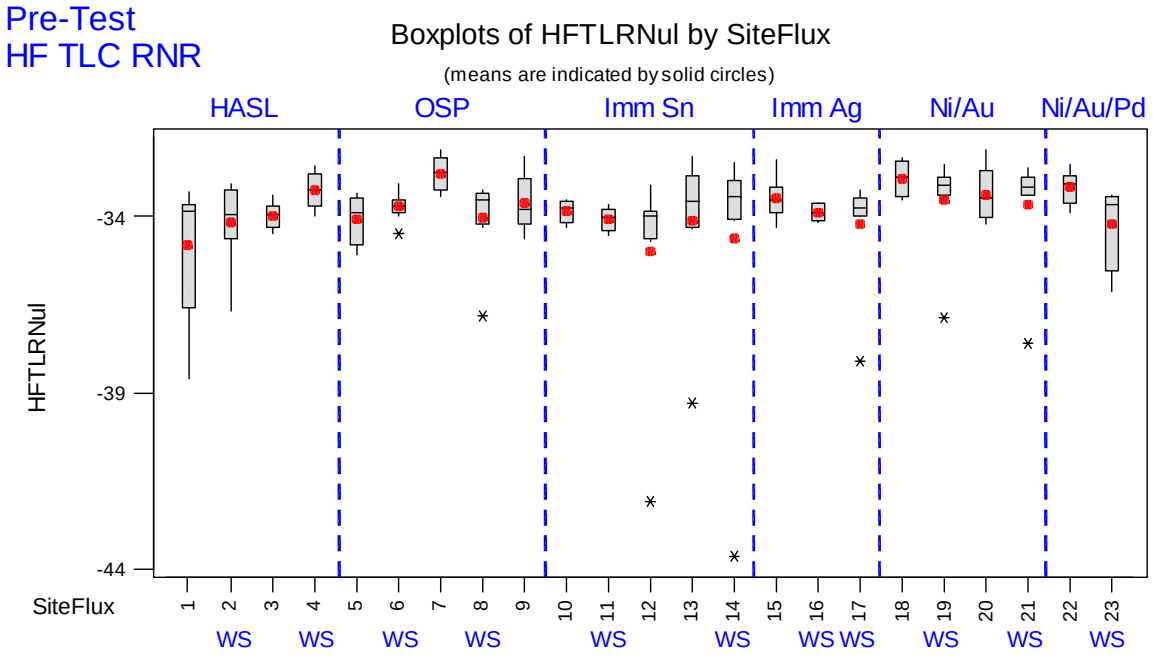

Figure F.34 Boxplot Displays for HF TLC RNR Measurements (dB) at Pre-test by Surface Finish

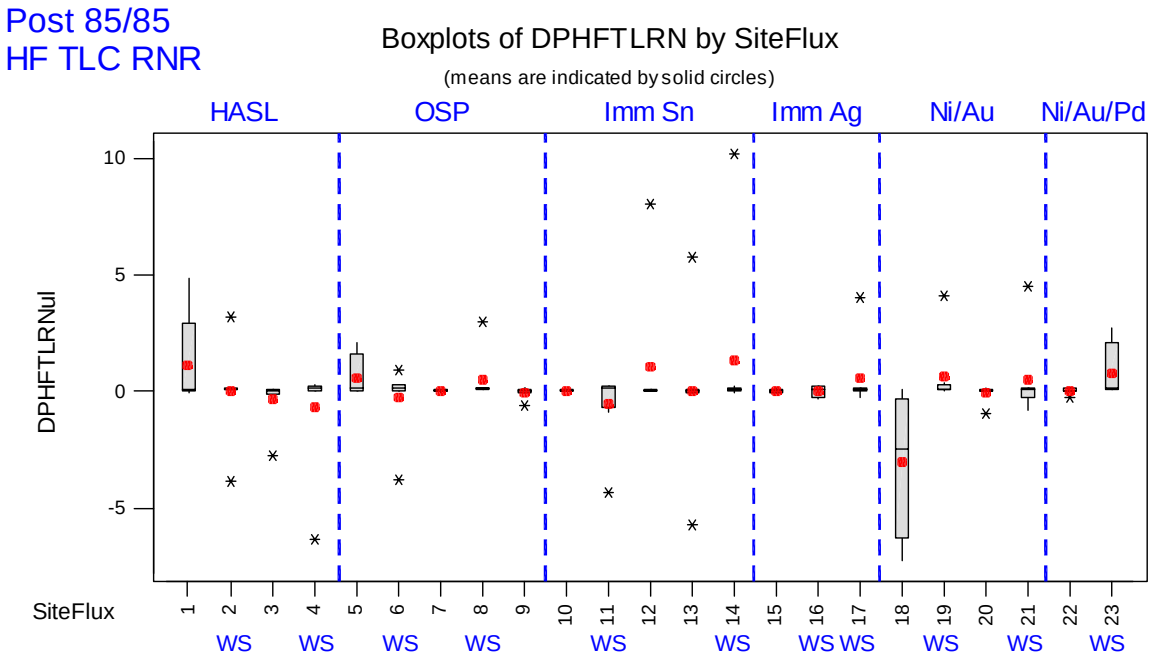

Figure F.35 Boxplot Displays for HF TLC RNR at Post 85/85 - Pre-test Measurements (dB) by Surf. Finish
(Acceptance Criterion = <10 dB increase over Pre-test)

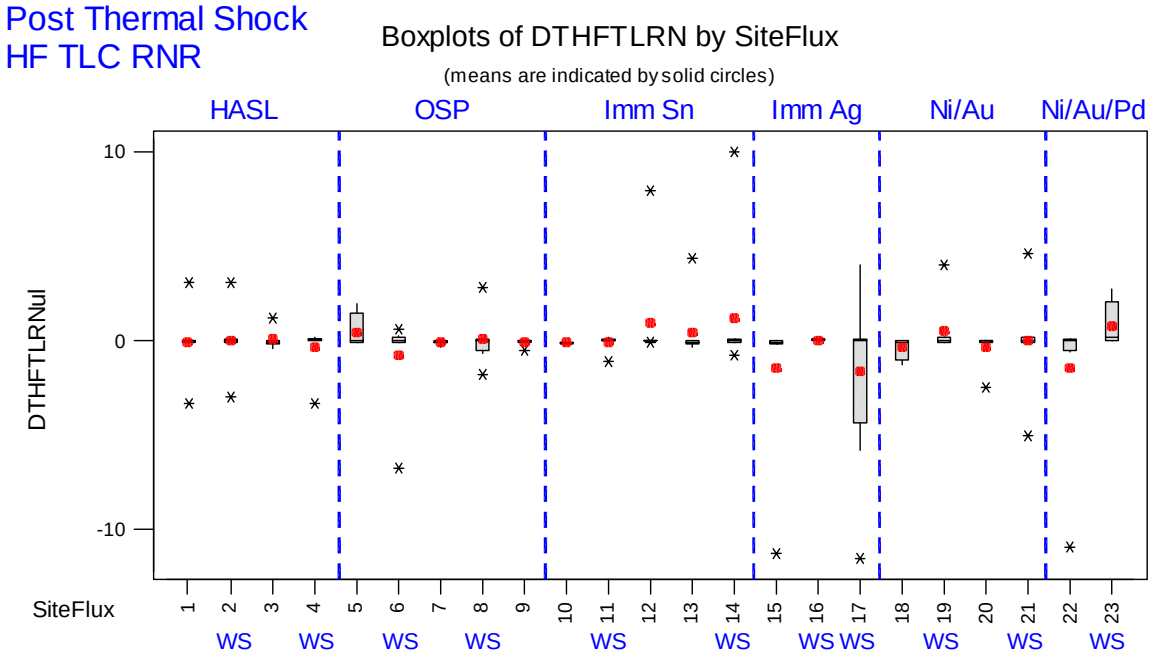

Figure F.36 Boxplot Displays for HF TLC RNR Post TS - Pre-test Measurements (dB) by Surface Finish
(Acceptance Criterion = <10 dB increase over Pre-test)

Post Thermal Shock
10-Mil Pads

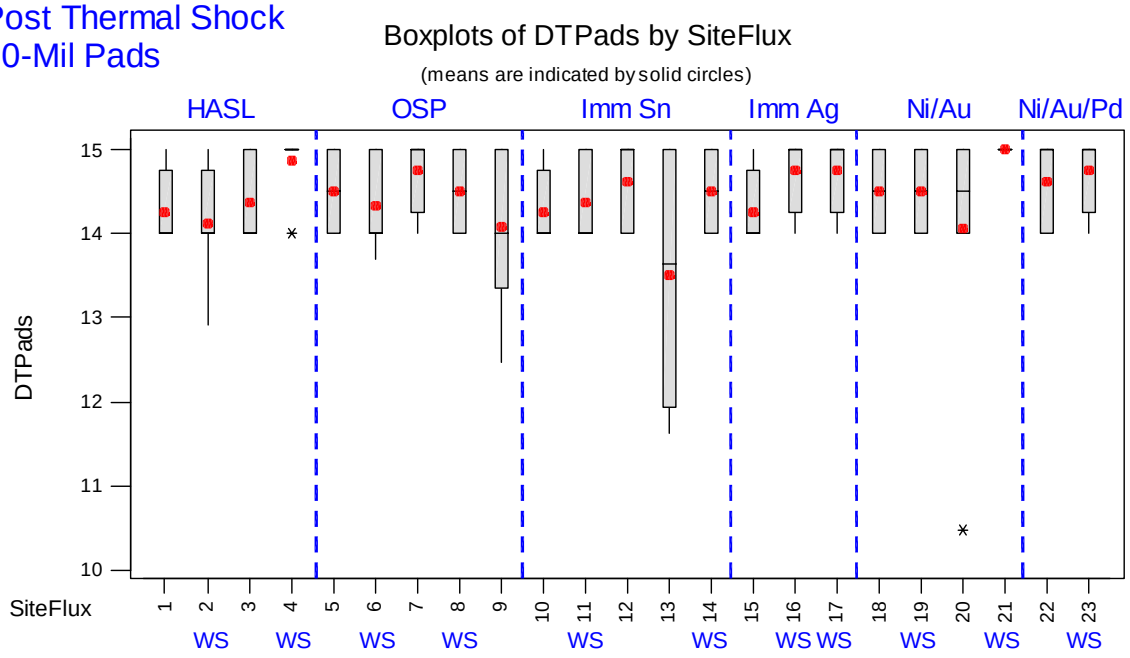

Figure F.37 Boxplot Displays for 10-Mil Pad Post TS - Pre-test Measurements (log_{10} ohms) **by Surf. Finish**
(Acceptance Criterion = Resistance > 7.7 log_{10} ohms)

Post Mechanical Shock
10-Mil Pads

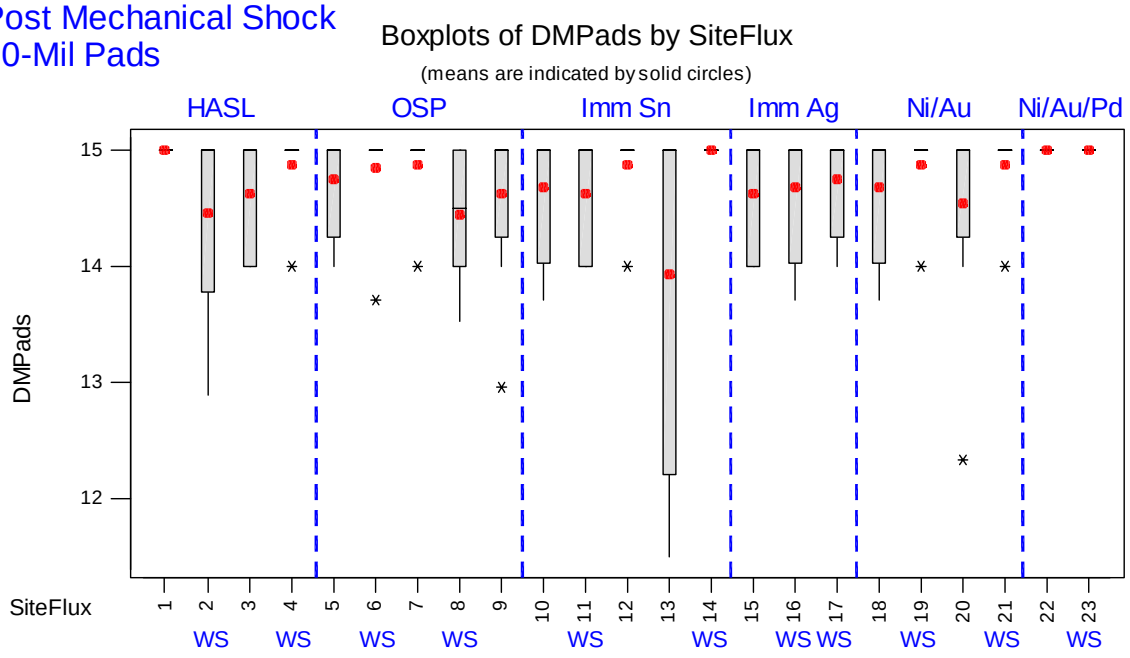

Figure F.38 Boxplot Displays for 10-Mil Pad Post MS - Pre-test Measurements (log_{10} ohms) **by Surf. Finish**
(Acceptance Criterion = Resistance > 7.7 log_{10} ohms)

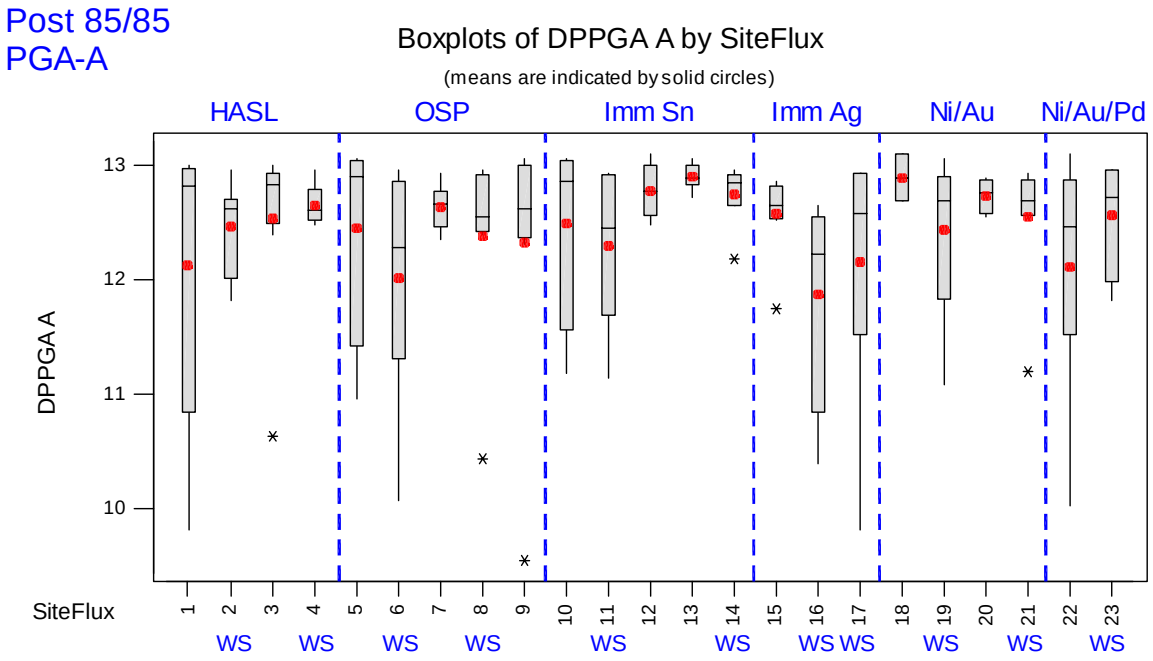

Figure F.39 Boxplot Displays for PGA-A Post 85/85 - Pre-test Measurements (log_{10} ohms) **by Surface Finish**
(Acceptance Criterion = Resistance > 7.7 log_{10} ohms)

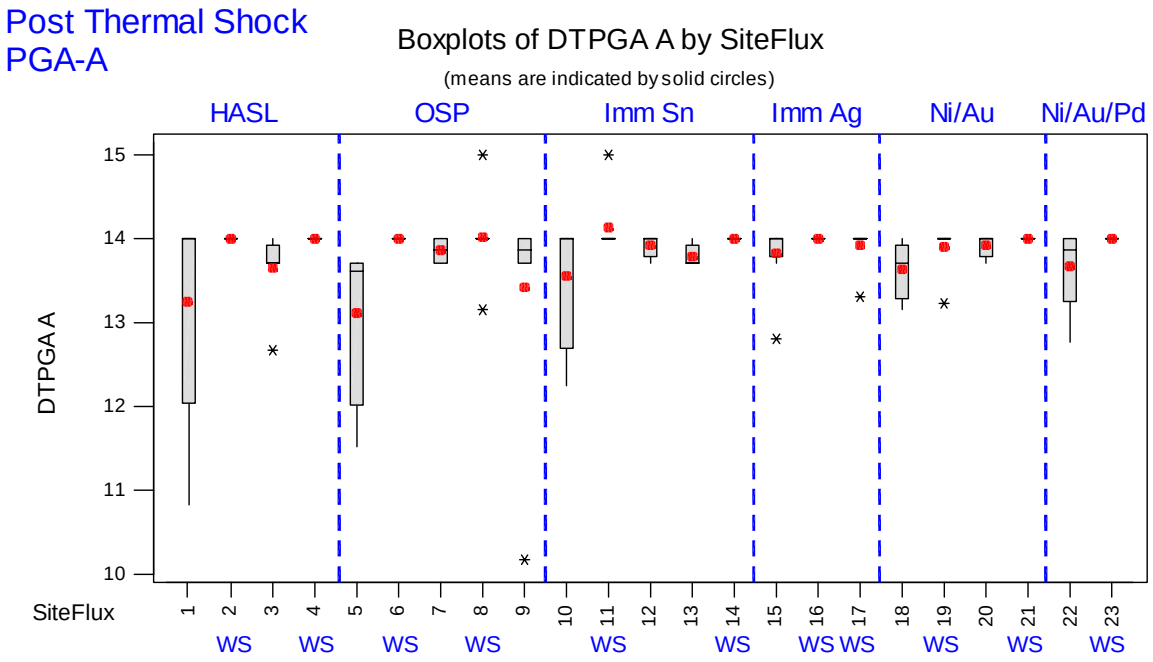

Figure F.40 Boxplot Displays for PGA-A Post TS - Pre-test Measurements (log_{10} ohms) **by Surface Finish**
(Acceptance Criterion = Resistance > 7.7 log_{10} ohms)

Post Mechanical Shock
PGA-A

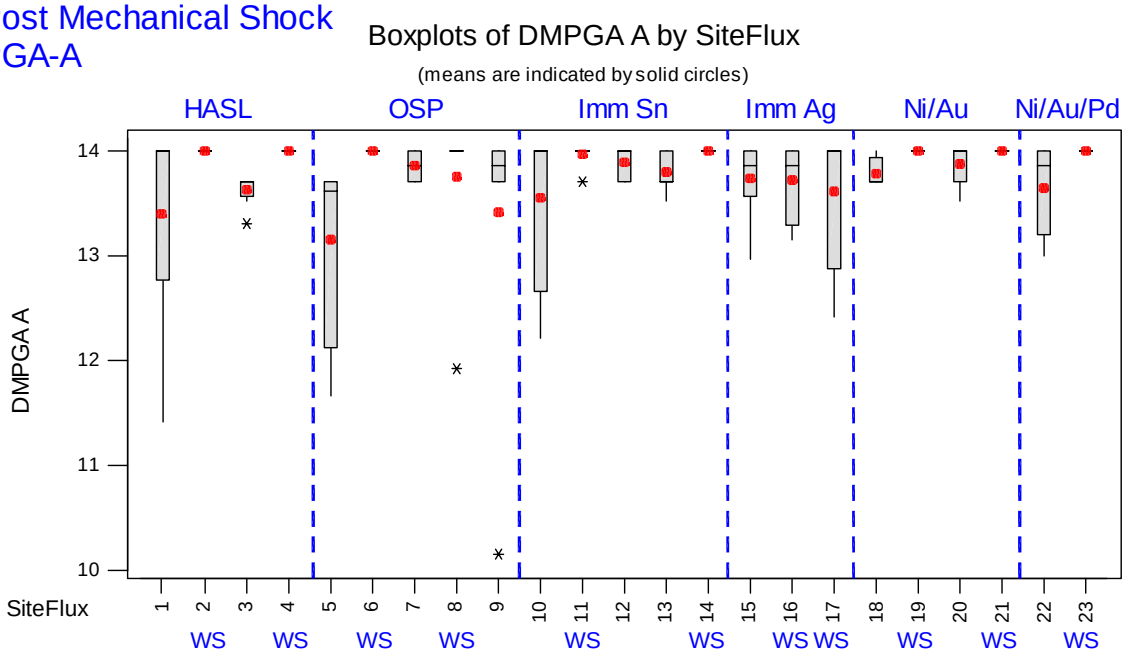

Figure F.41 Boxplot Displays for PGA-A Post MS - Pre-test Measurements (log_{10} ohms) **by Surface Finish**
(Acceptance Criterion = Resistance > 7.7 log_{10} ohms)

Post 85/85
PGA-B

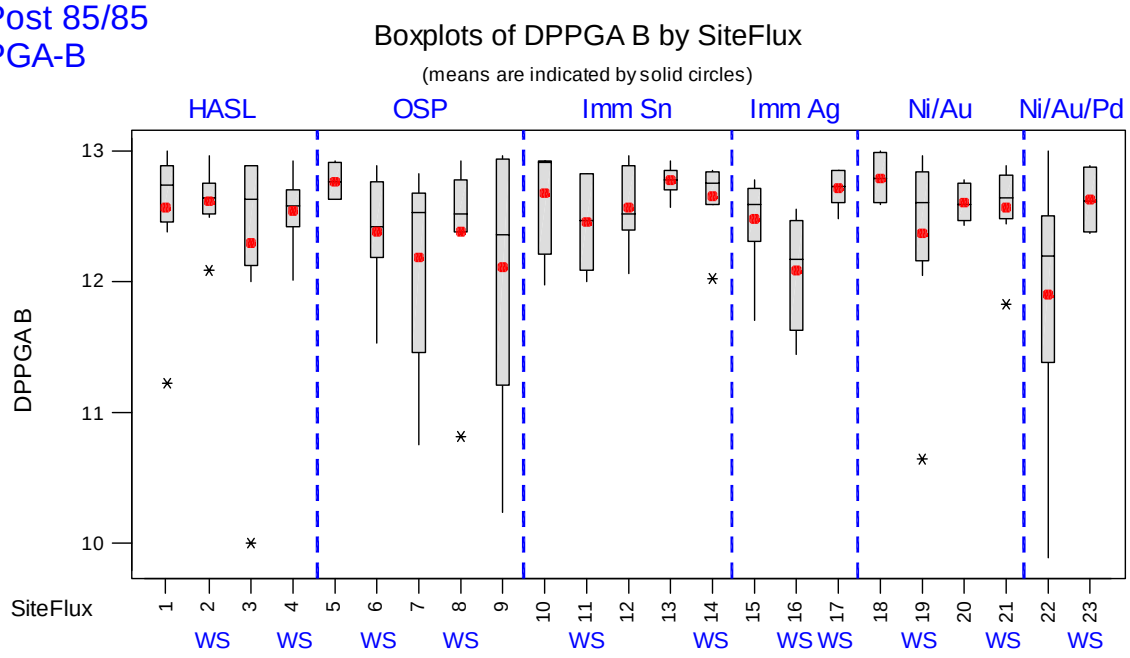

Figure F.42 Boxplot Displays for PGA-A Post 85/85 - Pre-test Measurements (log_{10} ohms) **by Surface Finish**
(Acceptance Criterion = Resistance > 7.7 log_{10} ohms)

Post Thermal Shock
PGA-B

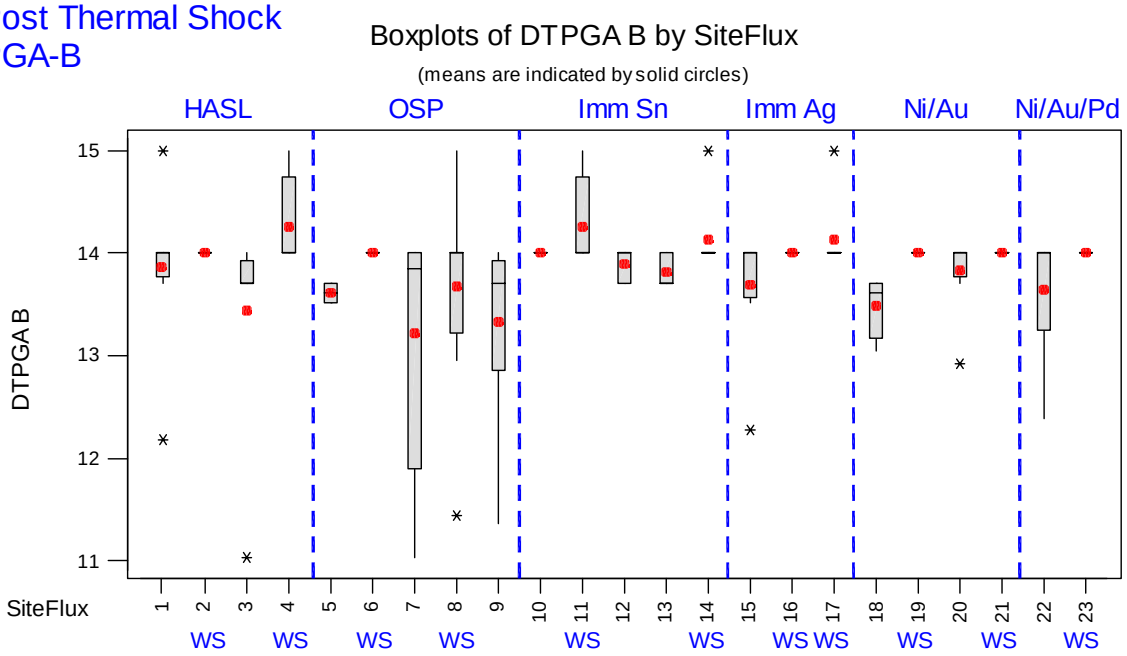

Figure F.43 Boxplot Displays for PGA-A Post TS - Pre-test Measurements (log_{10} ohms) **by Surface Finish**
(Acceptance Criterion = Resistance > 7.7 log_{10} ohms)

Post Mechanical Shock
PGA-B

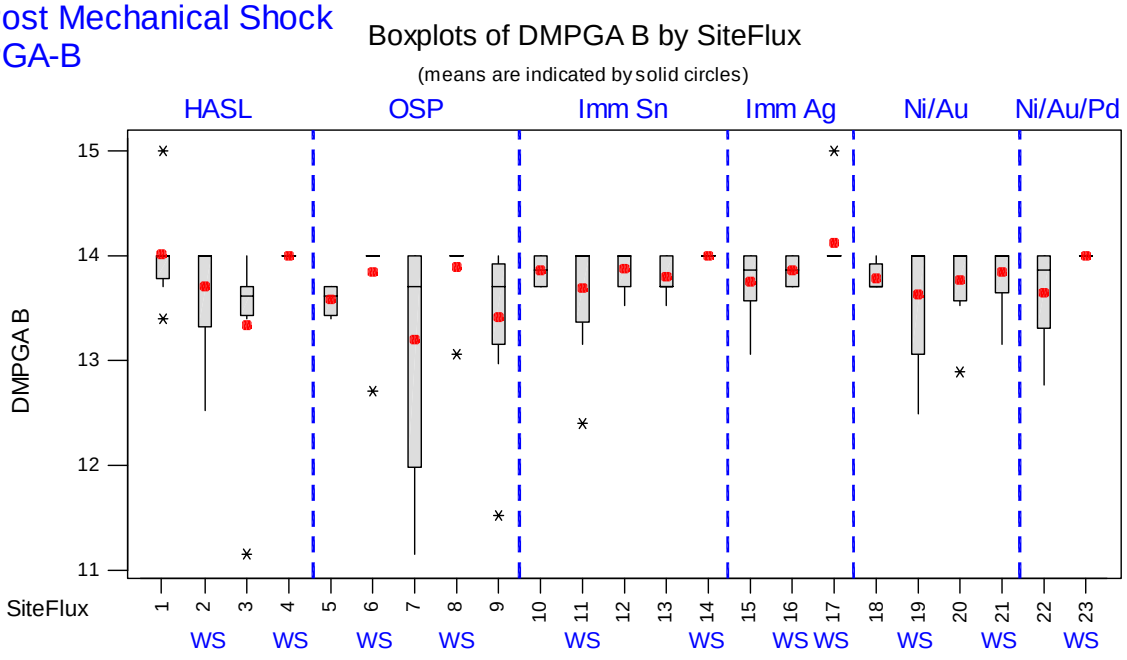

Figure F.44 Boxplot Displays for PGA-A Post MS - Pre-test Measurements (log_{10} ohms) **by Surface Finish**
(Acceptance Criterion = Resistance > 7.7 log_{10} ohms)

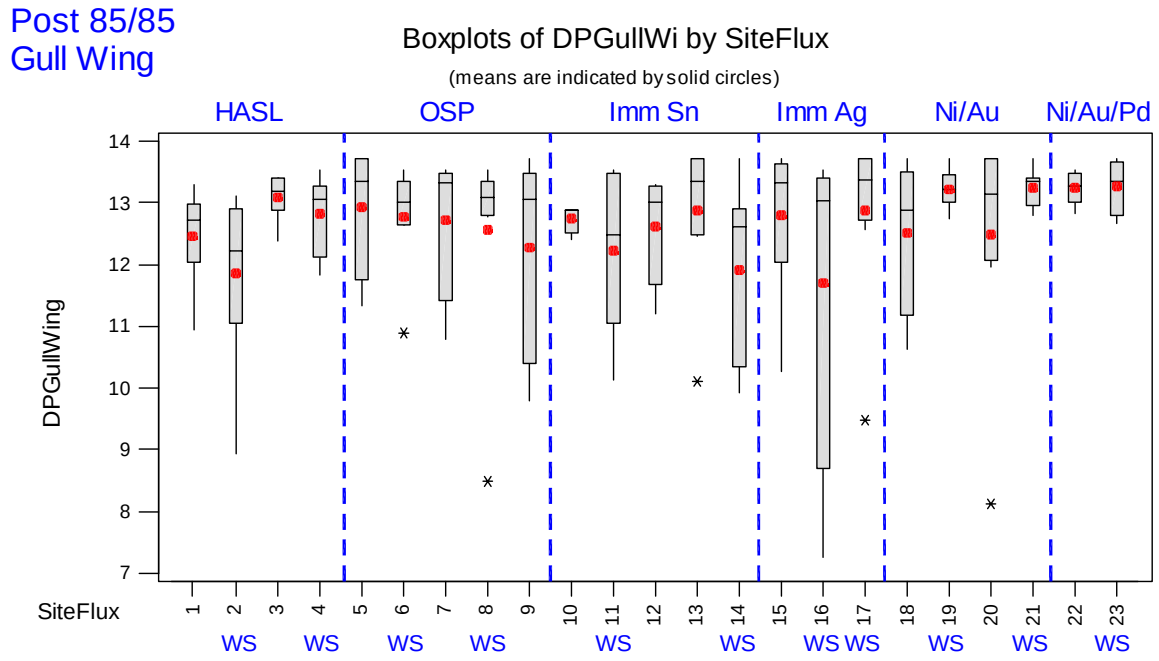

Figure F.45 Boxplot Displays for the Gull Wing Post 85/85 - Pre-test Measuremts. (log_{10} ohms) **by Surf. Fin.**
(Acceptance Criterion = Resistance > 7.7 log_{10} ohms)

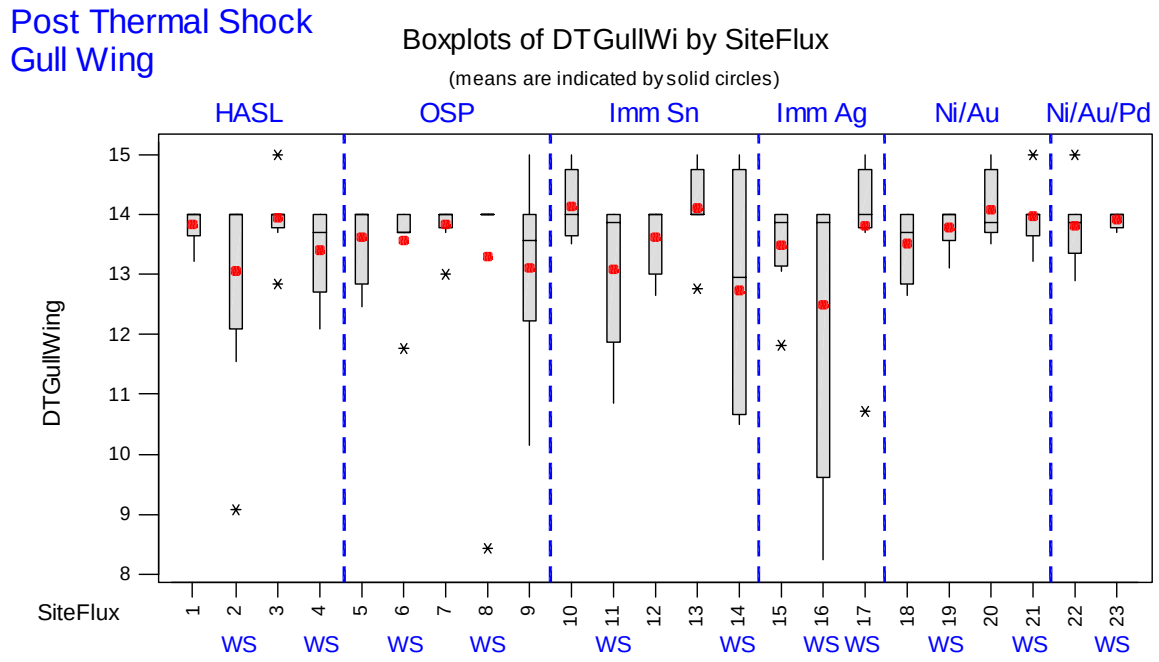

Figure F.46 Boxplot Displays for the Gull Wing Post TS - Pre-test Measurements (log_{10} ohms) **by Surf. Fin.**
(Acceptance Criterion = Resistance > 7.7 log_{10} ohms)

Post Mechanical Shock
Gull Wing

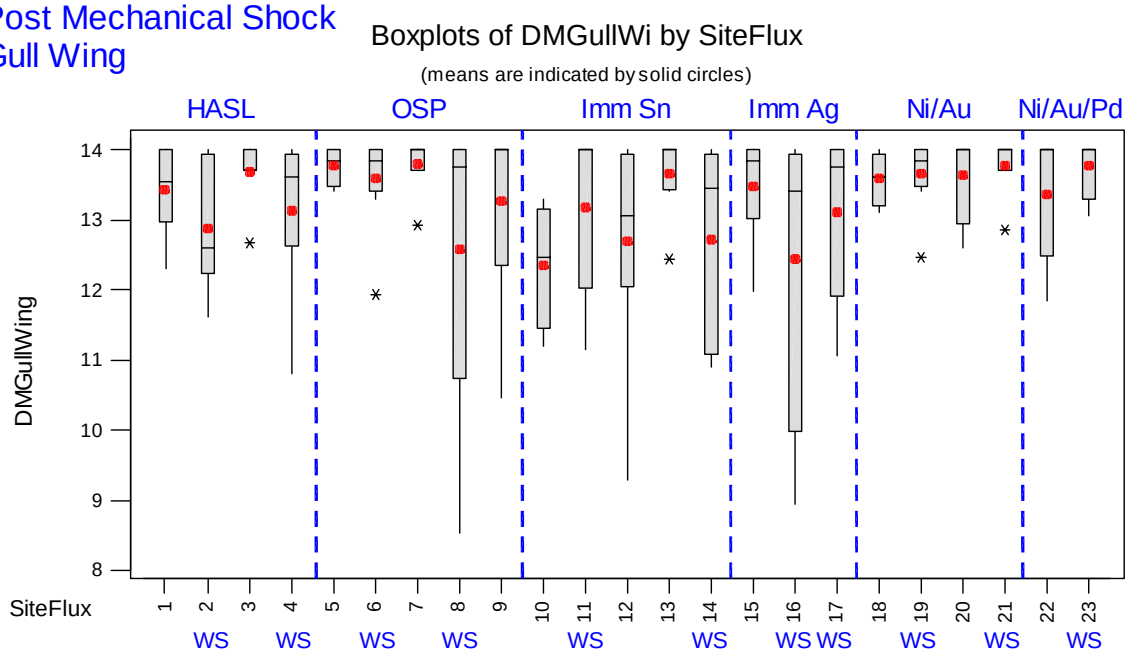

Figure F.47 Boxplot Displays for the Gull Wing Post MS - Pre-test Measurements (log_{10} ohms) **by Surf. Fin.**
(Acceptance Criterion = Resistance > 7.7 log_{10} ohms)

Pre-Test
Stranded Wire 1

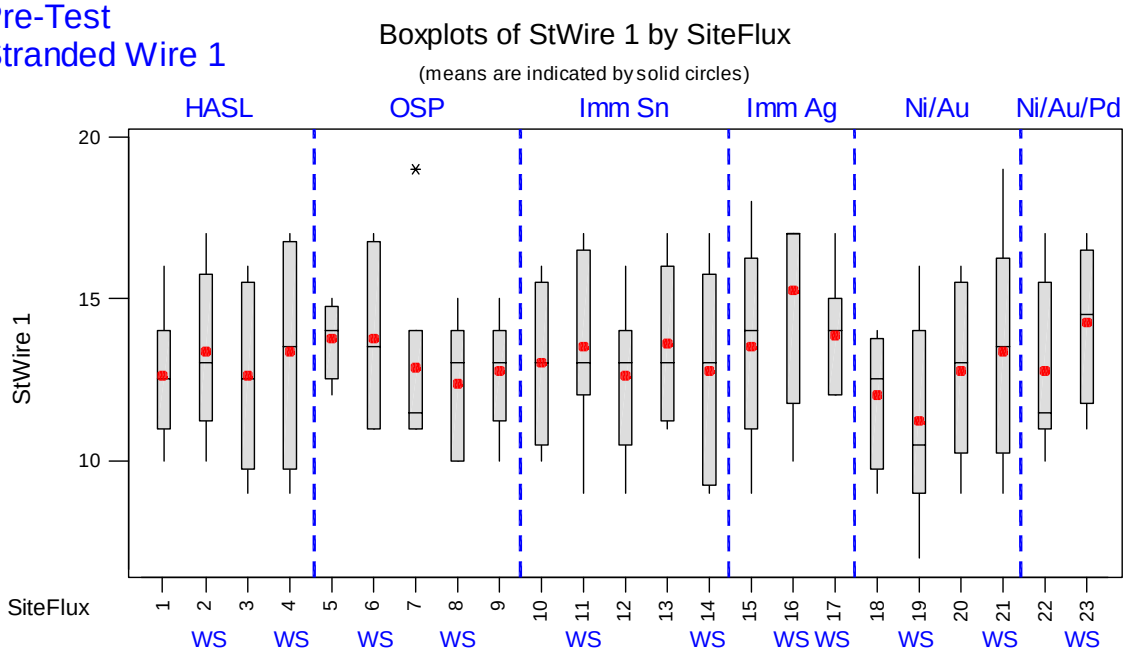

Figure F.48 Boxplot Displays for the Stranded Wire 1 Measurements (volts) at Pre-test by Surface Finish

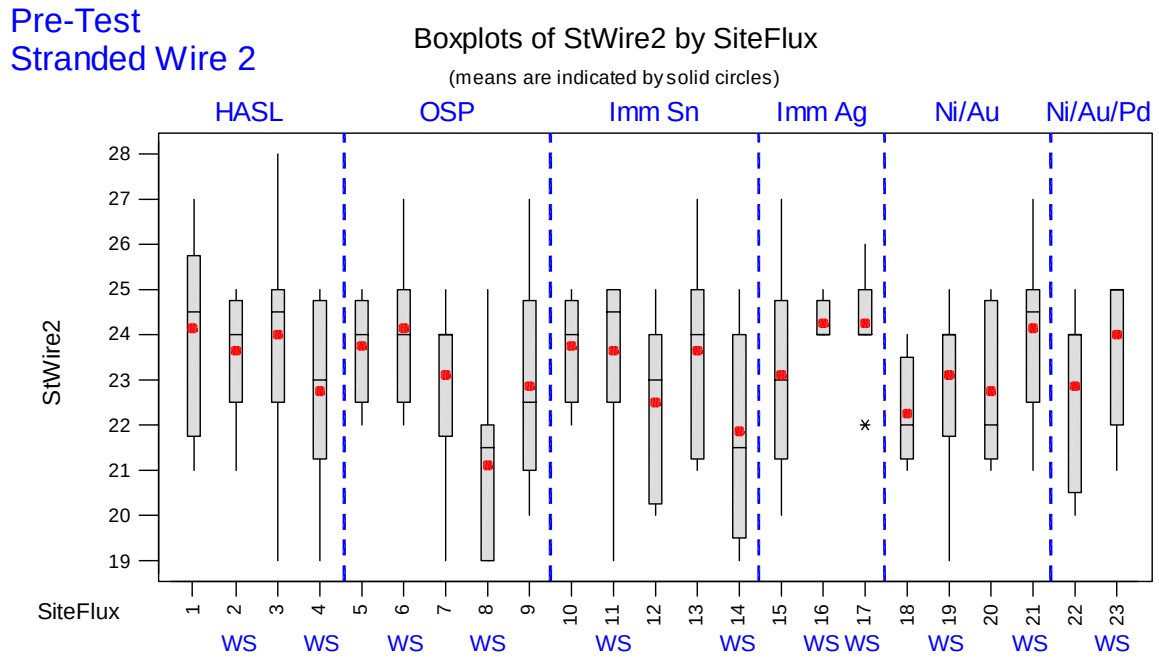

Figure F.49 Boxplot Displays for the Stranded Wire 2 Measurements (volts) at Pre-test by Surface Finish

F.10 Design and CCAMTF Baseline Testing of the Test PWA

F.10.1 Test PWA

As mentioned in Chapter 4, the primary test vehicle used in both the DfE project and in the CCAMTF evaluation of low-residue technology was an electrically functional PWA. This assembly was designed at Sandia National Laboratories in Albuquerque based on input from LRSTF members and from military and industry participants during open review meetings held by the task force. The PWA measures 6.05" x 5.8" x 0.062" and is divided into six sections, each containing one of the following types of electronic circuits:

- High current low voltage (HCLV)
- High voltage low current (HVLC)
- High speed digital (HSD)
- High frequency (HF)
- Other networks (ON)
- Stranded wire (SW)

The layout of the functional assembly is shown in Figure F.50. The components in the HCLV, HVLC, HSD, and HF circuits represent two principal types of soldering technology:

- Plated through hole (PTH)—leaded components are soldered through vias in the circuit board by means of a wave soldering operation
- Surface mount technology (SMT)—leadless components are soldered to pads on the circuit board by passing the circuit board through a reflow oven.

The other networks (ON) are used for current leakage measurements: 10-mil pads, a socket for a PGA, and a gull wing. The two stranded wires (SW) are hand soldered.

The subsections for PTH and SMT components form separate electrical circuits. The PWA includes a large common ground plane, components with heat sinks, and mounted hardware.

Each subsection shown in Figure F.50 contains both functional and nonfunctional components (added to increase component density). A 29-pin PTH edge connector is used for circuit testing. High frequency connectors are used to ensure proper impedance matching and test signal fidelity as required. Board fabrication drawings, schematics, and a complete listing of all components are available by contacting the authors of this report. A discussion of each of the sections of the test PWA is now given. This discussion is supplemented with baseline test results for each of the 23 electrical responses listed in Table 4.1.

F.10.2 High Current Low Voltage

The HCLV section of the board is in the upper left-hand corner of PWA (see Figure F.50). The upper left-hand portion of this quadrant contains PTH components with SMT components immediately beneath.

Purpose of the HCLV Experiment

Performance of high-current circuits is affected by series resistance. Resistance of a conductor (including solder joints) is determined by the following equation:

$$R = \frac{\rho L}{A_c} ohms(\Omega) \tag{F.7}$$

where ρ = resistivity, the proportionality constant
L = length of the conductor
A_C = cross-sectional area of the conductor (solder joints)

Resistance is most likely to change due to cracking or corrosion of the solder joint that may be related to the soldering process. These conditions decrease the cross-sectional area of the solder joints, thus increasing resistance as shown in Equation F.7. Use of high current to test solder joint resistance makes detection of a change in resistance easier. A 5 Amperes (A) current was selected as a value that would cover most military applications. A change of resistance is most conveniently determined by measuring the steady state performance of the circuit, which will now be discussed.

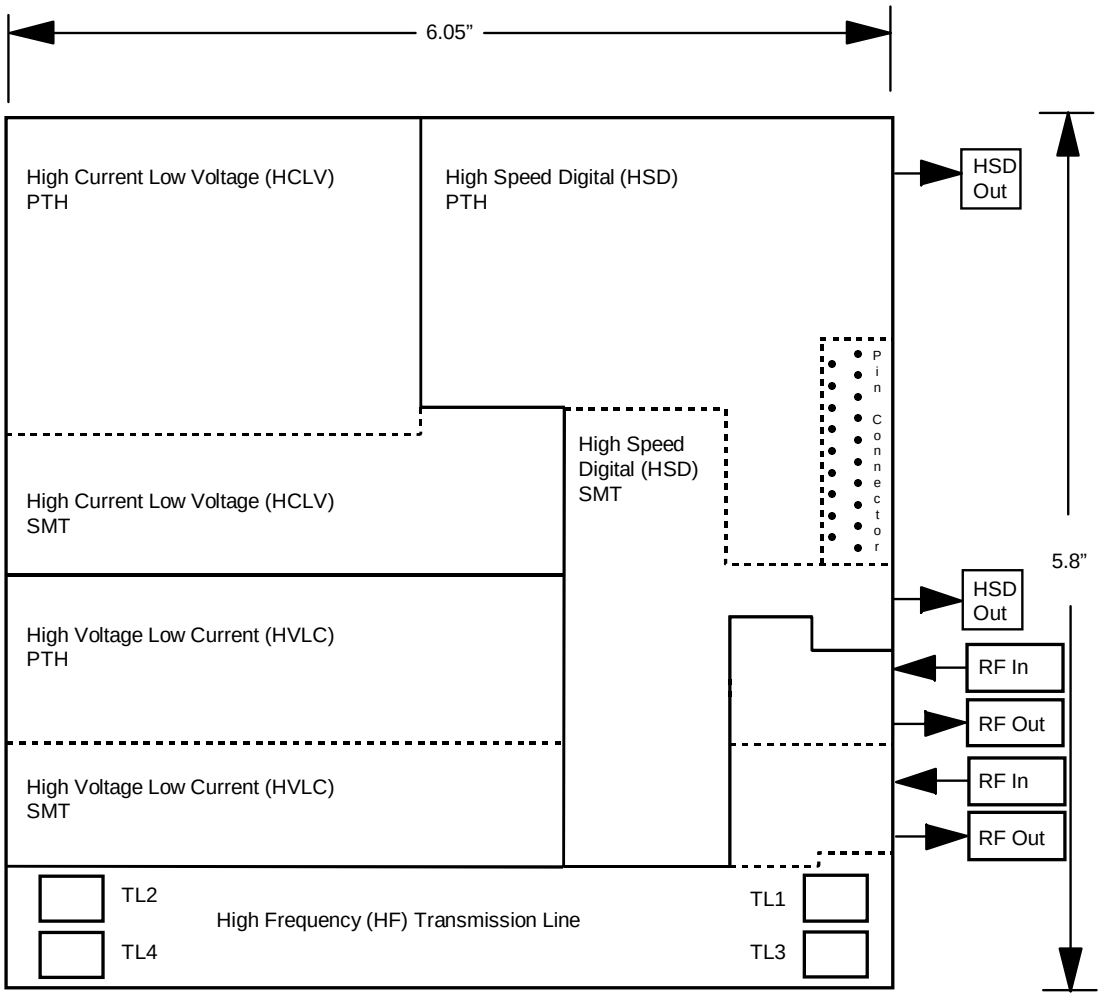

Figure F.50 Layout of the PWA Illustrating the Four Major Sections and Subsections

Steady State Circuit Performance

Overall circuit resistance, R_{total}, is the parallel combination of the seven resistors, R_1, R_2, ..., R_7, (all resistors = 10Ω) used in the HCLV circuit:

$$\frac{1}{R_{total}} = \frac{1}{R_1} + \frac{1}{R_2} + \frac{1}{R_2} + \cdots + \frac{1}{R_7} = \frac{7}{10\Omega} \tag{F.8}$$

$$R_{total} = \frac{10\Omega}{7} \tag{F.9}$$

Since a current (I) of 5A will be applied to the circuit, the resulting voltage (V), according to Ohm's Law, is

$$V = IR = 5A \times \frac{10\Omega}{7} = 7.14V \tag{F.10}$$

Changes in resistance are thus detected by changes in voltage. However, a pulse width had to be chosen that would not overstress the circuit components. With current equally divided among the seven parallel resistors, the power (P) dissipated in each resistor, according to Joule's Law, is:

$$P = I^2 R = \left(\frac{5A}{7}\right)^2 \times 10\Omega = 5.1Watts(W) \tag{F.11}$$

Since the power rating for the PTH wire-wound resistor is 3W, the rating is exceeded by a factor of 1.7 for steady state (5.1 / 3). Design curves from the resistor manufacturer indicate the PTH wire-wound resistors could tolerate the excess power for about 100*ms*. The SMT resistors are rated at 1W, so the steady state rating is exceeded by a factor of five. With the manufacturer unable to provide the pulse current capability of the SMT resistors, a pulse derating factor could not be determined. A pulse width of 100μ*s* was selected, which is three orders of magnitude less than the capability of the wire-wound resistors. This width is also sufficiently long for the circuit to achieve steady state before the measurement is taken.

Circuit Board Design

Traces carrying the 5A current were placed on an inner layer of the circuit board because: (1) the primary concern was the possible degradation of the solder connections as discussed above and (2) the bulk electrical characteristics (resistivity) of the traces should not be affected by flux residues. High-current trace widths were designed to be 250 mils whenever possible (following MIL-STD-275). This width with a 5A current should cause no more than a 30^oC temperature rise under steady-state conditions.

The resistor and capacitor values were selected to be readily available. If other values are used, care should be taken to not over-stress the parts, as discussed above.

Baseline Testing Results for HCLV

A gauge repeatability and reproducibility (GR&R) study (Iman et al, 1998) was conducted for the CCAMTF ATS as part of the CCAMTF program. The LRSTF PWA was utilized in this study. In particular, 120 LRSTF PWAs were tested for each of the following four surface finishes: OSP,

immersion Ag, immersion Au/Pd and HASL with solder mask. Half the PWAs in each surface finish group were processed with low-residue (LR) flux and the other half with water soluble (WS) flux. Data modeling showed that surface finish and flux type did not significantly affect the voltage measurements for HCLV PTH and HCLV SMT. Figures F.51 and F.52 provide dotplot displays of 4 × 120 = 480 voltage measurements for HCLV PTH and 480 voltage measurements for HCLV SMT, respectively. The summary statistics HCLV PTH and HCLV SMT voltages are given in Table F.31.

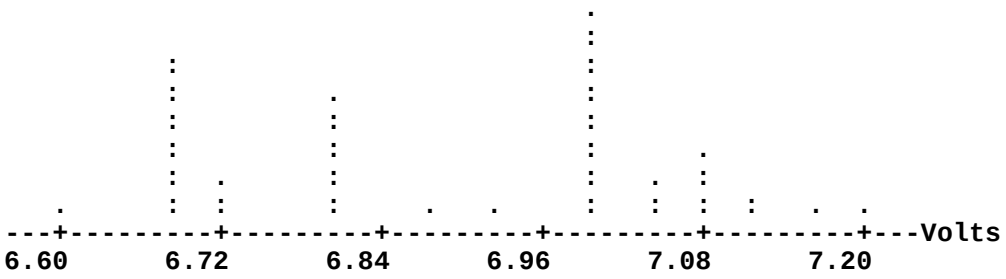

Figure F.51. Dotplot for 480 HCLV PTH Voltage Measurements (each dot represents up to 10 points)

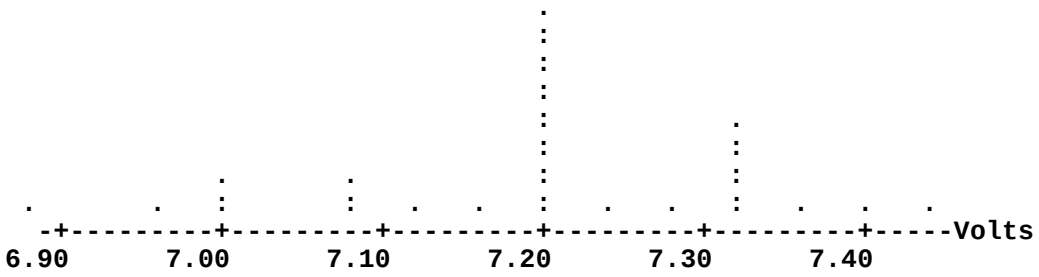

Figure F.52. Dotplot for 480 HCLV SMT Voltage Measurements (each dot represents up to 16 points)

Table F.31. Summary Statistics for HCLV Circuitry Test Measurements

Circuitry	Mean	Median	St. Dev.	Min	Max
HCLV PTH	6.88V	6.96	0.163	6.60	7.20
HCLV SMT	7.20V	7.20	0.106	6.88	7.44

F.10.3 High Voltage Low Current

The HVLC circuitry is immediately below the HCLV circuitry and above the high frequency transmission lines in Figure F.50. The PTH circuitry is in the upper part of this subsection and the SMT circuitry is in the lower part.

Purpose of the HVLC Experiment

Flux residues could decrease the insulation resistance between conductors. The impact of this decrease could be significant in circuits with a high voltage gradient across the insulating region. Decreased resistance can be detected by an increase in current when a high voltage is applied to the circuit. A voltage of 250V was selected as the high potential for this test. The change in leakage current is determined by measuring the steady-state performance of the circuit, which will now be discussed.

Steady State Circuit Performance

Steady-state operation of the HVLC circuit can be determined by considering only the resistors. The total resistance of the series combination is the sum of the resistances.

$$R_{total} = R_1 + R_2 + R_3 + R_4 = R_5 = 50\,M\Omega \tag{F.12}$$

since all resistors are 10MΩ each. From Ohm's law, the current flowing into the circuit with 250V applied is

$$I = \frac{V}{R} = \frac{250V}{50\,M\Omega} = 5\mu A \tag{F.13}$$

Care was taken to not overstress the individual components in the circuits. The voltage stress across each resistor-capacitor pair is one-fifth of the applied 250V, or 50V. The voltage ratings are 250V for the PTH resistors, 200V for the SMT resistors, and 250V for all the capacitors. Power rating is not a concern due to the low current.

Circuit Board Design

High voltage traces were placed next to ground potential traces by design. The spacings between the high voltage and intermediate traces were selected using MIL-STD-275.

Voltage	Spacing Between Traces (mils)
0 – 100	5
101 – 300	15
301 – 500	30

These guidelines were followed except the 5-mil spacing, where 10 mils was used to facilitate board fabrication. Table F.32 lists the voltage on various board circuit traces and the spacing to the adjacent ground trace.

Resistors and capacitors were selected to have readily available values—different values could have been used to achieve particular experimental goals. For instance, higher resistance values could be used with lower value capacitors. Reverse biased, low-leakage diodes could also be used for higher sensitivity to parasitic leakage resistance.

Baseline Testing Results for HVLC

Data modeling showed that surface finish and flux type had very little effect on the voltage measurements for HVLC PTH and HVLC SMT. Figures F.53 and F.54 provide dotplot displays of 480 voltage measurements for HVLC PTH and HVLC SMT, respectively. The summary statistics for HVLC PTH and HVLC SMT voltages are given in Table F.33. Note that two slight outliers for HVLC PTH are identified in Table F.33, but are not included in Figure F.53.

Table F.32 HVLC Circuit Board Trace Potentials

Technology	Trace Connected to:		Potential (V)	Trace Length at Potential (in)	Spacing (mils)
	Resistor	Capacitor			
PTH	R15	C21	250	0.8	30
			200	0.4	15
	R16	C22	200	0.4	15
			150	NA	
	R17	C23	150	NA	
			100	0.4	10
	R18	C24	100	0.4	10
			50	NA	
	R19	C25	50	NA	
SMT	R20	C26	250	5.0	30
			200	1.0	15
	R21	C27	200	1.0	15
			150	NA	
	R22	C28	150	NA	
			100	0.9	10
	R23	C29	100	0.9	10
			50	NA	
	R24	C30	50	NA	

NA = not applicable since no 50V or 150V traces were adjacent to ground potential

Table F.33 Summary Statistics for HVLC Circuitry Test Measurements (sans outliers)

Circuitry	Mean	Median	St. Dev.	Min	Max	Outliers	
HVLC PTH	5.04µA	5.04	0.024	4.972	5.148	5.203	5.232
HVLC SMT	4.95µA	4.95	0.011	4.914	4.976		

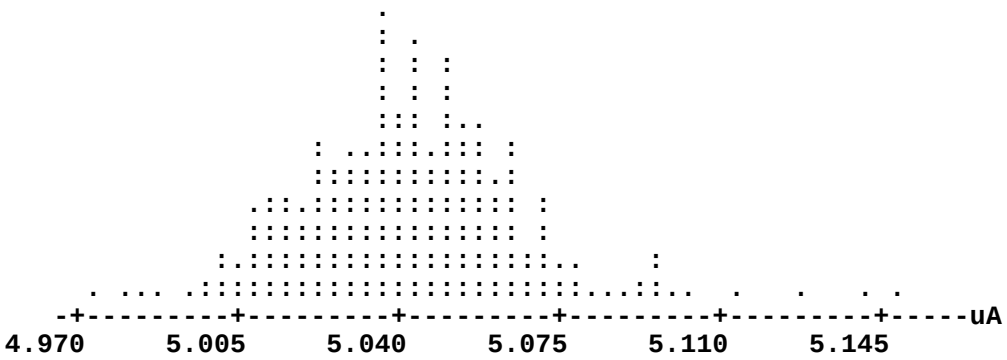

Figure F.53 Dotplot of 478 Voltage Measurements for HVLC PTH (each dot represents up to 2 points)

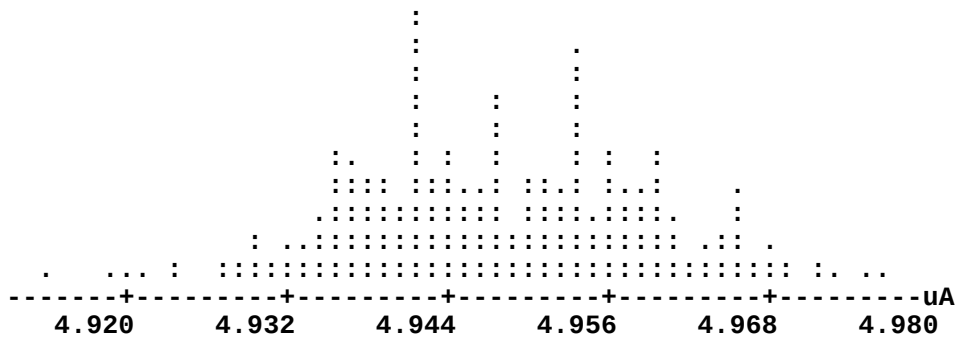

Figure F.54 Dotplot of 480 Voltage Measurements for HVLC SMT (each dot represents up to 2 points)

F.10.4 High Speed Digital

The HSD circuitry is in the upper right-hand corner of the LRSTF PWA shown in Figure F.50. This subsection contains the PTH circuitry and consists of two 14-pin Dual In-line Package (DIP) integrated circuits (ICs). The SMT subsection IC is a single 20-pin leadless chip carrier (LCC) package. Each of these ICs is a "Fast" bi-polar digital "QUAD-DUAL-INPUT-NAND-GATE." Both subsections contain two ceramic capacitors that bypass spurious noise on the power input line (VCC) to the ICs and an output high-frequency connector. Inputs to both subsections are applied through the edge-connector on the right side of the board. Figure F.55 shows a simplified schematic of the ICs.

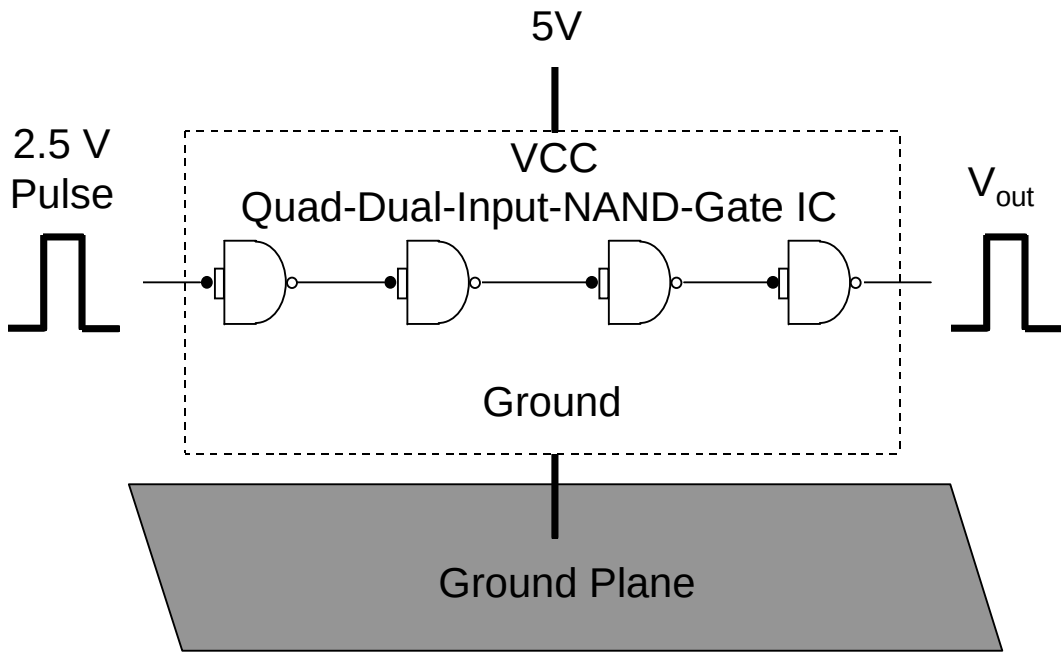

Figure F.55 Simplified Schematic of the ICs in the HSD Subsection

Purpose of the HSD Experiment

The output signal of each gate in Figure F.55 is opposite in polarity to the input signal. If the traces of these two signals are in close proximity on the printed circuit board (capacitively coupled), the gate switching speed might be affected by the presence of flux residues. A 5VDC bias is applied to the VCC inputs during environmental testing to accelerate aging. One PTH IC (U02) is hand soldered during assembly to introduce hand solder flux residue in the experiment.

Circuit Description

The schematic in Figure F.55 represents the ICs in the PTH and SMT subsections. The ICs are random logic circuits that are NAND (Not AND) gates. An AND gate's output is high only when all inputs are high. The logic of a NAND gate is opposite the logic of an AND gate. Therefore, the output of a NAND gate is low only when all inputs are high, otherwise the output is high. With the two connected inputs, the output of each gate is opposite the input. Since the four gates are connected in series, the output of the last gate is the same logic level (high or low) as the input, with a slight lag.

The output pulse does not change logic levels instantaneously, but the switching times from low to high (rise time) and from high to low (fall time) should be less than 7*ns*. ICs should perform within these criteria if the VCC input is 5±0.5V DC, the output load does not exceed specifications, and the circuit has a proper ground plane as shown in Figure F.55. The HSD circuits also provide an intermediate test for high frequencies, with switching time dictating a high frequency spectrum. The frequency spectrum of switching circuits can be expressed in terms of bandwidth (BW). For a switching circuit, the respective BWs (in Hertz) for rise (t_r) and fall (t_f) times are:

$$BW_r = \frac{0.35}{t_r} Hz \quad and \quad BW_f = \frac{0.35}{t_f} Hz \tag{F.14}$$

Bipolar technology was used rather than a complementary metal oxide semiconductor (CMOS) since it is not as vulnerable to electrostatic discharge (ESD) damage. Available military bipolar technologies have the following typical switching speeds and bandwidths:

Technology	Typical $t_{r\ or\ f}$ (ns)	Bandwidth (MHz)
5404 TTL	12	29
54LS04 Low Power Schottky	9	39
54S04 Schottky	3	117
54F04 Advanced Schottky (Fast)	2.5	140

The Fast technology was selected since it had the shortest switching time and largest bandwidth, which provides the widest frequency spectrum for this test.

Circuit Board Design

Ground planes were provided for proper circuit operation of the ICs. The PTH subcircuit utilized the large common ground plane on layer 3 since most of the input and output traces are on layer 4. Since the SMT circuit traces are on the top layer, a smaller ground plane was added on layer 2. The "QUAD-DUAL-INPUT-NAND-GATE" was selected since other solder studies of national attention have used that particular type of IC, which makes direct comparisons with these studies possible.

Baseline Testing Results for HSD

Data modeling showed that surface finish and flux type had very little effect on the total propagation delay measurements (msec) for HSD PTH and HSD SMT. Figures F.56 and F.57 provide dotplot displays of 480 voltage measurements for HSD PTH and HSD SMT, respectively. The summary statistics HSD PTH and HSD SMT total propagation delay are given in Table F.34 (Note one slight outlier for HSD PTH).

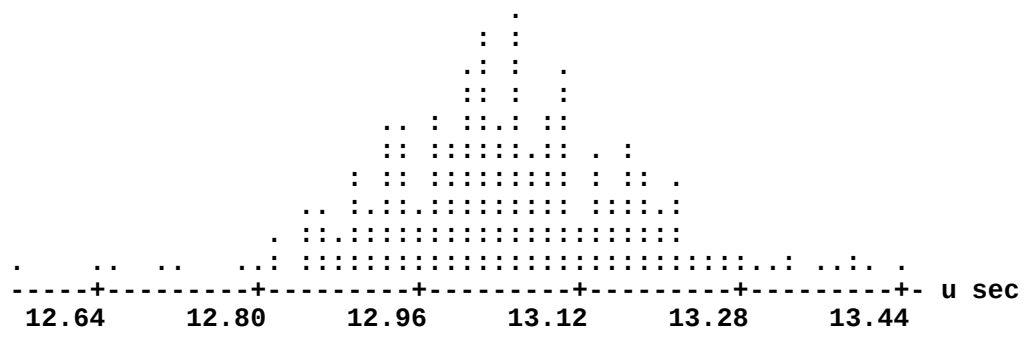

Figure F.56 Dotplot of 480 Measurements of Total Propagation Delay for HSD PTH (each dot represents up to 2 points)

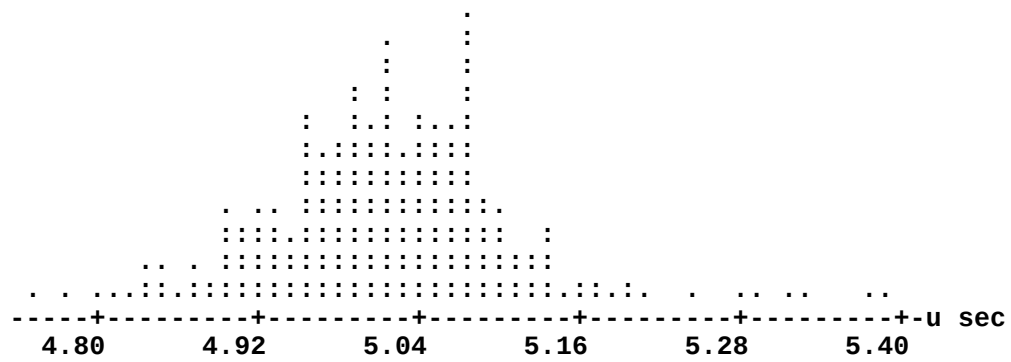

Figure F.57 Dotplot of 480 Measurements of Total Propagation Delay for HSD SMT (each dot represents up to 2 points)

Table F.34 Summary Statistics for HSD Circuitry Total Propagation Delay (μsec) Test Measurements (sans outliers)

Circuitry	Mean	Median	St. Dev.	Min	Max	Outliers	
HSD PTH	13.04μ sec	13.04	0.124	12.56	13.44	14.40	
HSD SMT	5.02μ sec	5.02	0.086	4.75	5.39	4.20	4.29

F.10.5 High Frequency

The HF section shown in the lower right-hand corner of Figure F.50 contains two major subsections, the low-pass filters (LPF) and the transmission line coupler (TLC). The TLC traces on layer 4 of the board are on the backside of the board. The LPF/PTH subsection is above the LPF/SMT subsection. Each of these subsections has discrete ceramic capacitors and three inductor-capacitor (LC) filters, with the inductor printed on the circuit board in a spiral pattern. The HF circuits allow evaluation of circuit performance up to 1G*Hz* (1000*MHz*).

Purpose of the High Frequency Experiment

Flux residues may affect the performance of LPF printed circuit inductors and transmission lines due to parasitic resistances and parasitic capacitances. Since the transmission lines are separated by only 10 mils, flux residues between the lines may affect their performance.

LPF Circuit Description

An inductor-capacitor (LC) LPF consists of a series inductor followed by a shunt capacitor. A low-frequency signal passes through the LPF without any loss since the inductor acts as a short circuit and the capacitor acts as an open circuit for such signals. Conversely, a high-frequency signal is blocked by the LPF since the inductor acts as an open circuit and the capacitor acts as a short circuit for such signals.

When a sine wave test signal is passed through an LPF, its amplitude is attenuated as a function of frequency. The relationship between the output and input voltage amplitudes can be expressed as a transfer function. The transfer function, V_{out} / V_{in}, was measured to determine any effects of the l ow-residue fluxes.

The transfer function is measured in decibels (dB) as a function of frequency. A decibel can be expressed in terms of voltage as follows:

$$dB = 20\log_{10}\left(\frac{|V_{out}|}{|V_{in}|}\right) \qquad \text{(F.15)}$$

The PTH transfer function differs from the SMT transfer function due to the self inductance of the capacitor through-hole leads.

LPF Circuit Board Design

The three LC LPFs for each of the SMT and PTH circuits were designed to have the following cutoff frequencies: 800, 400, and 200 *MHz*. Cutoff frequency is that frequency for which the transfer function is -3 *dB*. The respective component values chosen for the LC filters are 16 *nH* (nano-Henries) and 6.4 *pF* (pico-Farads), 32 *nH* and 13 *pF*, and 65 *nH* and 24 *pF*. Most LPF circuitry was placed on Layer 1, with Layer 2 used as a ground plane. Crossovers needed to connect the LPF circuits are on Layer 4.

The LPF circuits were designed to operate with a 50Ω test system, so all interconnect traces longer than 0.10 *in* were designed as 50Ω transmission lines to avoid signal distortion. The LPF circuits were predicted to have less than 2 *dB* loss below 150 *MHz*, approximately 6 *dB* loss near 235

MHz, and greater than 40 *dB* loss at 550 *MHz* and beyond. The measured response of the LPF/SMT circuit is close to that predicted except that the transfer function decreases more rapidly than predicted above 350 *MHz*. As stated previously, the PTH circuit transfer function did not perform similarly to the SMT, particularly at frequencies above 150 *MHz*.

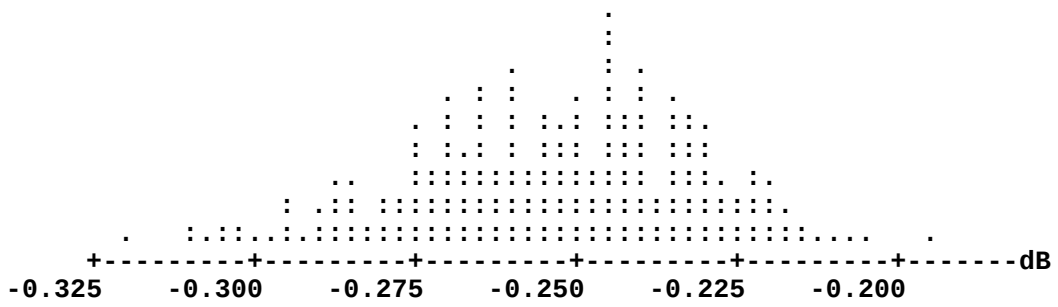

Figure F.58 Dotplot of 473 Measurements of the Response for HF PTH at 50 MHz (each dot represents up to 2 points)

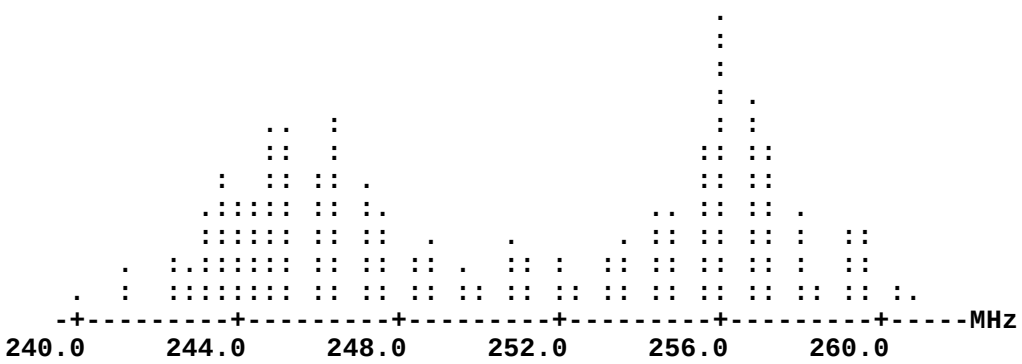

Figure F.59 Dotplot of 472 Measurements of the Frequency for HF PTH at –3dB (each dot represents up to 2 points)

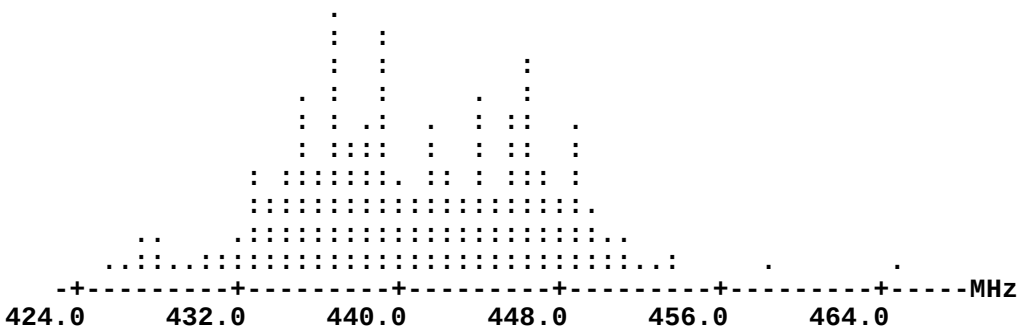

Figure F.60 Dotplot of 474 Measurements of the Frequency for HF PTH at –40dB (each dot represents up to 2 points)

Baseline Testing Results for HF LPF

Data modeling showed that surface finish and flux type had slights effects on the HF LPF frequencies and responses for HF PTH 50 MHz, HF PTH f(–3dB), HF PTH f(–40dB), HF SMT 50 MHz, and HF SMT f(-3dB). The response, HF SMT f(-40dB), was 5 to 12 MHz lower for PWA with OSP, immersion Ag, or immersion Au/Pd surface finishes. However, the range of frequencies for this response was only from 630.7 MHz to 680.60 MHz, so the changes in frequency are relatively small. Figures F.58 to F.59 provide dotplot displays of 480 measurements for the six HF LPF responses. The summary statistics for these responses are given in Table F.35 (Note there are several outliers identified in this table).

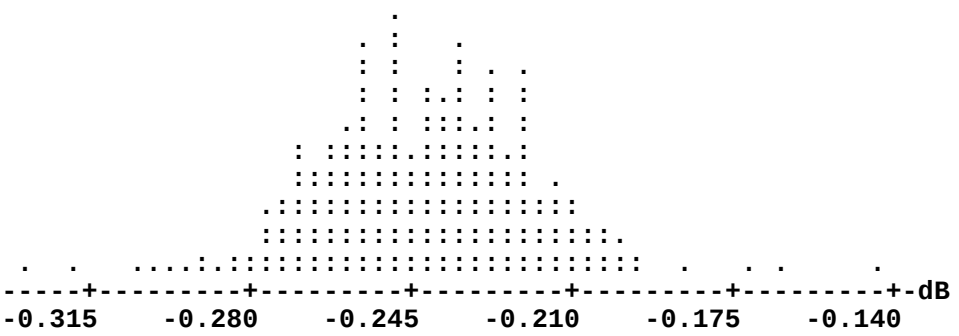

Figure F.61 Dotplot of 473 Measurements of the Response for HF SMT at 50 MHz (each dot represents up to 2 points)

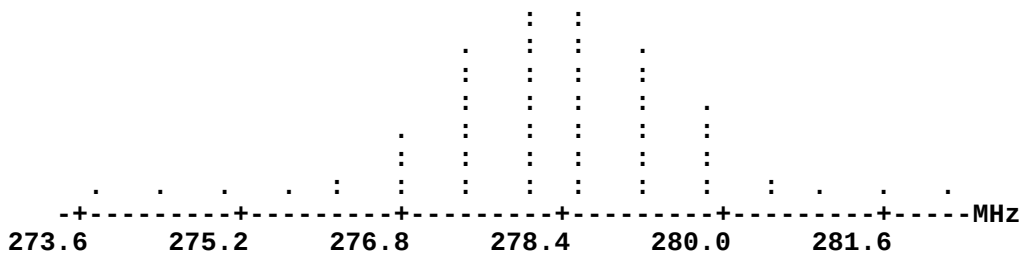

Figure F.62 Dotplot of 469 Measurements of the Frequency for HF SMT at –3dB (each dot represents up to 7 points)

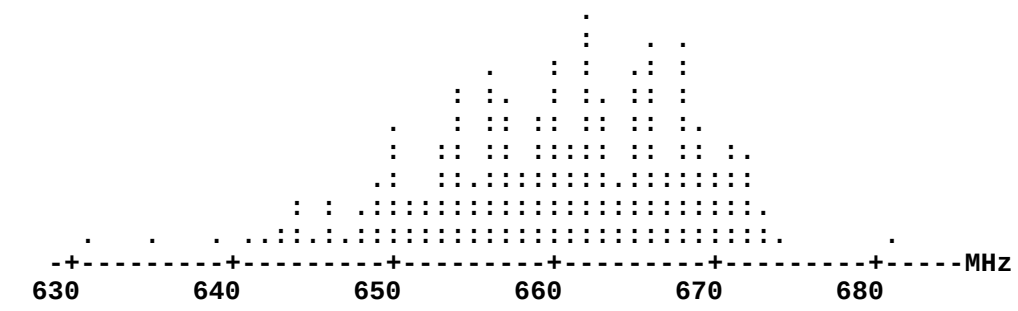

Figure F.63 Dotplot of 469 Measurements of the Frequency for HF SMT at –40dB (each dot represents up to 2 points)

The distribution in Figure F.59 is different from the other 22 electrical responses in that it displays a bimodal distribution for HF PTH f(-3dB) with one group of frequencies centered at approximately 245MHz and the other group at 256MHz. Data modeling showed that the differences between these

two groups were not related to any of the experimental parameters (surface finish or flux) nor were they related to fixture or time of test. A possible explanation for the bimodal distribution is differences in date lots for the components. However, date lot information were not recorded prior to processing and thus, the date lot hypothesis cannot be confirmed. Since the JTP acceptance criterion is based on change after exposure to environmental conditions, the bimodal distribution could potentially be important if the measurements were not repeatable. Twenty board serial numbers were randomly selected for retest to see if the measurements were repeatable with 10 boards from the distribution centered at 245MHz and 10 boards from the distribution centered at 256MHz. These two groups of 10 were equally split between fixtures A and B on the CCAMTF ATS. Table F.36 gives the differences between the initial baseline measurements and those from the repeat test. The differences in this table are all quite small. The correlation of the measurements on fixture A is 0.995 and on fixture B it is 0.982, which indicates excellent repeatability. Thus, other than being a curiosity, the bimodal distribution for HF PTH f(-3dB) will have no practical effect on the test results.

Table F.35 Summary Statistics for 393 Test Measurements for Response (dB) or Frequency (MHz) for HF LPF (sans outliers)

Circuitry	**Mean**	**Median**	**St. Dev.**	**Min**	**Max**	**Outliers**	
HF PTH 50 MHz	-0.254 dB	-0.252	0.022	-0.319	-0.194	-0.351	-0.150
						-0.148	-0.138
						-0.130	-0.107
						-0.096	
HF PTH –3dB	250.6 MHz	250.7	5.65	240.0	260.8	227.4	230.5
						305.3	306.5
						307.1	307.7
						308.3	308.9
HF PTH –40dB	440.7 MHz	440.1	6.01	425.3	464.4	506.6	507.2
						507.8	513.1
						513.7	514.3
HF SMT 50 MHz	-0.242 dB	-0.242	0.023	-0.329	-0.144	-0.447	-0.074
						-0.066	-0.062
						-0.061	
HF SMT –3dB	278.3 MHz	278.6	1.20	273.8	282.2	225.2	295.8
						299.4	301.8
						302.9	302.9
						355.2	381.9
						383.1	384.3
						389.6	
HF SMT –40dB	660.2 MHz	661.0	7.66	630.7	680.6	694.8	701.9
						708.5	719.8
						721.5	758.3
						862.8	872.3
						877.7	890.2
						924.6	

Table F.36 Results from Repeat Testing of the HF PTH f(-3dB) Circuit

	Fixture A			Fixture B		
Test	**Baseline**	**Repeat**	**Difference**	**Baseline**	**Repeat**	**Difference**
1	244.2	243.0	1.23	242.4	243.0	-0.57
2	245.3	244.8	0.55	244.2	245.3	-1.14
3	246.5	246.5	-0.03	245.3	245.9	-0.64
4	247.1	247.1	-0.03	246.5	244.2	2.34
5	253.1	254.3	-1.15	248.9	250.1	-1.19
6	255.4	255.4	-0.04	253.7	255.4	-1.74
7	256.0	256.0	-0.03	254.8	255.4	-0.64
8	257.2	257.8	-0.61	256.0	258.4	-2.41
9	259.0	259.0	0.00	257.8	258.4	-0.61
10	259.6	259.0	0.60	259.0	259.0	0.00

TLC Circuit Description

Figure F.64 shows a diagram of the TLC subsection. The LPFs described above are *lumped element* circuits since the capacitors are discrete components. The TLC lines are *distributed element* circuits with the resistors, inductors, and capacitors distributed along the lines. A circuit model for the lines is shown in Figure F.65.

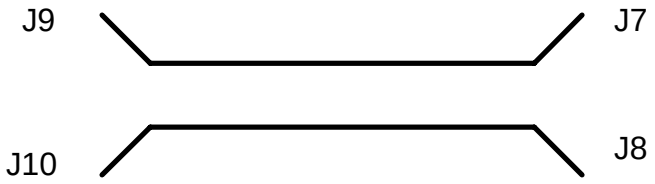

Figure F.64 Diagram of the HF/TLC Subsection

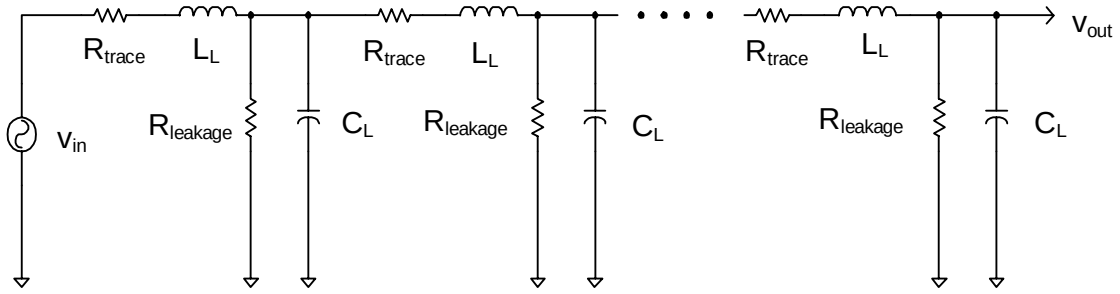

Figure F.65 HF/TLC Distributed Element Model

The inductance and capacitance for a transmission line with a ground plane are, respectively:

$$L_L = 0.085 R_0 \sqrt{\varepsilon_r}\, nH / in \qquad \text{(F.16)}$$

$$C_L = \frac{85}{R_0}\sqrt{\varepsilon_r}\, pF / in \qquad \text{(F.17)}$$

where R_0 = characteristic resistance and ε_r = dielectric constant of the board material.

The TLC R_o was designed to be 50Ω for operation with a 50Ω test system. For FR-4 epoxy (board substrate material), L_L is about 9.6 *nH*/*in* and C_L is about 3.8 *pF*/*in*.

The TLC was tested with a sine wave signal similar to the one used in testing the LPFs. The source resistance was 50Ω and the three output terminals were connected to 50Ω loads.

TLC Circuit Board Design

The transmission line coupler (TLC) circuit has a pair of coupled 50Ω transmission lines with required measurable performance frequencies less than 1000 *MHz*. Layer 4 of the printed wiring board (PWB) was used to route the TLC circuit, with Layer 3 used as the ground plane. The TLC circuit is a 5 *in* long pair of 0.034 *in* wide 50Ω transmission lines spaced 0.010 *in* apart. The circuit design incorporated the board dielectric constant of about 3.8 and the .020 *in* spacing between copper layers. A computer-aided circuit design tool (Libra) was used to model the TLC circuit. Performance measured on a test PWB agreed very closely with the forward and reverse coupling predictions between 45 *MHz* and 1000 *MHz*.

Baseline Testing Results for HF TLC

Data modeling showed that surface finish and flux type had very slight effect on the HF TLC frequencies and responses for HF TLC 50 MHz, HF TLC 500 MHz, HF TLC 1000 MHz, HF TLC Reverse Null Frequency, and HF TLC Reverse Null Response. Figures F.66 to F.70 provide dotplot displays of 480 measurements for the five HF TLC responses. Summary statistics for these responses are given in Table F.37 (Note the outliers identified in this table).

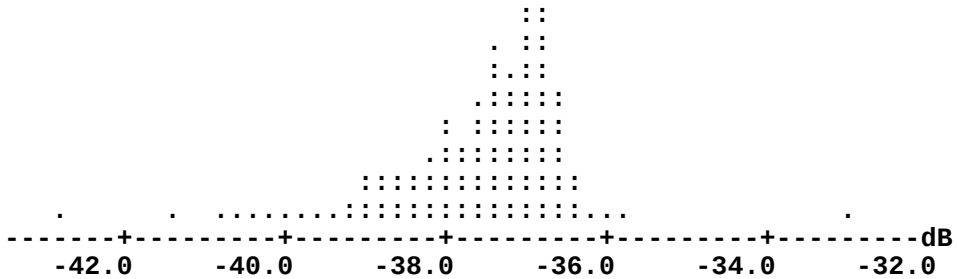

Figure F.66 Dotplot of 479 Measurements of the Response for HF TLC at 50 MHz (each dot represents up to 4 points)

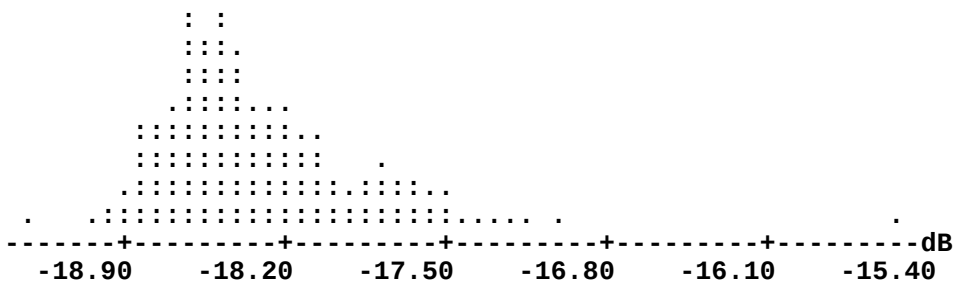

Figure F.67 Dotplot of 479 Measurements of the Response for HF TLC at 500 MHz (each dot represents up to 3 points)

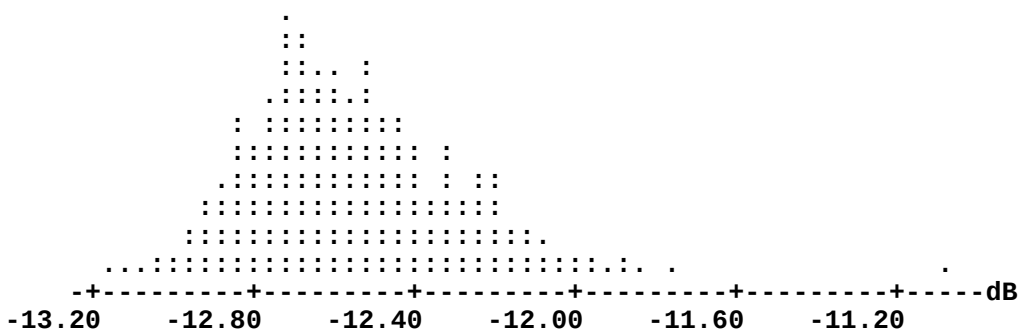

Figure F.68 Dotplot of 478 Measurements of the Response for HF TLC at 1000 MHz (each dot represents up to 2 points)

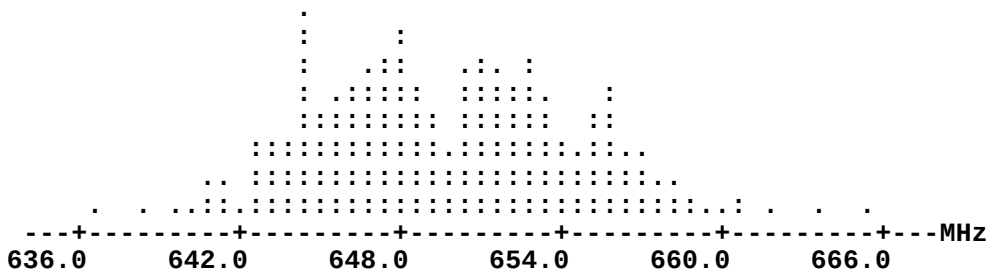

Figure F.69 Dotplot of 479 Measurements of the HF TLC Reverse Null Frequency (each dot represents up to 2 points)

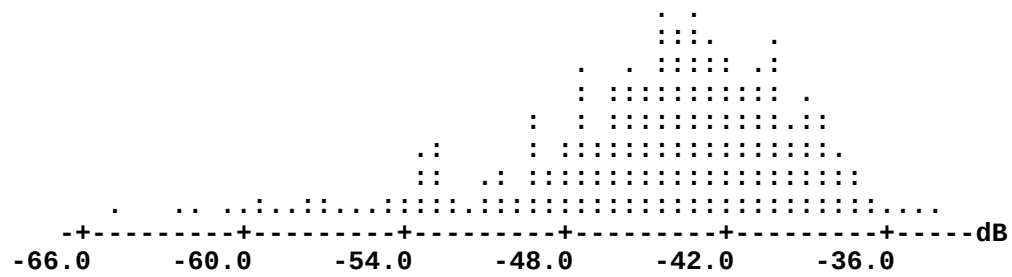

Figure F.70 Dotplot of 479 Measurements of the HF TLC Reverse Null Response (each dot represents up to 2 points)

Table F.37 Summary Statistics for 480 Test Measurements for Response (dB) or Frequency (MHz) for HF TLC (sans outliers)

Circuitry	Mean	Median	St. Dev.	Min	Max	Outliers	
HF TLC 50 MHz	-37.57 dB	-37.34	0.974	-42.74	-33.05	-6.13	
HF TLC 500 MHz	-18.34 dB	-18.43	0.403	-19.29	-15.57	-6.90	
HF TLC 1000 MHz	-12.56 dB	-12.60	0.258	-13.15	-11.07	-7.05	-8.94
HF TLC RNF	649.6 MHz	649.1	4.77	636.6	665.1	935.3	
HF TLC RNR	-44.82 dB	-44.01	5.25	-64.89	-34.12	-9.67	

F.10.6 Other Networks (Leakage Currents)

The test PWA also contains three test patterns to provide tests for current leakage: (1) the pin grid array (PGA), (2) the gull wing (GW), and (3) 10-mil spaced pads. A 100V source was used to generate leakage currents.

Purpose of the Experiments

The PGA, GW, and 10-mil pads allow leakage currents to be measured on test patterns that are typical in circuit board layouts. These patterns contain several possible leakage paths and the leakage could increase with the presence of flux residues and environmental exposure. In addition, solder mask was applied to portions of the PGA and GW patterns to evaluate its effect on leakage currents and the formation of solder balls.

Pin Grid Array

The PGA hole pattern has four concentric squares that are electrically connected by traces on the top layer of the board as shown in Figure F.71. The pattern also has four vias just inside the corners of the innermost square that are connected to that square. Four vias were placed inside the innermost square to trap flux residues. Two leakage current measurements were made: (1) between the two inner squares (PGA-A) and (2) between the two outer squares (PGA-B), as shown in Figure F.71. Solder mask covers the holes of the two outer squares on the bottom layer, allowing a direct comparison of similar patterns with and without solder mask.

Rather than an actual PGA device, a socket was used since it provided the same soldering connections as a PGA device. Also, obtaining leakage measurements on an actual PGA is nearly impossible due to complexity of its internal semiconductor circuits.

Gull Wing

The upper half of the topmost GW lands and the lower half of the bottom most GW lands were covered with solder mask to create a region that is susceptible to the formation of solder balls. The lands were visually inspected to detect the presence of solder balls. A nonfunctional GW device is installed with every other lead connected to a circuit board trace forming two parallel paths around the device. Total leakage current measurements were made on adjacent lands of the GW device

10-mil Pads

The 10-mil pads were laid out in two rows of five pads each. The pads within each row were connected on the bottom layer of the board and leakage between the rows was measured.

Baseline Testing Results for Leakage Currents

The leakage currents are converted to resistance (ohms) through the basic equation $R = V/I$. Since the applied voltage is 100 V and the current is measured in nanoamps, this equation can be expressed as $\log_{10} R = 11 - \log_{10} I$.

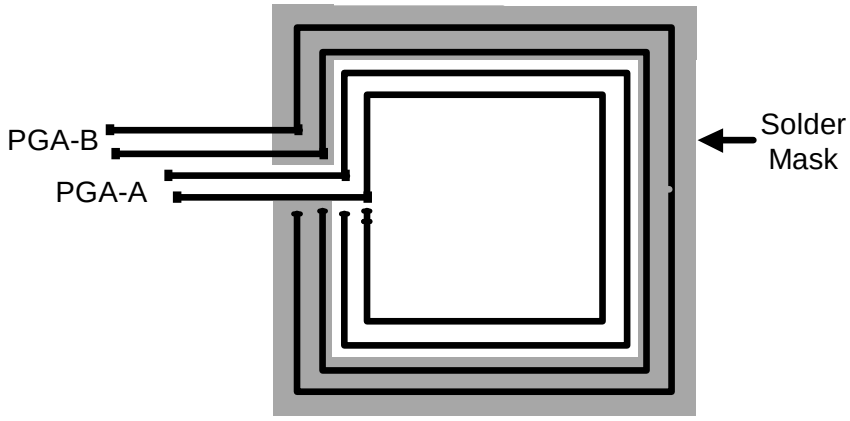

Figure F.71 PGA Hole Pattern with Solder Mask

Table F.38 Significant Coefficients for the GLM Analyses of Leakage Currents

Experimental Variables	10-Mil Pad	PGA A	PGA B	Gull Wing
Constant	11.43	10.63	9.88	11.57
OSP	0.68	0.92	1.22	0.61
Immersion Ag	0.59	0.84	1.22	0.67
Immersion Au/Pd	0.28	0.49	1.52	0.40
Flux	1.61	1.77	2.74	0.89
OSP*Flux	-0.33		-0.60	
Ag*Flux	-0.37	-0.26	-0.90	
Au/Pd*Flux			-0.90	-0.31
Model R^2	60.99	74.52	88.12	35.04
Standard Deviation	0.606	0.542	0.432	.681

General linear modeling (GLM) results for $\log_{10}$ R are given in Table F.38. The GLM results show that surface finish and flux type strongly affect leakage currents. To illustrate these effects, dotplot displays of 480 measurements for the four leakage responses are given by surface finish and flux in Figures F.72 to F075 and by flux in Figure F.76. The summary statistics for these responses are given in Tables F.39 and F.40.

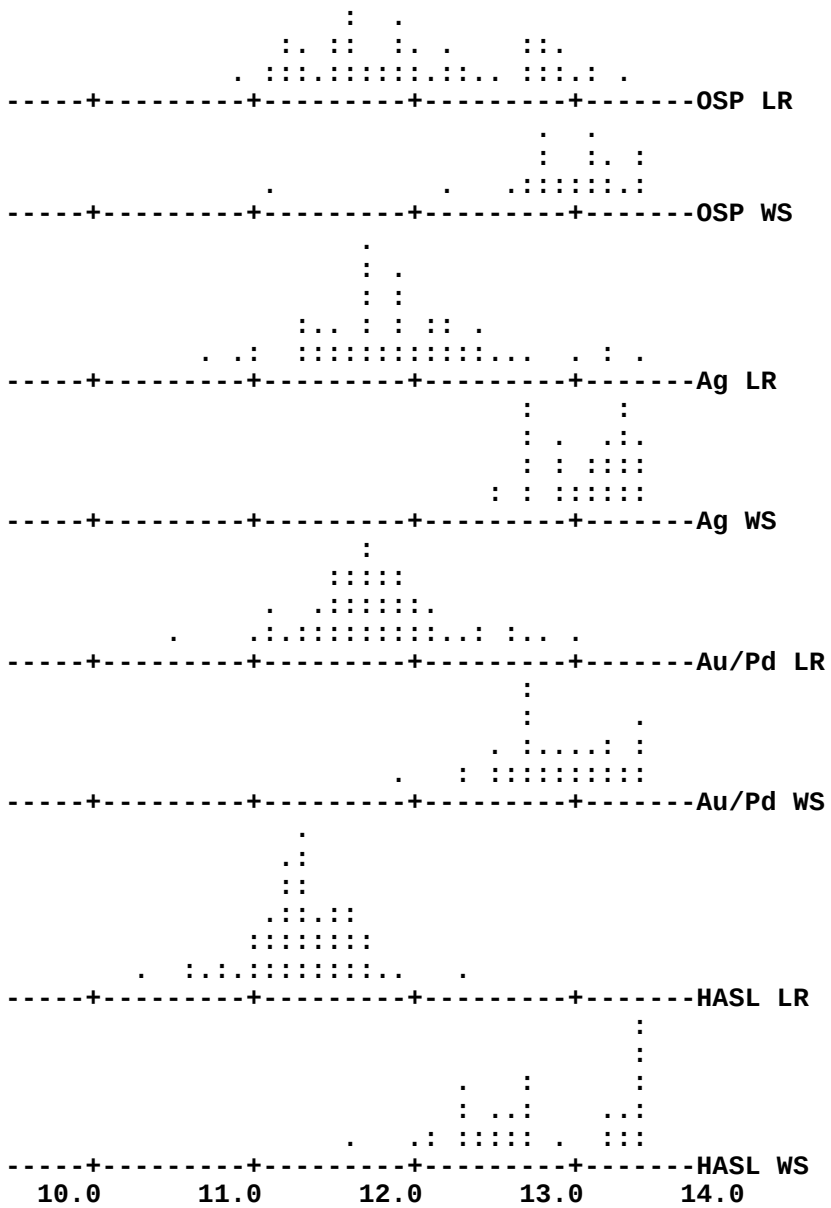

Figure F.72 Dotplots for 480 Measurements of Leakage on 10-Mil Pads by Surface Finish and Flux

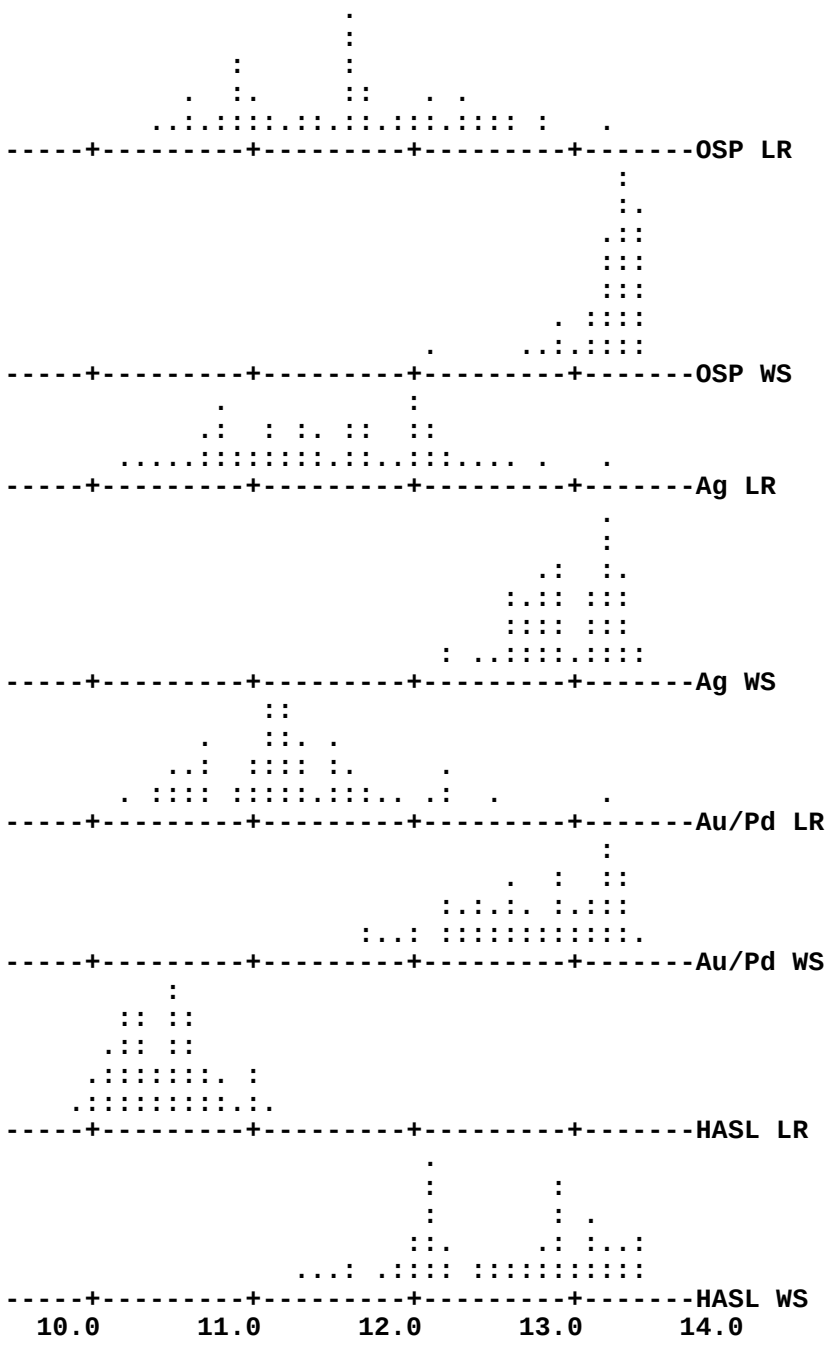

Figure F.73 Dotplots for 480 Measurements of Leakage on PGA A by Surface Finish and Flux

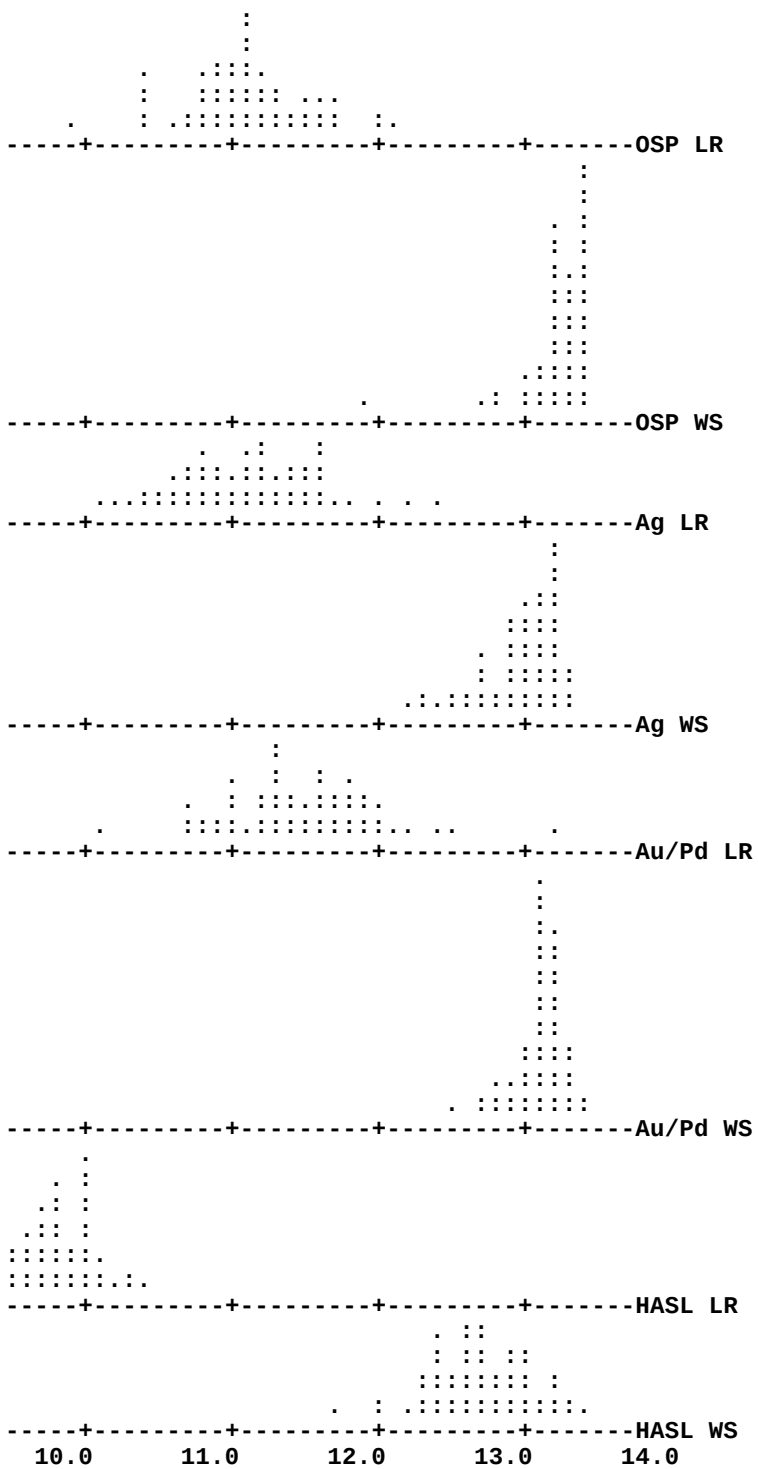

Figure F.74 Dotplots for 480 Measurements of Leakage on PGA B by Surface Finish and Flux

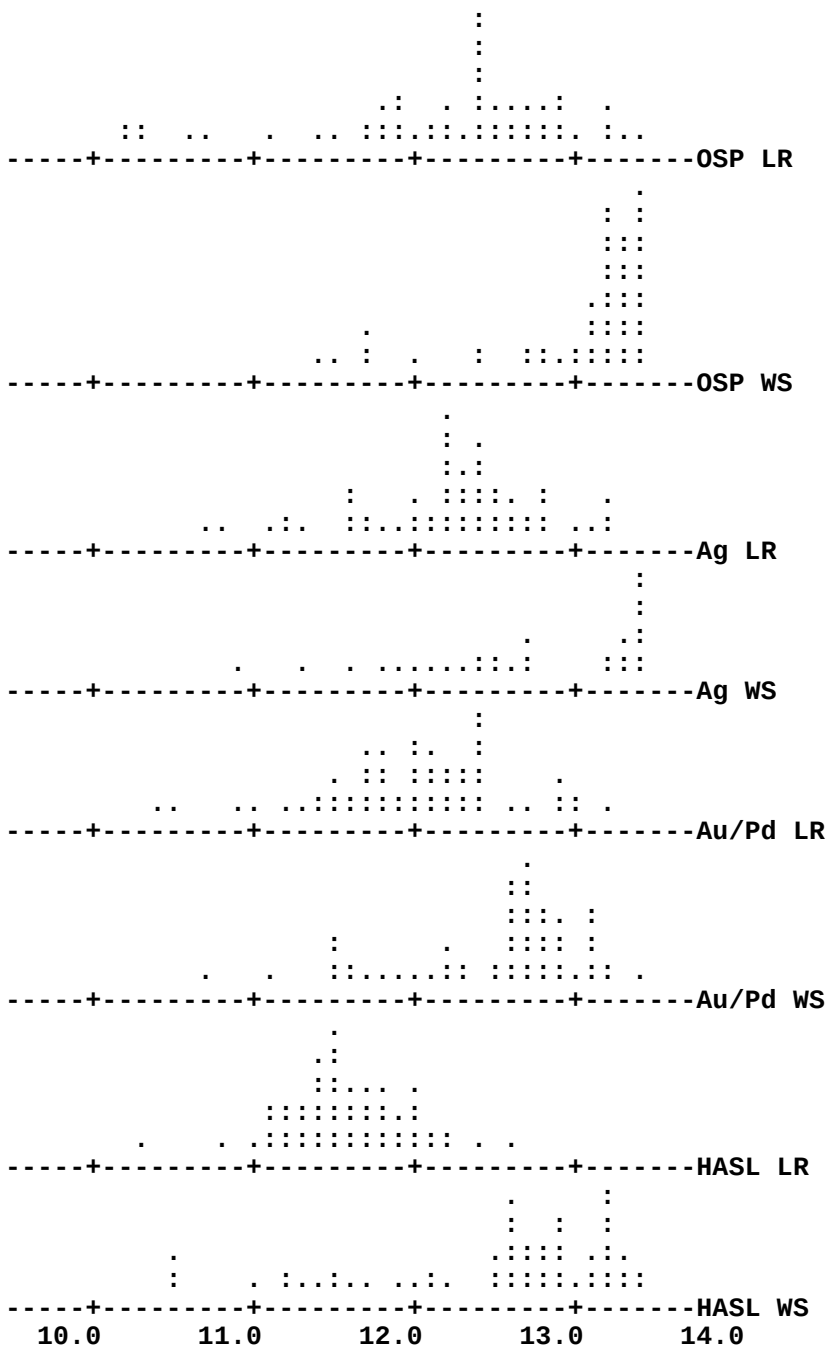

Figure F.75 Dotplots for 480 Measurements of Leakage on the Gull Wing by Surface Finish and Flux

Table F.39 Summary Statistics for Leakage Currents Test Measurements by Surface Finish and Flux

Circuitry	Surface Finish	Flux	Mean	Median	St. Dev.	Min	Max
10-Mil Pads	**OSP**	**LR**	12.11	11.94	0.77	10.91	15.00
		WS	13.39	13.52	0.55	11.12	14.00
	Immersion Ag	**LR**	12.02	11.90	0.76	10.73	15.00
		WS	13.26	13.30	0.38	12.48	14.00
	Immersion Au/Pd	**LR**	11.81	11.73	0.54	10.47	14.00
		WS	13.22	13.22	0.60	11.91	15.00
	HASL	**LR**	11.29	11.29	0.33	10.34	12.30
		WS	13.15	13.40	0.67	11.57	15.00
PGA A	**OSP**	**LR**	11.59	11.62	0.67	10.38	13.15
		WS	13.28	13.30	0.26	12.12	13.70
	Immersion Ag	**LR**	11.47	11.39	0.66	10.16	13.22
		WS	12.98	12.94	0.33	12.18	14.00
	Immersion Au/Pd	**LR**	11.23	11.20	0.56	10.18	13.15
		WS	12.78	12.80	0.62	11.67	15.00
	HASL	**LR**	10.45	10.46	0.28	9.94	11.10
		WS	12.56	12.66	0.58	11.29	13.40
PGA B	**OSP**	**LR**	11.10	11.11	0.43	9.91	12.09
		WS	13.23	13.30	0.25	11.85	13.52
	Immersion Ag	**LR**	11.10	11.12	0.47	10.13	12.40
		WS	12.94	13.00	0.27	12.19	13.30
	Immersion Au/Pd	**LR**	11.47	11.44	0.50	10.09	13.15
		WS	13.16	13.10	0.39	12.51	15.00
	HASL	**LR**	9.74	9.75	0.29	9.11	10.35
		WS	12.70	12.70	0.35	11.65	13.40
Gull Wing	**OSP**	**LR**	12.15	12.40	0.90	9.01	13.52
		WS	13.10	13.22	0.65	11.44	16.00
	Immersion Ag	**LR**	12.23	12.32	0.60	10.66	13.52
		WS	13.14	13.46	0.70	10.91	14.00
	Immersion Au/Pd	**LR**	11.99	12.02	0.57	10.35	13.22
		WS	12.53	12.66	0.64	10.69	14.00
	HASL	**LR**	11.57	11.52	0.39	10.26	12.62
		WS	12.44	12.70	0.86	9.48	13.52

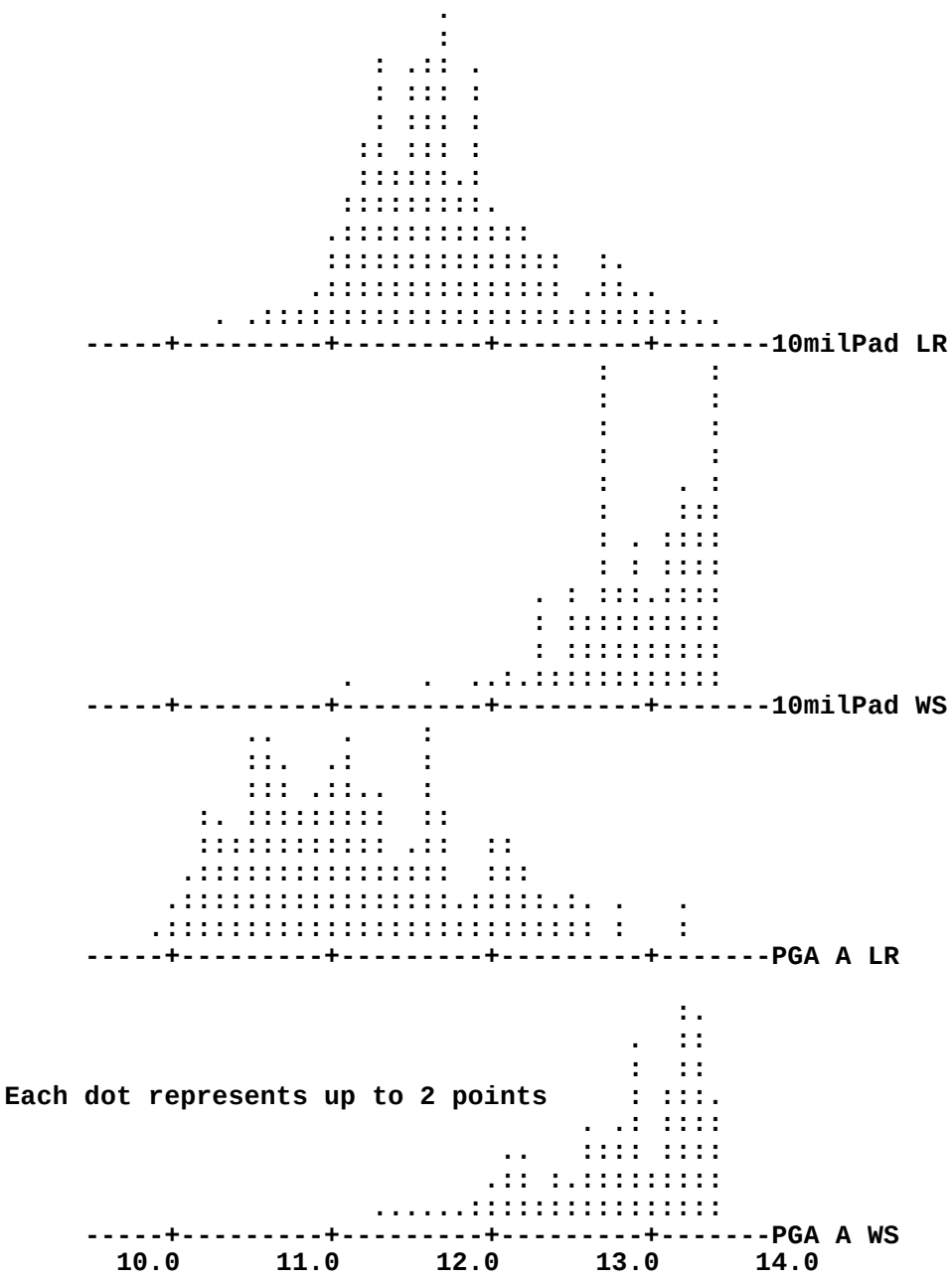

Figure F.76 Dotplots for 480 Leakage Measurements by Flux

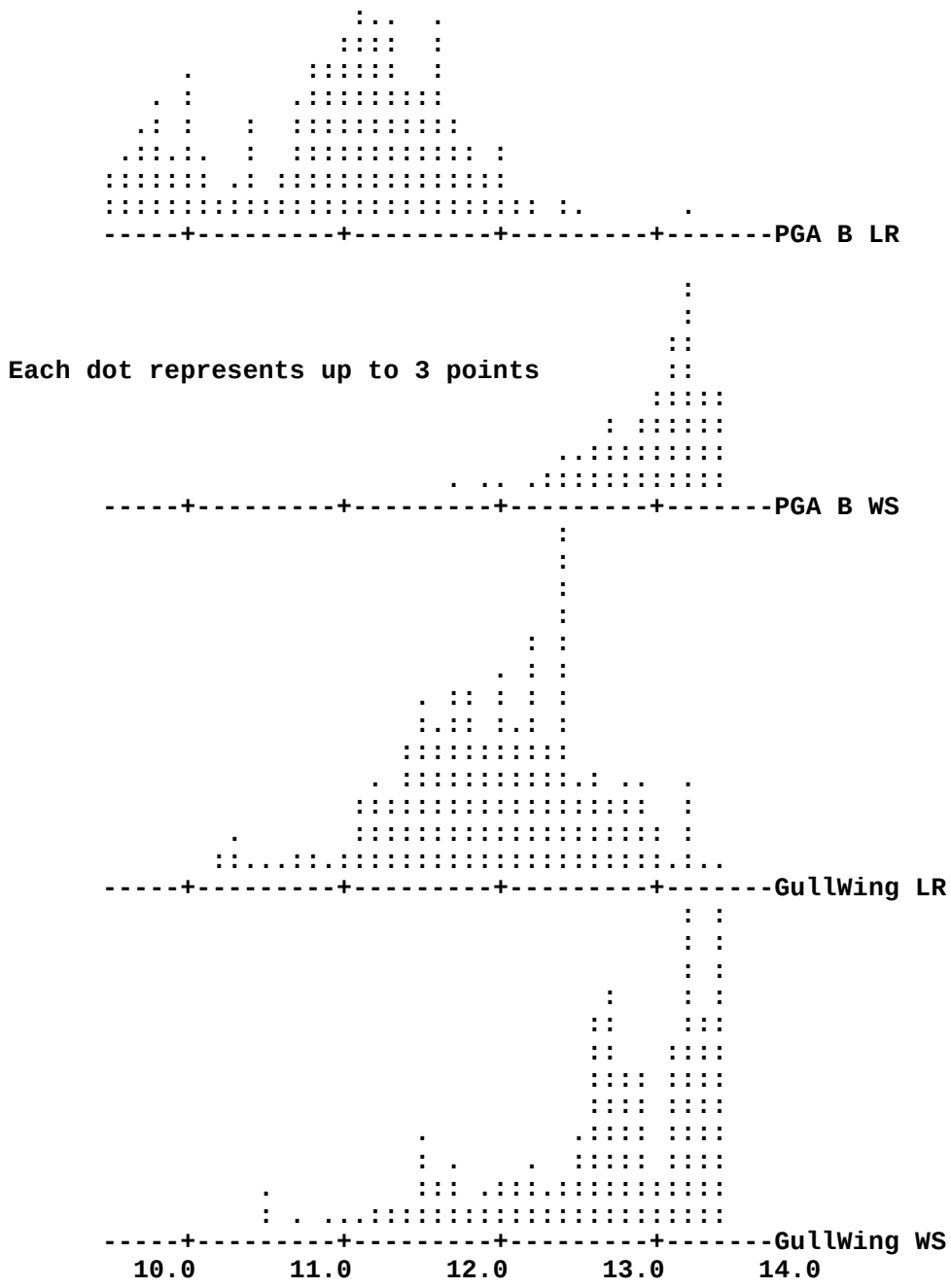

Figure F.76 Continued

F.10.7 Stranded Wires

Two 22-gauge stranded wires were hand soldered just to the left of the edge connector. One wire was soldered directly into the board through holes and the other were soldered to two terminals, E17 and E18. Each wire is 1.5 *in* long, is silver coated, and has white PTFE insulation. All wires were stripped, tinned, and cleaned in preparation for the soldering process.

Purpose of the Stranded Wire Experiment

Stranded wires were used to evaluate flux residues and subsequent corrosion.

Table F.40 Summary Statistics for Leakage Currents Test Measurements by Flux

Circuitry	Flux	Mean	Median	St. Dev.	Min	Max
10-Mil Pads	**LR**	11.80	11.68	0.70	10.34	15.00
	WS	13.25	13.30	0.56	11.12	15.00
PGA A	**LR**	11.18	11.10	0.72	9.94	13.22
	WS	12.90	13.00	0.54	11.29	15.00
PGA B	**LR**	10.85	11.00	0.79	9.11	13.15
	WS	13.01	13.07	0.38	11.65	15.00
Gull Wing	**LR**	11.99	12.02	0.68	9.01	13.52
	WS	12.80	12.94	0.78	9.48	16.00

Circuit Description

The 5A 100µs pulse used to test the HCLV circuit was injected into each of the stranded wires for electrical test. A separate PWB trace was connected to each end of the stranded wire. Test wires were connected to the separate traces allowing to provide the means to measure the voltage drop across the stranded wires. In this manner, the voltage drop was measured independently from any voltage drop in the test wires conducting the 5A pulse to the stranded wires.

Baseline Testing Results for Stranded Wires

Surface finish and flux type had very little effect on the HF TLC frequencies and responses for HF TLC 50 MHz, HF TLC 500 MHz, HF TLC 1000 MHz, HF TLC Reverse Null Frequency, and HF TLC Reverse Null Response. Figures F.77 and F.78 provide dotplot displays of 480 measurements for the two stranded wire voltages. The summary statistics for these responses are given in Table F.41.

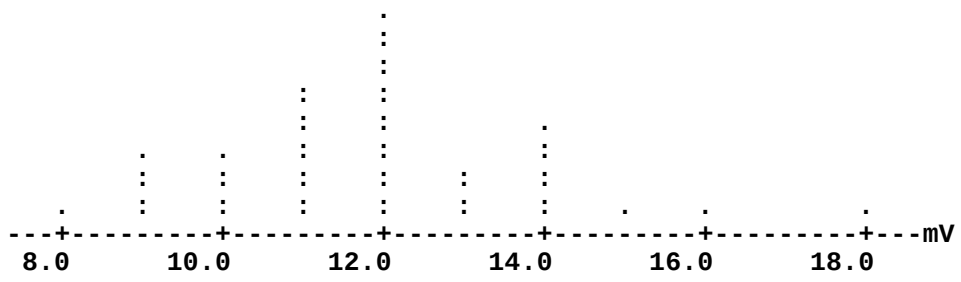

Figure F.77 Dotplots for 480 Voltage Measurements for Stranded Wire 1 (each dot represents up to 11 points)

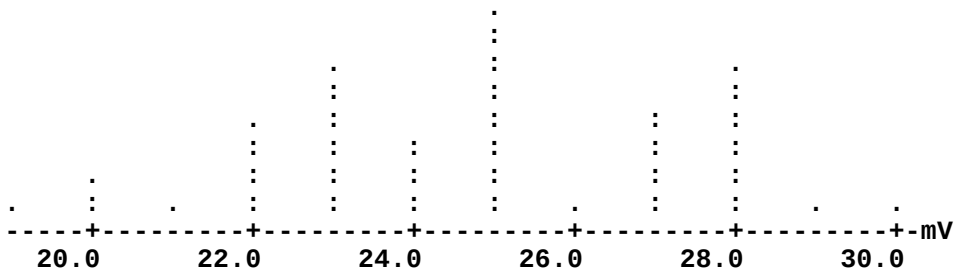

Figure F.80 Dotplots for 476 Voltage Measurements for Stranded Wire 2 (each dot represents 8 points)

Table F.41 Summary Statistics for Stranded Wires Voltage Test Measurements

Circuitry	Mean	Median	St. Dev.	Min	Max	Outliers
Stranded Wire 1	11.75mV	12.00	1.60	8.00	18.00	
Stranded Wire 2	24.82mV	25.00	2.41	19.00	30.00	42,43, 45, 45

F.10.8 Summary Statistics for All Baseline Measurements

For ease of reference, Table F.42 gives the summary statistics for all 23 electrical responses from the test PWA.

F.10.9 Listing of Components

All functional component types conformed to commercial specifications and were ordered pre-tinned (to the extent possible). Components were not pre-cleaned before use. A listing of all components is given in the Table F.43.

Table F.42 Summary Statistics for All Baseline 480 Measurements (sans outliers)

Circuitry	Mean	Median	St. Dev.	Min	Max	Outliers
High Current Low Voltage						
HCLV PTH	6.88V	6.92	0.16	6.60	7.20	
HCLV SMT	7.20V	7.20	0.10	6.88	7.44	
High Voltage Low Current						
HVLC PTH	5.04µA	5.04	0.024	4.972	5.148	5.203 5.232
HVLC SMT	4.95µA	4.95	0.011	4.914	4.976	
High Speed Digital						
HSD PTH	13.04µ sec	0.12	13.04	12.56	13.44	14.40
HSD SMT	5.02µ sec	0.08	5.02	4.75	5.39	
High Frequency Low Pass Filter						
HF PTH 50 MHz	-0.254 dB	-0.253	0.024	-0.319	-0.194	-0.351 -0.150 -0.148 -0.138 -0.130 -0.107 -0.096
HF PTH –3dB	250.5 MHz	249.2	5.74	230.5	260.8	227.6 230.5 305.3 306.5 307.2 307.7 308.3 308.9
HF PTH –40dB	440.5 MHz	440.1	5.96	425.3	464.4	506.6 507.2 507.8 513.1 513.7 514.3
HF SMT 50 MHz	-0.242 dB	-0.241	0.022	-0.329	-0.173	-0.447 -0.164 -0.144 -0.074 -0.066 -0.062 -0.061
HF SMT –3dB	278.4 MHz	278.6	1.21	273.8	282.2	225.2 295.8 299.4 301.8 302.9 302.9 355.2 381.9 383.1 384.3 389.6
HF SMT –40dB	660.7 MHz	661.6	7.46	639.0	680.6	694.8 701.9 708.5 719.8 721.5 758.3 862.8 872.3 877.7 890.2 924.6
High Frequency Transmission Line Coupler						
HF TLC 50 MHz	-37.61 dB	-37.38	0.957	-42.74	-33.05	-6.13
HF TLC 500 MHz	-18.31 dB	-18.40	0.389	-19.29	-15.57	-6.90
HF TLC 1000 MHz	-12.55 dB	-12.58	0.254	-13.15	-11.07	-7.05 -8.94
HF TLC RNF	649.5 MHz	649.1	4.87	636.6	665.1	935.3
HF TLC RNR	-44.68 dB	-43.96	5.208	-64.89	-34.12	-9.67
Leakage (resistance in log 10 ohms)						
10-Mil Pads (LR)	11.79	11.69	0.64	10.63	15.00	
10-Mil Pads (WS)	13.27	13.40	0.56	11.12	15.00	
PGA A (LR)	11.17	11.11	0.70	10.01	13.15	
PGA A (WS)	12.89	13.05	0.52	11.29	14.00	
PGA B (LR)	10.84	11.04	0.80	9.11	12.46	
PGA B (WS)	13.01	13.10	0.34	11.65	13.52	
Gull Wing (LR)	12.03	12.05	0.66	10.15	13.52	
Gull Wing (WS)	12.81	12.96	0.71	10.52	14.00	
Stranded Wire						
Stranded Wire 1	11.75mV	12.00	1.50	8.00	18.00	
Stranded Wire 2	24.71mV	25.00	2.38	19.00	30.00	42, 43, 45, 45

Table F.43 Listing of Components for the Test PWA

MFG P/N	Description	Quantity per Assembly	Supplier
ACC916228-2	PGA Socket, 18X18 (223 PINS)	1	AMP
350-60-2	6 Split washer	3	Barnhill Bolt
402-632-38-0110	6-32 UNC Mach Screw	3	Barnhill Bolt
231-632-A-2	6-32 UNC Mach Screw Nut	3	Barnhill Bolt
RWR89N10R0FR	Resistor, 10 Ohm, Axial	7	Dale
M55342M09B10MOM	Resistor, 10 Ohm, Surface Mnt	7	Dale
RLR07C1005FR	Resistor,10Meg Axial	5	Dale
M55342M09B10POM	Resistor,10Meg Surface Mount	5	Dale
2309-2-00-44-00-07-0	Swage pin	17	Harrison HEC
KA29/127BPMCTH	29 Pin Connector,Pretin	1	Hypertonics
C1825N474K5XSCxxxx	CAP, .47 UF, Surf Mnt	7	Kemet
C0627104K1X5CS7506	CAP, 0.1 UF, Radial	7	Kemet
C1825N104K1XRC	CAP, 0.1 UF, Surf Mnt	7	Kemet
C062T105K5X5CSxxxx	CAP, 1 UF, Radial	7	Kemet
C052G130J2G5CR	CAP, 13 PF, Radial	1	Kemet
CDR31BP130BJWR	CAP, 13 PF, Surf Mnt	1	Kemet
C052G240J2G5CRxxxx	CAP, 24 PF, Radial	1	Kemet
C0805N240J1GRC37317537	CAP, 24 PF, Surf Mnt	1	Kemet
C0805N629B1GSC37317535	CAP, 6.2 PF ±0.5%, Surf Mnt	1	Kemet
C052G629D2G5CR7535	CAP, 6.2 PF, ±0.5%, Radial	1	Kemet
JM38510/33001B2A	20 Pin LCC	1	TI (808810.1001)
JM38510/33001BCA	14 Pin Dual-In-Line	2	TI (808810.1)
QFP80T25	80 Pin SQ Flat Pack	1	Top Line
CS1	Cap	1	Top Line
CKR06	Cap	2	Top Line
SC1210E7Axxxx	Cap	13	Top Line
D034	Diode	13	Top Line
RN65	Resistor	1	Top Line
RN55(sub for CS1, Qty 800)	Resistor	5	Top Line
SR1210E7A	Resistor	18	Top Line
T05	Transistor	4	Top Line
TO220M-3	Transistor	3	Top Line
5162-5013-09	Connector, RF, OMNI Spec	10	TTI
131-3701-201	Sub for 5162-5013-09	10	Penstock

F.11 Design for the Environment Printed Wiring Board Project Performance Demonstration Methodology for Alternative Surface Finishes

Note: This methodology is based on input from members of a Performance Demonstration Technical Workgroup, which includes representatives of the printed wiring board (PWB) industry manufacturers, assemblers, and designers; industry suppliers; public interest group; Environmental Protection Agency (EPA); the University of Tennessee Center for Clean Products and Clean Technologies; and other stakeholders. As the testing continues, there may be slight modifications to this methodology.

I. OVERVIEW

A. Goals

The U.S. Environmental Protection Agency's (EPA=s) Design for the Environment (DfE) Printed Wiring Board (PWB) Project is a cooperative partnership among EPA, the PWB industry, public interest groups, and other stakeholders. The project encourages businesses to incorporate environmental concerns into their decision-making processes, along with the traditional parameters of cost and performance, when choosing which technologies and processes to implement. To accomplish this goal, the DfE PWB Project collects detailed data on the performance, cost, and risk aspects of one Ause cluster@ or manufacturing operation, and makes it available to all interested parties. This use cluster focuses on surface finishes used in PWB manufacturing. Analyses on the performance, cost, and risk of several alternative surface finishes will be conducted throughout this project, and the results will be documented in the final project report, titled the *Cleaner Technologies Substitutes Assessment* or CTSA. This methodology provides the general protocol for the performance demonstration portion of the DfE PWB Project. The CTSA is intended to provide manufacturers and designers with detailed information so that they can make informed decisions, taking environmental and health risks into consideration, on what process is best suited for their own facility.

Surface finishes are applied to PWBs to prevent oxidation of exposed copper on the board, thus ensuring a solderable surface when components are added at a later processing stage . Specifically, the goals of the DfE PWB Surface Finishes Project are:

1) to standardize existing information about surface finish technologies;
2) to present information about surface finish technologies not in widespread use, so PWB manufacturers and designers can evaluate the environmental and health risks, along with the cost and performance characteristics, among different technologies; and
3) to encourage PWB manufacturers and designers to follow the example of this project and evaluate systematically other technologies, practices, and procedures in their operations that affect the environment.

B. General Performance Demonstration Plan

The most widely used process for applying surface finishes in commercial PWB shops is hot air solder leveling (HASL). In this process, tin-lead is fused onto exposed copper surfaces. This process was selected as the focus of the Design for the Environment Project because HASL is a source of lead waste in the environment and because there are several alternative surface finishes available on the market. A comprehensive evaluation of these technologies, including performance, cost, and risk, however, has not been conducted. In addition, a major technical concern is that the HASL process

does not provide a level soldering surface for components.
The general plan for the performance demonstration portion of the Project is to collect data on alternative surface finish processes during actual production runs at sites where the processes are already in use. Demonstration facilities will be nominated by suppliers. These sites may be customer production facilities, customer testing facilities (beta sites), or supplier testing facilities, in that order of preference. Each demonstration site will receive standardized test boards which they will run through their surface finish operation during their normal production operation.

The test vehicle design will be tested on the test board designed by the Sandia National Laboratory Low-Residue Soldering Task Force (LRSTF). The same test vehicle was used by the Circuit Card Assembly and Materials Task Force (CCAMTF). CCAMTF is a joint industry and military program evaluating several alternative technologies including Organic Solderability Preservative (OSP), Immersion Silver, Electroplated Palladium/Immersion Gold, Electroless Nickel/Immersion Gold, and Electroplated Palladium. CCAMTF conducted initial screening tests on coupons for each of these surface finishes, however, they will conduct functionality tests only for the OSP (thick), Electroplated Palladium/Immersion Gold, and Immersion Silver technologies.

II. PERFORMANCE DEMONSTRATION PROTOCOL

A. Technologies to be Tested

The technologies that the DfE Project plans to test include:

1. HASL (baseline)
2. OSP – Thick
3. Immersion Tin
4. Immersion Silver
5. Electroless Nickel/Immersion Gold
6. Nickel/Palladium/Gold

B. Step One: Identify Suppliers and Test Sites/Facilities

Performance Demonstration Technical Workgroup members identified suppliers of the above product lines. Any supplier of these technologies who wanted to participate was eligible to submit its product line, provided that it agreed to comply with the testing methodology and submit the requested information, including chemical formulation data. All proprietary information submitted is bring handled as Confidential Business Information. For each product line submitted, the supplier completed a Supplier Data Sheet detailing information on the chemicals used, equipment requirements, waste treatment recommendations, any limitations of the technology, and other information on the product line.

Performance demonstration sites were nominated by suppliers. They identified sites that are currently using their alternative surface finish product line in the following order of preference:
- customer production facilities (first preference)
- beta sites – customer testing facilities (second preference)
- supplier testing facilities (third preference)

The final number of product lines evaluated for each type of alternative surface finish was determined based on the number of suppliers interested in participating and on the resources available. Each

accepted product line was tested at one or two sites. If a supplier has more than one substantially different product line within a technology, the supplier was allowed to submit names of test facilities for each of the products.

C. Step Two: Fabricate Test Vehicles

Test board were fabricated based on the Sandia National Laboratory Low-Residue Soldering Task Force (LRSTF) test board design. This general design was also used in the CCAMTF testing. For the DfE Project, uncoated test boards with comb pattern spacing of 8 mil, 12 mil, 16 mil, and 20 mil will be used.

All test boards are of the same design, and were fabricated at a single shop to minimize the variables associated with board production. All manufacturing steps, up to but not including the soldermask application, were completed by the test board fabricator. For each supplier's product line, 24 boards were shipped to the demonstration site where the alternative surface finish was applied, beginning with the soldermask application step.

The design of the LRSTF PWB was based on input from a large segment of the manufacturing community, and thus reflects the multiple requirements of the commercial sector. Each quadrant of the LRSTF PWA contain one of the following types of circuity:

High-current low-voltage (HCLV)
High-voltage low current (HVLC)
High speed digital (HSD)
High frequency (HF)

The components in each quadrant represent two principal types of soldering technology:

Plated through hole (PTH) – leaded components are soldered through vias in the circuit board by means of a wave soldering operation.
Surface mount technology (SMT) – components manufactured with solder tips on two of their opposite ends are temporarily attached to the substrate with an adhesive and then they are soldered to pads on the circuit board by passing the circuit board through a reflow oven to reflow the solder tips.

The LRSTF PWA also has two stranded wires (SW) that are secured to the circuit board with hand soldering, such as used in repair operations. This assembly also contains other networks that are used to monitor current leakage.

D. Step Three: Collect Background Information

After the suppliers identified appropriate test facilities and completed a supplier data sheet, an independent observer contacted the designated facilities. The observer scheduled a date for the on-site performance demonstration. A questionnaire was sent to each facility prior to the site visit to collect information on the surface finish technology used and background information on the facility, such as the size and type of product produced. On the day of the performance demonstration, the observer reviewed the background questionnaire and discussed any ambiguities with the facility contect.

E. Step Four: Conduct the Surface Finish Performance Demonstration

After test boards were distributed to the demonstration sites, the surface finish performance demonstrations were conducted. The surface finish was applied to the test boards as part of the normal production run at the facility. The test boards were placed in the middle of the run to reflect actual production conditions. The facility applied the solder mask it normally uses in production. The usual process operator operated the line to minimize error due to unfamiliarity with the technology. All test boards were processed in the same production run.

On the day of the performance demonstration, the observer collected data on the surface finish process. During the demonstration, the observer recorded information on surface finish technology performance, including information on chemicals, equipment, and waste treatment methods used. In addition, other information needed for the performance, cost, or risk analyses, as described below, was collected.

1. **Product Cost:** A cost per square foot of panel processed will be calculated. This number will be based on information provided by product suppliers, such as purchase price, recommended bath life and treatment/disposal methods, and estimated chemical and equipment costs per square foot panel per day. Any "real world" information from PWB manufacturers, such as actual dumping frequencies, treatment/disposal methods, labor requirements, and chemical and equipment costs, will be collected during performance demonstrations, as required for use in the cost analysis. The product cost may differ for difference shop throughput categories.
2. **Product Constraints:** Information on any incompatibilities such as soldermask, flux, substrate type, or assembly process will be included. This information will be submitted by the suppliers and may also be identified as a result of the performance demonstrations.
3. **Special storage, safety, and disposal requirements:** Information on flammability or special storage requirements of the chemicals used in the process will be requested from the suppliers. Suppliers will provide recommendations on disposal or treatment of wastes associated with the use of their product lines. Information on these issues was also collected from participating facilities during the performance demonstrations. The storage and disposal costs will be a factor in determining the adjusted cost of the product. This project does not entail a life cycle analysis for disposal of the boards.
4. **Ease of use:** During the performance demonstration, the physical effort required to use the various surface finishes effectively will be qualitatively assessed based on the judgement of the operator in comparison to the baseline technology, HASL. Specific questions such as the following will be asked: What process operating parameters are needed to ensure good performance? What are the ranges of those parameters, and is there much flexibility in the process steps? How many hours of training are required to use this type of surface finish?
5. **Duration of Production Cycle:** The measured time of the surface finish application process and the number of operators required will be recorded during the performance demonstration. This information will be used to measure the labor costs associated with the use of the product line. Labor costs will be based on the operator time required to run the process using an industry standard worker wage. The process cycle has been defined as the activities following soldermask application up to, but not including, gold tab plating. The facilities participating in the performance demonstration will use the same soldermask they typically use in production conditions. The observer recorded the type of soldermask used, and information on the facilities' experiences with other soldermasks to determine if any known incompatibilities exist.

6. **Effectiveness of Technology, Product Quality:** The performance characteristics of the assembled boards will be tested after all demonstrations are complete and the boards are assembled with the functional components. Circuit electrical Performance will be tested to assess the circuit performance of the functional test vehicle under applicable environmental stress. Circuit Reliability Testing (functional tests) conditions will include Thermal Shock and Mechanical Shock. These tests are described in greater detail in Step 5. Qualitative information on shelf life considerations were collected through the performance demonstrations, where applicable.
7. **Energy and Natural Resource Data:** Information will be collected from the suppliers and during the performance demonstrations to evaluate the variability of energy consumption for the use of different surface finishes. The analysis will also address material use rates and how the rates vary with the different surface finishes.
8. **Exposure Data:** Exposure data will be used to characterize chemical exposures associated with the technologies. Exposure information collected during the performance demonstration may be supplemented with data from other sources, where available.

F. Step Five: Assemble and Test the Boards

After the surface finish was applied to the test boards at each demonstration facility, the facility sent the processed boards to one site for assembly. Two different assembly processes were used: a halide-free, low-residue flux and a halide-containing, water-soluble flux. Table 1 shows the different assembly methods, and number of test vehicles used for each method. The boards were not assembled as originally planned, resulting in the uneven distribution of assembly methods.

Table 1: Test Vehicle Distribution by Site and Flux

Site #	Surface Finishes*	# of Boards Assembled with Low Residue Flux	# of Boards Assembled with Water Soluble Flux	Total Boards by Site and by Surface Finish
1	HASL	8	8	16
2	HASL	0	8	8
6	HASL	8	0	8
	HASL Totals	16	16	32
3	OSP-Thick	4	8	12
13	OSP-Thick	8	8	16
16	OSP-Thick	8	0	8
	OSP Totals	20	16	36
4	Immersion Tin	0	8	8
5	Immersion Tin	4	8	12
10	Immersion Tin	8	0	8
11	Immersion Tin	8	0	8
	Immersion Tin Totals	20	16	36
8	Immersion Silver	0	8	8
9	Immersion Silver	8	4	12
	Immersion Silver Totals	8	12	20
7	Electroless Ni/Immersion Au	0	8	8
12	Electroless Ni/Immersion Au	8	0	8
14	Electroless Ni/Immersion Au	4	8	12
	NI/Au Totals	12	16	28
	Subtotals	84	80	
		Total test boards: 164		

* Corresponding board identification numbers are listed in Appendix A.

Following assembly, the performance characteristics of the assembled boards will be tested. Testing will include Circuit Electrical Performance testing and Circuit Reliability Testing.

Circuit Electrical Performance

This test assesses the circuit performance of a functional test vehicle under applicable environmental stress. The assembled test vehicles will be exposed to 85 ^{o} C at 85% relative humidity for 3 weeks. The assemblies will be tested prior to exposure, and at the end of three weeks of exposure. Good experimental design practices will be followed to control extraneous sources of variation. For example, the assemblies will be placed randomly in the test chamber. If all assemblies cannot be accommodated in the test chamber at the same time, they will be randomized to maintain balance among the experimental factors at each test time. A staggered ramp will be used to prevent condensation (during ramp-up, the temperature will be raised to test level before the humidity is raised and the procedure will be reversed during ramp-down). The pre-tests and post-tests will be identical.

Circuit Reliability Testing
The same test vehicles used to test circuit electrical performance will be used for the circuit reliability tests, which include:

- Thermal Shock
- Mechanical Shock

The electrical functionality of the LRSTF PWA will be evaluated through 23 electrical responses, as follows:

HCLV PTH voltage
HCLV SMT voltage
Stranded wire 1 voltage
Stranded wire 2 voltage
HVLC PTH current
HVLC SMT current
10-mil spaced pads current leakage
PGA A current leakage
PGA B current leakage
Gull wing current leakage
HSD PTH total propagation delay
HSD SMT total propagation delay
HF LPF PTH 50 MHz response
HF LPF PTH frequency response at –3 dB
HF LPF PTH frequency response at –40 dB
HP LPF SMT 50 MHz response
HF LPF SMT frequency response at –3 dB
HF LPF SMT frequency response at –40 dB
HF TLC 50 MHz forward response
HF TLC 500 MHz forward response
HF TLC 1000 MHz forward response
HF TLC reverse null frequency
HF TLC reverse null response

Table 2 shows the total number of electrical responses that will be measured.

Table 2. Number of Tests to be Conducted

Test Environment	Number of PWBs	Number of Test Times	Number of Tests	Number of Electrical Responses Measured
85/85	164	2	164 x 2 = 328	164 x 2 x 23 = 7,544
Thermal Shock		1	164 x 1 = 164	164 x 1 x 23 = 3,772
Mechanical Shock		1	164 x 1 = 164	164 x 1 x 23 = 3,722
Totals	**164**	**4**	**656**	**15,088**

G. Analyze Data and Present Results

The details of the data analysis and results are presented in the "Technical Proposal for this project, in Appendix B.

III. PERFORMANCE DEMONSTRATION PARTICIPANT REQUIREMENTS

A. From the Facilities/Process Operators:

1. Participating facilities were contacted by the project observer to arrange a convenient data for the performance demonstration. The observer sent a fact sheet describing the facility's role in the project.
2. Each facility was asked to complete a background questionnaire prior to the scheduled date of the performance demonstration and return it to the observer.
3. Each facility was asked to make its process line/process operators available to run the 24 test boards on the agreed upon date.
4. The process operator met with the independent observer before running the test boards through the line to explain the unique aspects of the line to the observer. The process operator was asked to be available to assist the independent observer in collecting information about the line.

B. From the Suppliers of the Process Line Alternatives:

1. Suppliers were asked to submit product data sheets, on which they provided information on product formulations, product constraints, recommended disposal/treatment etc. The information, including chemical formulation information, was requested prior to testing. Any proprietary information was submitted to the University of Tennessee as Confidential Business Information.
2. Suppliers were asked to identify and contact the demonstration sites.
3. Suppliers were asked to attend the on-site performance demonstration if they wishes to do so, but they were not required to attend.

Attachment A to this Methodology lists "Identification Numbers for Assembled Boards." To conserve space this information as not been reprinted as part of the CTSA.

Attachment B to this Methodology is the "Technical/Management Proposal for Validation of Alternatives to Lead Containing Surface Finishes." This Attachment contains the testing and analysis methodology submitted by Dr. Ronald L. Inman, President, Southwest Technology Consultants in Albuquerque, MN. Dr. Inman's methodology and results are presented in Chapter 6 of the CTSA and in Appendix F, and therefore, Attachment B of the Methodology is not repeated here.